A Systematic Approach for Seismic Evaluation and Retrofit of RC Buildings in Severe Earthquake Prone Area

Thesis submitted in partial fulfillment

for the Award of Degree

Doctor of Philosophy

by

MANGESHKUMAR RAJKUMAR SHENDKAR

DEPARTMENT OF CIVIL ENGINEERING
INDIAN INSTITUTE OF TECHNOLOGY
(BANARAS HINDU UNIVERSITY)
VARANASI - 221005

18061508 **August 2022**

6. RESULTS AND DISCUSSION

6.1 General

The preliminary seismic assessment of existing RC structures is done based on the Earthquake Disaster Risk Index (EDRI) method. The adaptive pushover analysis, Quadrants assessment method, and Material strain limit approach are used for the detailed seismic assessment purpose. The masonry infills are also accounted in the seismic analysis of reinforced concrete frame. In this study the several parameters, *viz.*, strength, ductility, response reduction factor, etc. can be obtained out from capacity curves before and after the retrofit of buildings.

6.2 Earthquake disaster risk index of 120 RC buildings

A calculation of hazard, exposure, vulnerability & risk of all existing reinforced concrete buildings is presented in Table 6.1 & EDRI of Koyna-Warna region is presented in Table 6.2.

Table 6.1 Details of hazard (H), exposure (E) & vulnerability (V) of all existing RC buildings

Sr. No.	H Actual	H Allowable	E Actual	E Allowable	V Actual	V Allowable	R Actual	R Allowable	Risk	Damage
1	0.80	0.80	0.25	1.00	1	1.00	0.20	0.80	0.25	Slight
2	0.80	0.80	0.24	1.00	1	1.00	0.19	0.80	0.24	Slight
3	0.80	0.80	0.23	1.00	1	1.00	0.18	0.80	0.23	Slight
4	0.80	0.80	0.18	1.00	1	1.00	0.14	0.80	0.18	No
5	0.80	0.80	0.32	1.00	1	1.00	0.26	0.80	0.32	Slight
6	0.80	0.80	0.32	1.00	1	1.00	0.26	0.80	0.32	Slight
7	0.80	0.80	0.32	1.00	1	1.00	0.26	0.80	0.32	Slight
8	0.80	0.80	0.33	1.00	1	1.00	0.26	0.80	0.33	Slight
9	0.80	0.80	0.32	1.00	1	1.00	0.26	0.80	0.32	Slight
10	0.80	0.80	0.42	1.00	1	1.00	0.34	0.80	0.42	Moderate
11	0.80	0.80	0.34	1.00	1	1.00	0.27	0.80	0.34	Slight
12	0.80	0.80	0.35	1.00	1	1.00	0.28	0.80	0.35	Slight
13	0.80	0.80	0.43	1.00	1	1.00	0.34	0.80	0.43	Moderate
14	0.80	0.80	0.34	1.00	1	1.00	0.27	0.80	0.34	Slight
15	0.80	0.80	0.33	1.00	1	1.00	0.26	0.80	0.33	Slight
16	0.80	0.80	0.33	1.00	1	1.00	0.26	0.80	0.33	Slight
17	0.80	0.80	0.32	1.00	1	1.00	0.26	0.80	0.32	Slight
18	0.80	0.80	0.31	1.00	1	1.00	0.25	0.80	0.31	Slight
19	0.80	0.80	0.26	1.00	1	1.00	0.21	0.80	0.26	Slight
20	0.80	0.80	0.38	1.00	1	1.00	0.30	0.80	0.38	Slight
21	0.80	0.80	0.38	1.00	1	1.00	0.30	0.80	0.38	Slight
22	0.80	0.80	0.35	1.00	1	1.00	0.28	0.80	0.35	Slight
23	0.80	0.80	0.41	1.00	1	1.00	0.33	0.80	0.41	Moderate
24	0.80	0.80	0.48	1.00	1	1.00	0.38	0.80	0.48	Moderate
25	0.80	0.80	0.48	1.00	1	1.00	0.38	0.80	0.48	Moderate
26	0.80	0.80	0.42	1.00	1	1.00	0.34	0.80	0.42	Moderate
27	0.80	0.80	0.45	1.00	1	1.00	0.36	0.80	0.45	Moderate
28	0.80	0.80	0.48	1.00	1	1.00	0.38	0.80	0.48	Moderate
29	0.80	0.80	0.55	1.00	1	1.00	0.44	0.80	0.55	Moderate
30	0.80	0.80	0.35	1.00	1	1.00	0.28	0.80	0.35	Slight
31	0.80	0.80	0.41	1.00	1	1.00	0.33	0.80	0.41	Moderate
32	0.80	0.80	0.37	1.00	1	1.00	0.30	0.80	0.37	Slight
33	0.80	0.80	0.56	1.00	1	1.00	0.45	0.80	0.56	Moderate
34	0.80	0.80	0.90	1.50	1	1.00	0.72	1.20	0.60	Severe
35	0.80	0.80	0.71	1.50	1	1.00	0.56	1.20	0.47	Moderate

36	0.80	0.80	1.88	1.50	1	1.00	1.50	1.20	1.00	Collapse
37	0.80	0.80	0.88	1.00	1	1.00	0.70	0.80	0.88	Collapse
38	0.80	0.80	1.32	1.50	1	1.00	1.05	1.20	0.88	Collapse
39	0.80	0.80	0.81	1.00	1	1.00	0.65	0.80	0.81	Collapse
40	0.80	0.80	0.98	1.00	1	1.00	0.78	0.80	0.98	Collapse
41	0.80	0.80	0.96	1.00	1	1.00	0.77	0.80	0.96	Collapse
42	0.80	0.80	0.83	1.00	1	1.00	0.66	0.80	0.83	Collapse
43	0.80	0.80	0.81	1.00	1	1.00	0.65	0.80	0.81	Collapse
44	0.80	0.80	0.96	1.00	1	1.00	0.77	0.80	0.96	Collapse
45	0.80	0.80	0.98	1.00	1	1.00	0.78	0.80	0.98	Collapse
46	0.80	0.80	0.32	1.00	1	1.00	0.26	0.80	0.32	Slight
47	0.80	0.80	1.27	1.00	1	1.00	1.01	0.80	1.00	Collapse
48	0.80	0.80	1.22	1.00	1	1.00	0.97	0.80	1.00	Collapse
49	0.80	0.80	0.29	1.00	1	1.00	0.23	0.80	0.29	Slight
50	0.80	0.80	0.29	1.00	1	1.00	0.23	0.80	0.29	Slight
51	0.80	0.80	0.29	1.00	1	1.00	0.23	0.80	0.29	Slight
52	0.80	0.80	1.77	1.00	1	1.00	1.41	0.80	1.00	Collapse
53	0.80	0.80	2.68	1.00	1	1.00	2.14	0.80	1.00	Collapse
54	0.80	0.80	0.91	1.25	1	1.00	0.73	1.00	0.73	Severe
55	0.80	0.80	0.83	1.25	1	1.00	0.66	1.00	0.66	Severe
56	0.80	0.80	0.36	1.00	1	1.00	0.29	0.80	0.36	Slight
57	0.80	0.80	3.56	1.00	1	1.00	2.84	0.80	1.00	Collapse
58	0.80	0.80	1.10	1.50	1	1.00	0.87	1.20	0.73	Severe
59	0.80	0.80	1.22	1.50	1	1.00	0.97	1.20	0.81	Collapse
60	0.80	0.80	2.72	1.00	1	1.00	2.17	0.80	1.00	Collapse
61	0.80	0.80	2.49	1.50	1	1.00	1.99	1.20	1.00	Collapse
62	0.80	0.80	2.49	1.50	1	1.00	1.99	1.20	1.00	Collapse
63	0.80	0.80	2.49	1.50	1	1.00	1.99	1.20	1.00	Collapse
64	0.80	0.80	1.20	1.50	1	1.00	0.96	1.20	0.80	Collapse
65	0.80	0.80	1.11	1.50	1	1.00	0.89	1.20	0.74	Severe
66	0.80	0.80	1.09	1.00	1	1.00	0.87	0.80	1.00	Collapse
67	0.80	0.80	2.18	1.50	1	1.00	1.74	1.20	1.00	Collapse
68	0.80	0.80	1.23	1.50	1	1.00	0.98	1.20	0.82	Collapse
69	0.80	0.80	1.63	1.00	1	1.00	1.30	0.80	1.00	Collapse
70	0.80	0.80	2.81	1.50	1	1.00	2.24	1.20	1.00	Collapse

71	0.80	0.80	3.77	1.00	1	1.00	3.01	0.80	1.00	Collapse
72	0.80	0.80	0.91	1.00	1	1.00	0.73	0.80	0.91	Collapse
73	0.80	0.80	1.64	1.00	1	1.00	1.31	0.80	1.00	Collapse
74	0.80	0.80	1.13	1.50	1	1.00	0.90	1.20	0.75	Severe
75	0.80	0.80	2.64	1.50	1	1.00	2.11	1.20	1.00	Collapse
76	0.80	0.80	2.40	1.50	0.42	1.00	0.80	1.20	0.67	Severe
77	0.80	0.80	1.36	1.00	1	1.00	1.09	0.80	1.00	Collapse
78	0.80	0.80	1.36	1.00	1	1.00	1.09	0.80	1.00	Collapse
79	0.80	0.80	2.25	1.00	1	1.00	1.80	0.80	1.00	Collapse
80	0.80	0.80	1.11	1.50	1	1.00	0.89	1.20	0.74	Severe
81	0.80	0.80	0.92	1.50	1	1.00	0.73	1.20	0.61	Severe
82	0.80	0.80	1.26	1.50	1	1.00	1.01	1.20	0.84	Collapse
83	0.80	0.80	0.85	1.00	1	1.00	0.68	0.80	0.85	Collapse
84	0.80	0.80	0.73	1.00	1	1.00	0.58	0.80	0.73	Severe
85	0.80	0.80	1.53	1.00	1	1.00	1.22	0.80	1.00	Collapse
86	0.80	0.80	1.19	1.50	1	1.00	0.95	1.20	0.79	Severe
87	0.80	0.80	0.88	1.00	1	1.00	0.70	0.80	0.88	Collapse
88	0.80	0.80	0.63	1.50	1	1.00	0.50	1.20	0.42	Moderate
89	0.80	0.80	0.62	1.00	1	1.00	0.49	0.80	0.62	Severe
90	0.80	0.80	0.90	1.50	1	1.00	0.72	1.20	0.60	Severe
91	0.80	0.80	3.35	1.50	1	1.00	2.67	1.20	1.00	Collapse
92	0.80	0.80	2.42	1.50	1	1.00	1.93	1.20	1.00	Collapse
93	0.80	0.80	0.84	1.25	1	1.00	0.67	1.00	0.67	Severe
94	0.80	0.80	2.28	1.50	1	1.00	1.82	1.20	1.00	Collapse
95	0.80	0.80	3.48	1.50	1	1.00	2.78	1.20	1.00	Collapse
96	0.80	0.80	0.80	1.00	1	1.00	0.64	0.80	0.80	Collapse
97	0.80	0.80	2.00	1.25	1	1.00	1.60	1.00	1.00	Collapse
98	0.80	0.80	1.51	1.00	1	1.00	1.20	0.80	1.00	Collapse
99	0.80	0.80	1.59	1.00	1	1.00	1.27	0.80	1.00	Collapse
100	0.80	0.80	0.74	1.00	1	1.00	0.59	0.80	0.74	Severe
101	0.80	0.80	0.69	1.00	1	1.00	0.55	0.80	0.69	Severe
102	0.80	0.80	0.69	1.00	1	1.00	0.55	0.80	0.69	Severe
103	0.80	0.80	0.69	1.00	1	1.00	0.55	0.80	0.69	Severe
104	0.80	0.80	0.69	1.00	1	1.00	0.55	0.80	0.69	Severe
105	0.80	0.80	0.75	1.00	1	1.00	0.60	0.80	0.75	Severe
106	0.80	0.80	0.72	1.00	1	1.00	0.57	0.80	0.72	Severe

107	0.80	0.80	0.75	1.00	1	1.00	0.60	0.80	0.75	Severe
108	0.80	0.80	0.75	1.00	1	1.00	0.60	0.80	0.75	Severe
109	0.80	0.80	2.09	1.50	1	1.00	1.66	1.20	1.00	Collapse
110	0.80	0.80	1.23	1.50	1	1.00	0.98	1.20	0.82	Collapse
111	0.80	0.80	3.67	1.50	1	1.00	2.93	1.20	1.00	Collapse
112	0.80	0.80	1.91	1.25	1	1.00	1.53	1.00	1.00	Collapse
113	0.80	0.80	0.93	1.00	1	1.00	0.74	0.80	0.93	Collapse
114	0.80	0.80	2.52	1.50	1	1.00	2.01	1.20	1.00	Collapse
115	0.80	0.80	1.01	1.25	1	1.00	0.81	1.00	0.81	Collapse
116	0.80	0.80	0.99	1.50	1	1.00	0.79	1.20	0.66	Severe
117	0.80	0.80	6.53	2.25	0.42	1.00	2.19	1.80	1.00	Collapse
118	0.80	0.80	0.84	1.00	1	1.00	0.67	0.80	0.84	Collapse
119	0.80	0.80	0.89	1.00	1	1.00	0.71	0.80	0.89	Collapse
120	0.80	0.80	1.06	1.25	1	1.00	0.85	1.00	0.85	Collapse

Table 6.2 Calculation of EDRI of all Surveyed Buildings and EDRI of Koyna-Warna region

Structure	**EDRI Calculation for Surveyed RC Buildings**			**EDRI Calculation from Census Data**		
	No. of buildings	Sum of Risk	EDRI Vulnerable	Approx. No. of RC buildings	Sum of Risk	EDRI of Koyna-Warna region
RC-MRF	120	84.18	0.7	5500	3858	0.7

Based on the Table 6.1 & 6.2, exposure and vulnerability factors play an important role to enhance the seismic risk index of the building. These two are the controllable factors for the risk index of structures. Earthquake disaster risk index of surveyed RC buildings is 0.7 obtained by sum of risk of all buildings to the total number buildings and earthquake disaster risk index of Koyna-Warna region is also 0.7 which is obtained by the extrapolation of sum of risk based on the approximate number of existing RC buildings.

6.2.1 Damage states of RC buildings based on the EDRI method

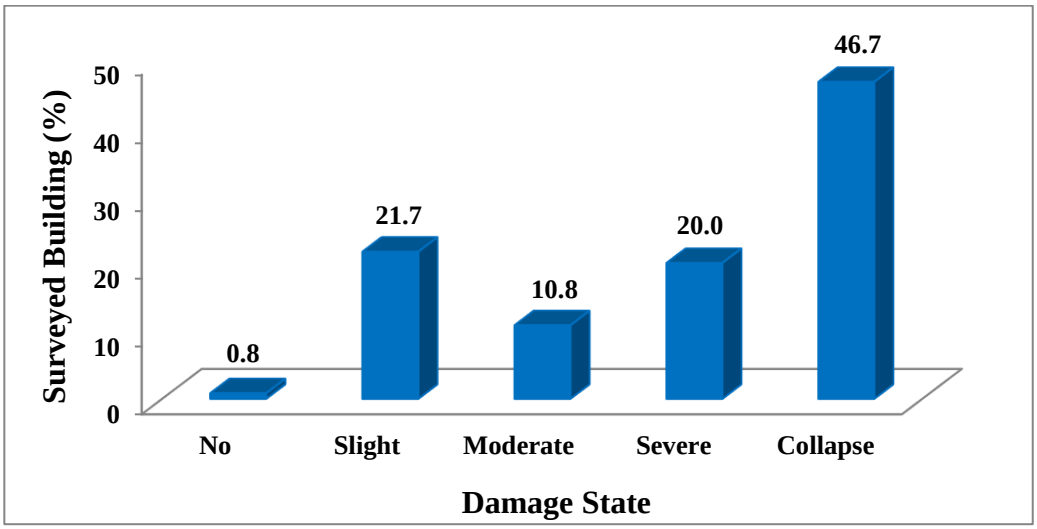

Figure 6.1 Damage states of RC buildings

Based on the study, it is found that the Koyna-Warna region has 46.7% of reinforced concrete sample buildings falling in the possible collapse category because, many buildings are constructed as a non-engineered in a hilly region, aging of structures, heavy rainfall conditions, etc. About 0.8 % and 21.7 % of sample buildings are falling in no damage and slight damage condition. The percentage of RC buildings in moderate and severe damage stage is 10.8 % and 20 % respectively. Also, irregular plan shapes, absence of continuous lintel bands, cracks in structural members, vegetation on the wall are the common observations in buildings that make them seismically more vulnerable.

6.2.2 Need for detailed evaluation of RC buildings

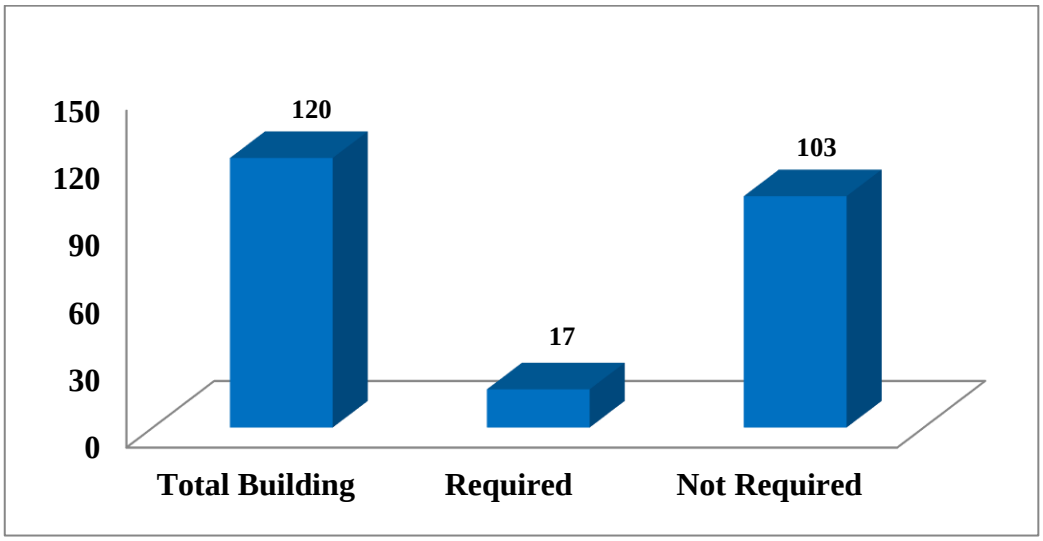

Figure 6.2 Requirement of detailed evaluation of RC buildings

Based on the EDRI results and IS 15988:2013 code, the buildings which are in moderate, severe, and collapse damage stage there is a need to go for a detailed evaluation except the single and double storey RC buildings having a total floor area less than 300 square meters. So there are seventeen RC buildings that need to go for a detailed evaluation out of 120 buildings.

6.2.3 Common structural and construction deficiencies and associated damages in RC buildings

The construction of RC buildings started after 1985. Even though the RC construction was started in early 1985, the engineered buildings are observed in only government quarters as per the design drawing and visual observation. Almost 80 % of existing RC buildings are either owner-built constructions constructed with the help of contractors by using thumb rules based on the discussion with owners, contractors & engineers. In the Koyna-Warna region the reinforced concrete buildings are constructed up to four & five storeys due to regional seismicity. Most of the buildings are being designed & built for gravity loads only. Architects play a major role in the design of buildings in this earthquake prone area. The government

buildings follow the earthquake resistant design philosophy. Most of the commercial buildings do not follow the FSI (Floor Space Index) rules as per the measured dimensions. The Koyna-Warna region is a hilly area so it is risky to construct mid-rise & high-rise buildings. All the government buildings constructed in this area are the mostly single or double storeyed. A nonstructural element such as shed is provided on the roof of each RC building. Common structural & construction deficiencies and associated damages as observed during the field visit are summarized in the following sections.

6.2.3.1 Soft Storey

(a) **(b)**

Figure 6.3 Open ground storey RC building constructed in Patan town

It is well known that soft storey (Open ground storey) failure in RC buildings is one of the major structural deficiencies. Most of the soft storey RC buildings collapsed during the Bhuj earthquake (2001) and hence, these buildings are more dangerous in the earthquake-prone area due to the absence of infills at the ground storey. In soft storey RC building, the ground storey is to be kept open for car parking purposes. In the field study, it was observed that one of the RC buildings is a soft storey building present in an earthquake-prone area (Patan town) as shown in Figure 6.3 and it is more vulnerable to earthquakes. As per the IS

13920: 2016, (ductile detailing code) minimum dimension of the column shall not be less than 300 mm. Here, we observed most of the columns having minimum dimensions are 230 mm in current construction practice which is not good for the building.

6.2.3.2 Vegetation on buildings

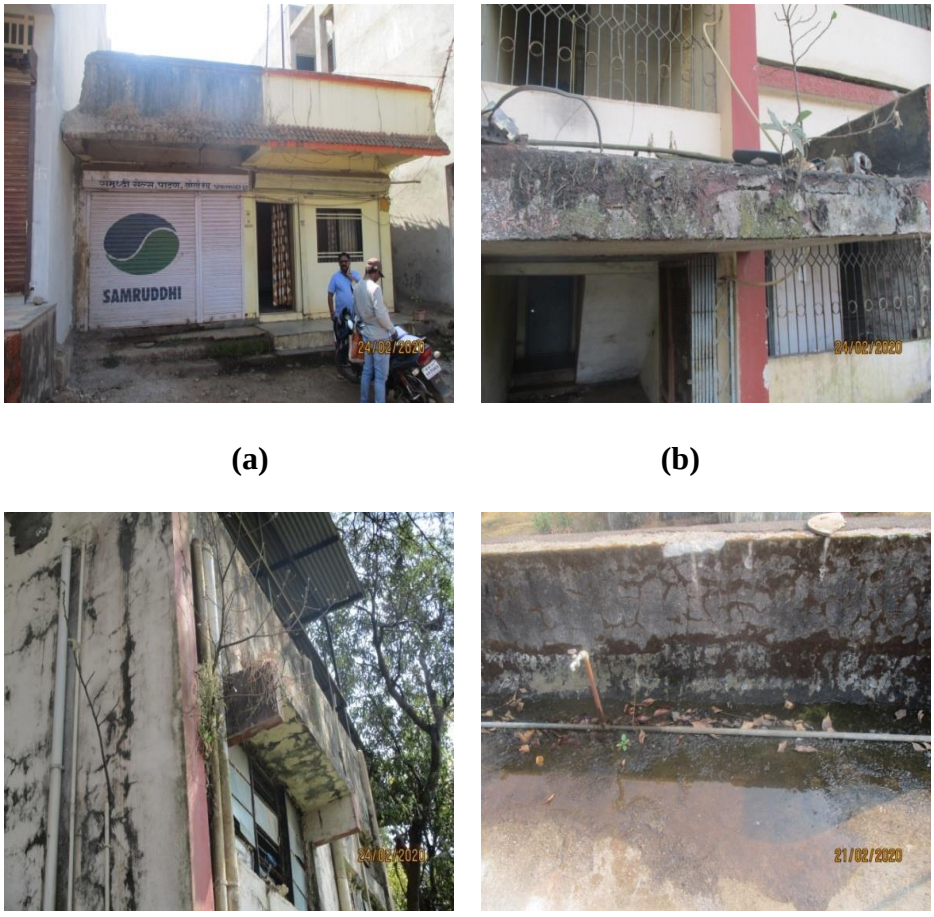

(a) **(b)**

(c) **(d)**

Figure 6.4 Growth of vegetation on roof, chajja, wall & parapet wall

Vegetation on the building is one of the major deficiencies observed. In the field study, we have observed that vegetation occurred on the roof, chajja, wall due to the heavy rainfall in this particular region as well as drainage pipe leakage. Initially, this vegetation seems to be in green color after a few months it appears to in brown color and ultimately it converts into black color. This vegetation may lead to the carbonation of concrete. The owner should carry

out maintenance of the building periodically to avoid such conditions. In this study, we observed such deficiency in many buildings as shown in Figure 6.4.

6.2.3.3 Deterioration of structural elements

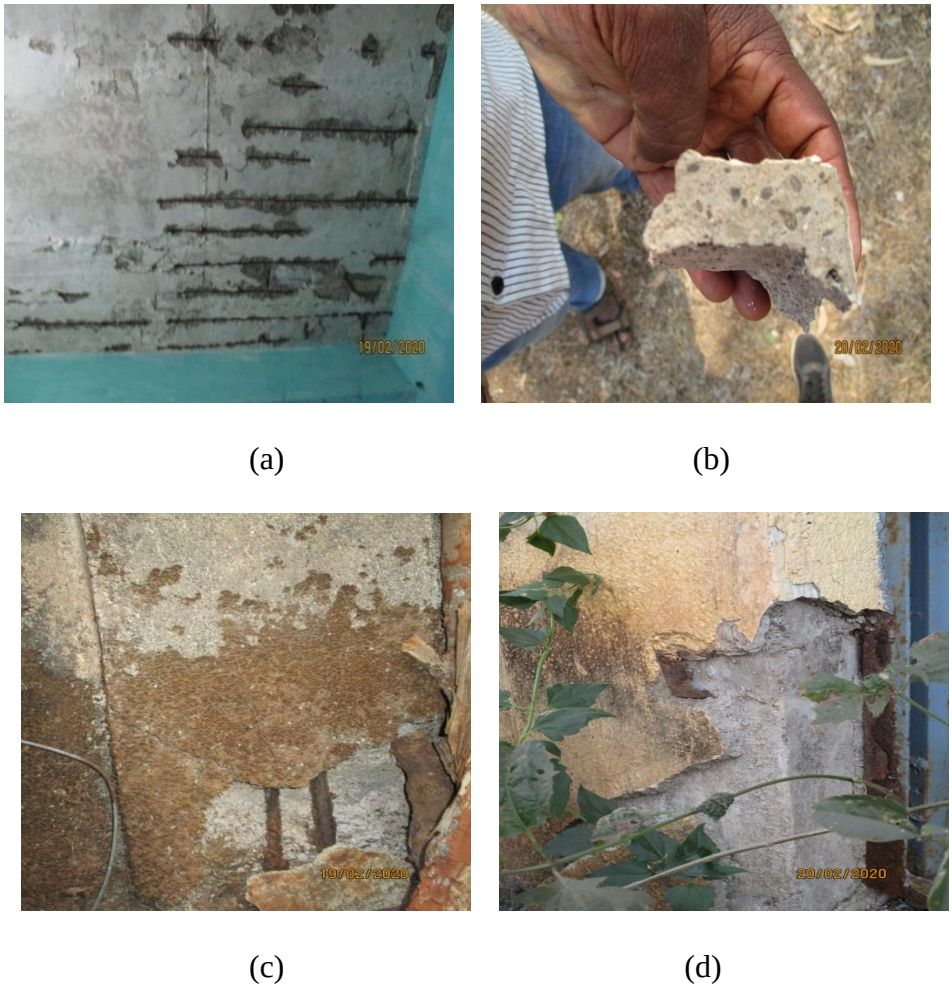

(a) (b)

(c) (d)

Figure 6.5 (a) Reinforcements are exposed out from slab, (b) Sample of cover concrete of column, (c) Corrosion of reinforcement, (d) Spalling of cover concrete

Structural elements are very important to maintain the overall structural integrity of the building. In the field study, we have observed the damage conditions of structural members like the spalling of cover concrete, corrosion of reinforcement. In many of the constructions, inadequate concrete cover is provided so due to less concrete cover provision reinforcements are exposed out & corroded. Similarly, in the case of slabs, we observed reinforcements are

corroded & exposed out due to many the reasons, *viz.*, material deterioration due to environmental conditions, poor quality of material & workmanship, also a provision of less concrete cover, etc. In this study, we have seen the concrete cover provided for the column is around 20 mm as shown in Figure 6.5 (b), and as per the Indian codal provisions, it should be 40 mm. So the structural failure is like a nightmare & it haunts the construction industry.

6.2.3.4 Building asymmetry & other deficiencies

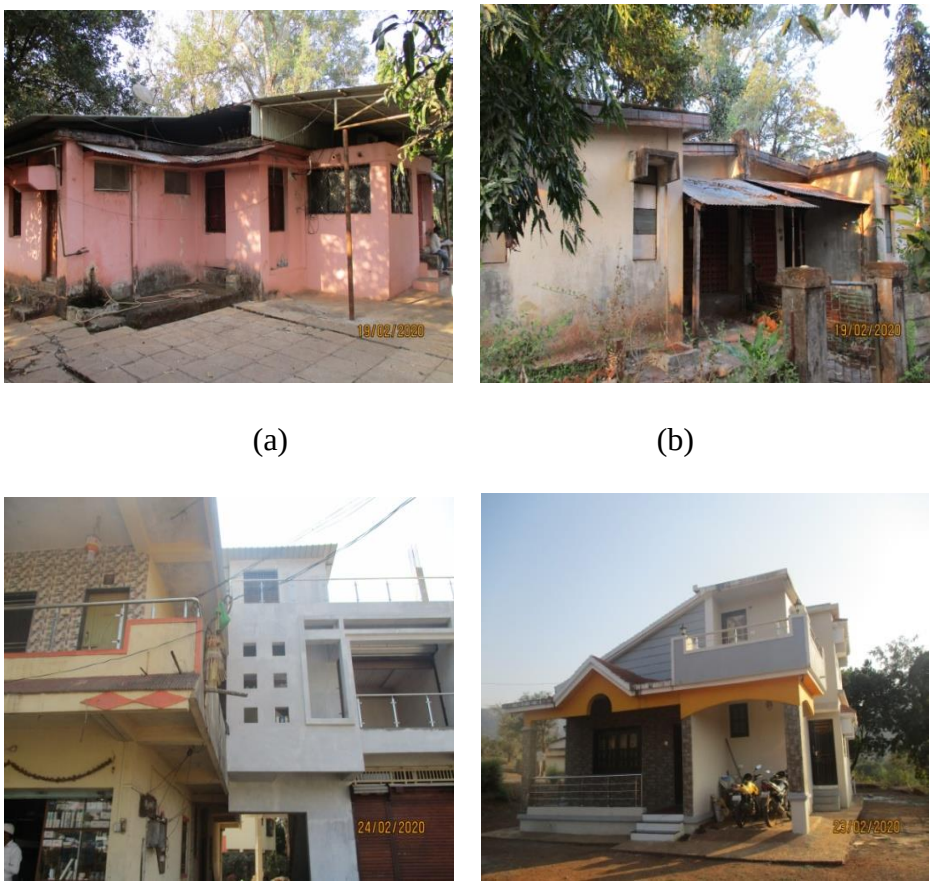

(a) (b)

(c) (d)

Figure 6.6 (a) Reentrant corner present in split roof structure, (b) Pitched roof structure, (c) Two RC buildings connected with each other, (d) Irregular structure

The geometrical configuration of the building is very important from an earthquake point of view. As per Figure 6.6, we have observed buildings having both plan irregularity and vertical

irregularity. The building must be symmetric in plan and should not have vertical irregularities to avoid the torsion effect. Also, the reentrant corners are present in most of the buildings. In the Koyna-Warna region, all the buildings are in a pitched roof style due to heavy rainfall conditions. Also, few buildings are in a split roof condition which is not good from an earthquake point of view. Frames don't have the symmetric lateral stiffness along both plan directions in most of the cases based on the observation. Few buildings are touching each other and so, there may be a possibility of a pounding effect in future earthquake events.

6.2.3.5 Cracks in buildings

(a)

(b)

(c)

(d)

(e) (f)

Figure 6.7 (a) Pop out of plaster, (b) horizontal crack propagate below the slab, (c) Shear crack at the corner of window, (d) Shrinkage cracks on wall, (e) Diagonal shear crack on column, (f) Crack on the junction of column and wall

Crack propagation is the initiation point of the failure of any structure. In this field study, we have observed different kinds of cracks in the buildings. Out of that, few are structural and the remaining are nonstructural cracks. Many columns of buildings are observed with a structural crack which is most probably a diagonal shear crack due to inadequate stirrups spacing. Peeling of plaster on the wall was observed due to dampness**.** Shrinkage cracks are also observed on the wall. Horizontal crack propagation below the slab was observed due to the deflection of the slab or corrosion of reinforcement in the beam. Vertical cracks were observed at the junction of wall and column due to the improper bond between the frame & infill. Shear cracks were observed at the corner of the opening for windows due to the concentration of stresses. All the observed cracks are shown in Figure 6.7

6.2.3.6 Settlement of buildings

(a) **(b)**

(c) **(d)**

Figure 6.8 (a) Buildings constructed on hill top (b) Backside portion of building (c) Collapsed wall due to settlement of soil, (d) Corner column foundation slightly damaged & loss of upper soil strata up to the foundation depth

Settlement of a building is a common geotechnical problem. In the field study, we have observed one commercial building is constructed in the hilly region & the behind portion of the building in a valley region. The backside ground portion of the building is settled moderately due to the loss of strength of soil. So the corner column foundation was slightly damaged & the temporary constructed infill wall was damaged completely. The major crack propagated through the ground due to the settlement problem. Some defects of a building is shown in Figure 6.8

6.2.3.7 Reinforcement in structural members

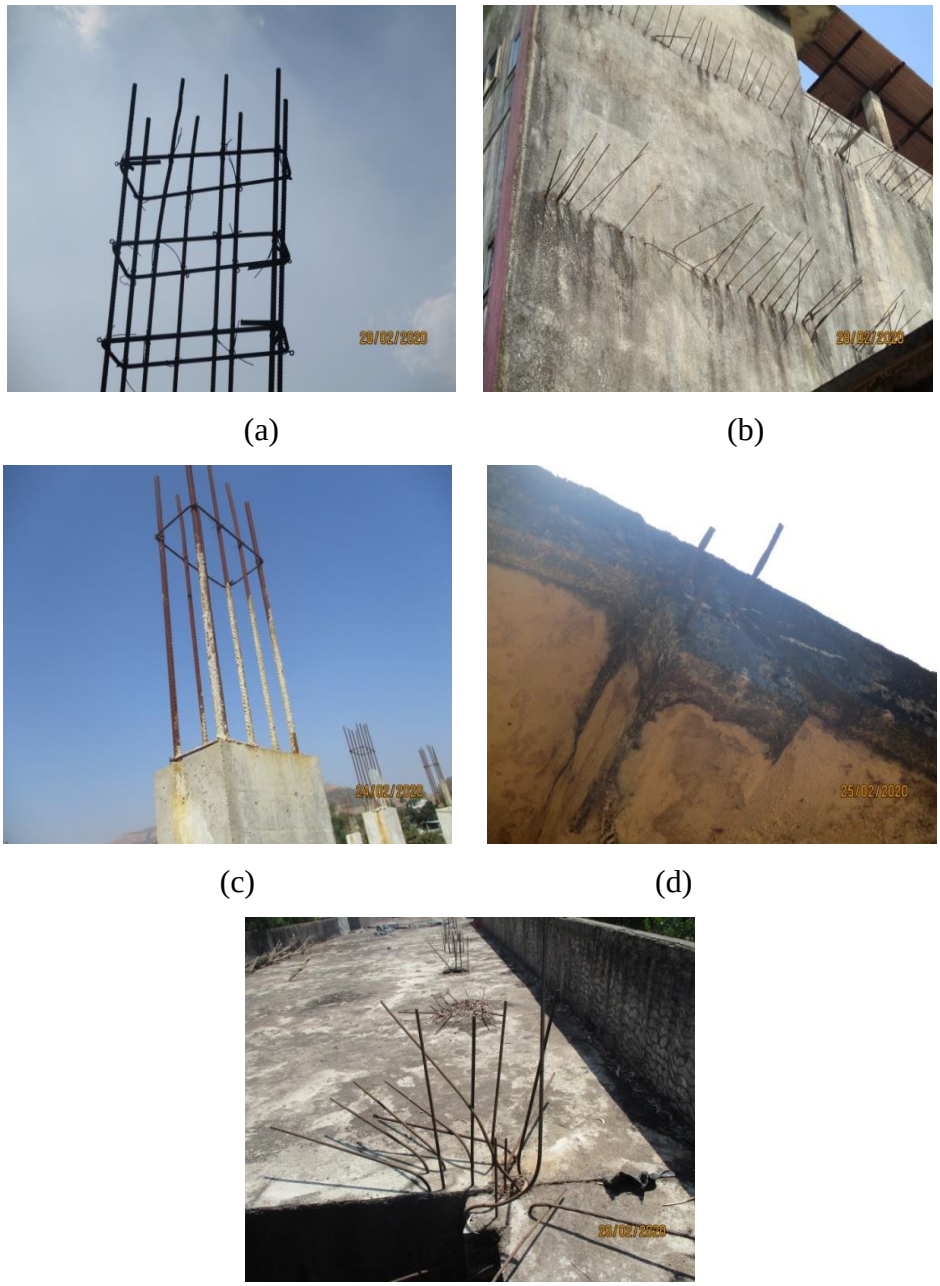

(a) (b)

(c) (d)

(e)

Figure 6.9 (a) Reinforcements are exposed to environment at terrace & stirrups bent at 90º (b) Reinforcements are exposed to environment at roof level (c) Corroded reinforcement bars, (d) Reinforcements are exposed from beam, (e) Condition of reinforcement bars at terrace.

Reinforcement is the most important building material. In field study, we have observed reinforcement bars are kept open at the terrace as well as roof level in most of the buildings so the bars get corroded due to exposure to the environment. Stirrups bend provision in column & beam is 90º based on the discussion with local engineers & contractors. As per the ductile detailing code, stirrups should be bent in 135°. Relevant Pictures of the reinforcements are shown in Figure 6.9

6.2.3.8 Damage conditions of buildings

(a) (b) (c)

(d) (e) (f)

Figure 6.10 Damage conditions of sample buildings

Figure 6.10 shows the different damage conditions of surveyed sample buildings. The slab leakage problem is observed almost in all buildings due to heavy rainfall. Structural cracks on the column, corroded reinforcement & spalling of cover concrete observed in columns, reinforcements are exposed out from slab, scaling of plaster, etc. There might be possible carbonation of concrete in the slabs, and columns of old buildings.

Based on the observation, it can be observed that damages occurred in current construction practices due to the following deficiencies:

1. Poor workmanship and rare maintenance of RC buildings.
2. Aging of structures.
3. The lesser concrete cover was provided to structural members.
4. Corrosion of reinforcement in structural members.
5. 90° hook is provided in the stirrups instead of 135° (IS 13920:2016 code)
6. The reduced strength of the column due to the deterioration of material.

6.2.3.9 Non-destructive tests on existing RC buildings

(a) (b)

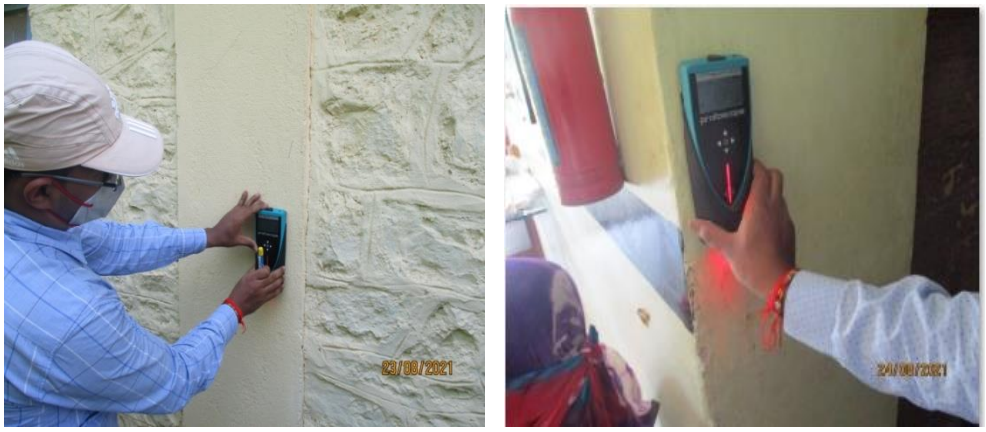

(c) (d)

Figure 6.11 Non-destructive tests on existing RC buildings

The non-destructive tests were carried out on existing RC buildings while doing the present study. Two types of non-destructive tests were conducted, *viz.,* rebound hammer and rebar locator. Rebound hammer is used to check the compressive strength of concrete and relar locator machine is used to detect the reinforcement diameter and concrete cover of structural members as shown in Figure 6.11.

6.3 Detailed seismic investigation of existing RC buildings

The plan, elevation, and structural details of building model: 1-17 have been already provided in chapter 5. The 17 deficient buildings have been analyzed by using SeismoStruct software. For each building capacity curves, damage patterns, and seismic design parameters have been developed to carry out the detailed seismic investigation towards determining the appropriate retrofitting measures.

6.3.1 Seismic investigation of model-1

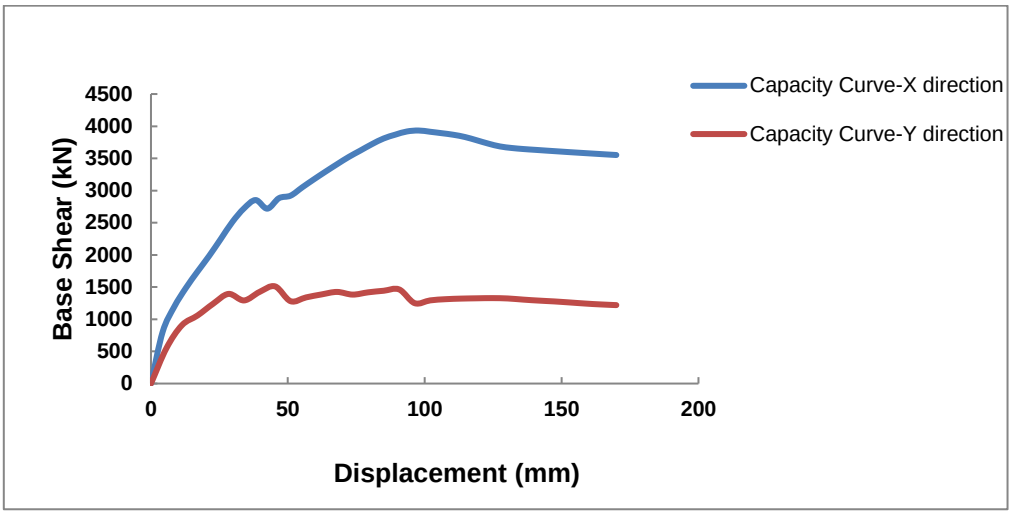

Figure 6.12 Capacity curves of model-1

As shown in Figure 6.12, the ultimate capacity of the building is higher in the X direction as compared to Y direction due to the structural configuration of building, and the remaining parameters are discussed in Table 6.3. The performance points of model-1 in X and Y direction are shown in Table 6.4 for life safety and collapse prevention purpose.

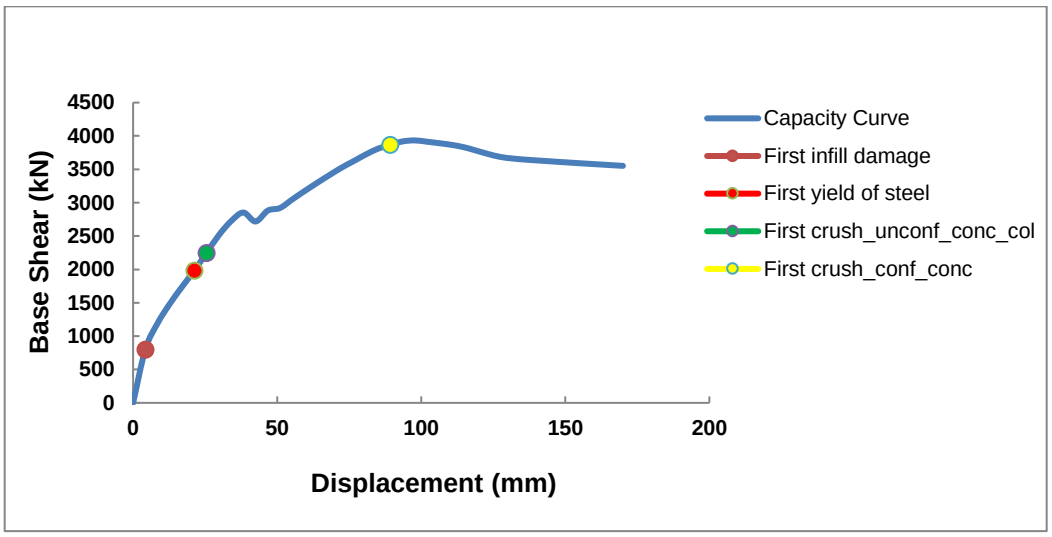

Figure 6.13 Damage pattern of model-1 in X direction

Figure 6.13 shows the damage pattern of model-1 in X direction. The first infill damage occurred at a base shear of 801.10 kN and a displacement of 4.25 mm. The first yielding of steel occurred at a base shear of 1983.86 kN and a displacement of 21.25 mm. The first crushing of the unconfined concrete column occurred at a base shear of 2247.24 kN and a displacement of 25.5 mm. And the first crushing of confined concrete occurred at a base shear of 3868.66 kN and a displacement of 89.25 mm.

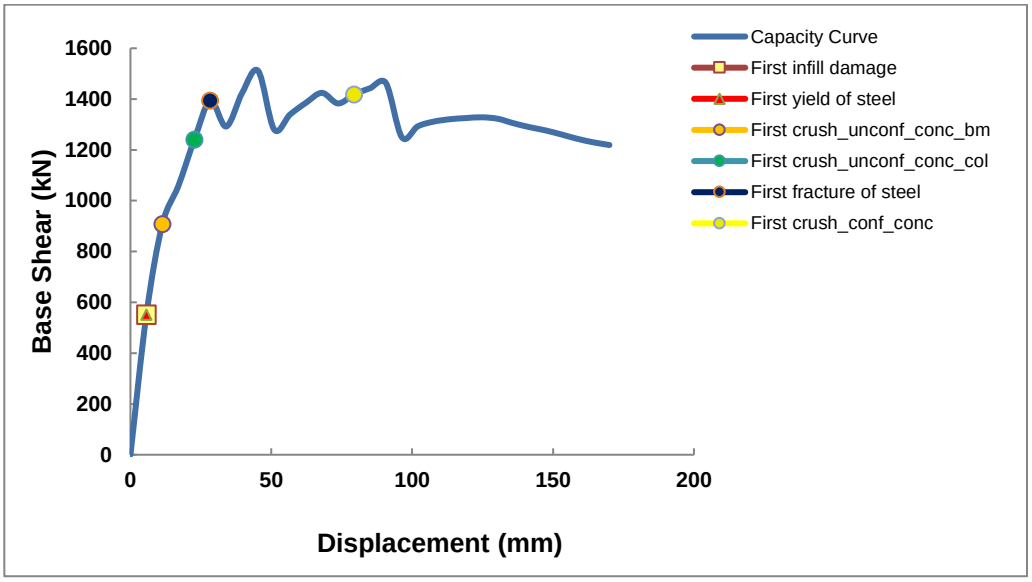

Figure 6.14 Damage pattern of model-1 in Y direction

Figure 6.14 shows the damage pattern of model-1in Y direction. The first infill damage and the first yielding of steel occurred at a base shear of 551.28 kN and a displacement of 5.67 mm. The first crushing of the unconfined concrete beam occurred at a base shear of 907.55kN and a displacement of 11.33 mm. The first crushing of the unconfined concrete column occurred at a base shear of 1239.44 kN and a displacement of 22.67 mm, the first fracture of steel occurred at a base shear of 1393.48 kN and a displacement of 28.33 mm, and the first crushing of confined concrete occurred at a base shear of 1417.97 kN and a displacement of 79.33 mm.

Table 6.3 Comparison of different parameters of Model-1			
Parameters			Remarks
	In X-axis	In Y-axis	
Ultimate capacity(kN)	3933.15	1510.65	The ultimate capacity is increased by 2.60 times in X-axis as compared to Y-axis
Yield displacement (mm)	26.40	13.10	The yield displacement is decreased by 50.37% in Y-axis as compared to X-axis
Maximum Displacement (mm)	97.75	45.33	The maximum displacement is decreased by 53.62 % in Y-axis as compared to X-axis
Ductility	3.70	3.46	The ductility is decreased by 6.48 % in Y-axis as compared to X-axis
Ductility Reduction Factor	2.53	2.43	The ductility reduction factor is decreased by 3.95 % in Y-axis as compared to X-axis
Overstrength factor	7.77	2.99	The overstrength factor is increased by 159.86 % in X-axis as compared to Y-axis
Time period (sec)	0.39	0.39	The time period is same in X and Y direction
R-factor	9.82	3.63	The R-factor is increased by 170.52 % in X-axis as compared to Y-axis

Table 6.4 Performance points of Model-1in X and Y direction				
Performance level	Displacement (mm**)**		Corresponding Base Shear (kN)	
	X direction	Y direction	X direction	Y direction
Life Safety (LS)	10.62	12.07	1338.91	927.15
Collapse Prevention (CP)	18.22	25.96	1809.94	1328.97

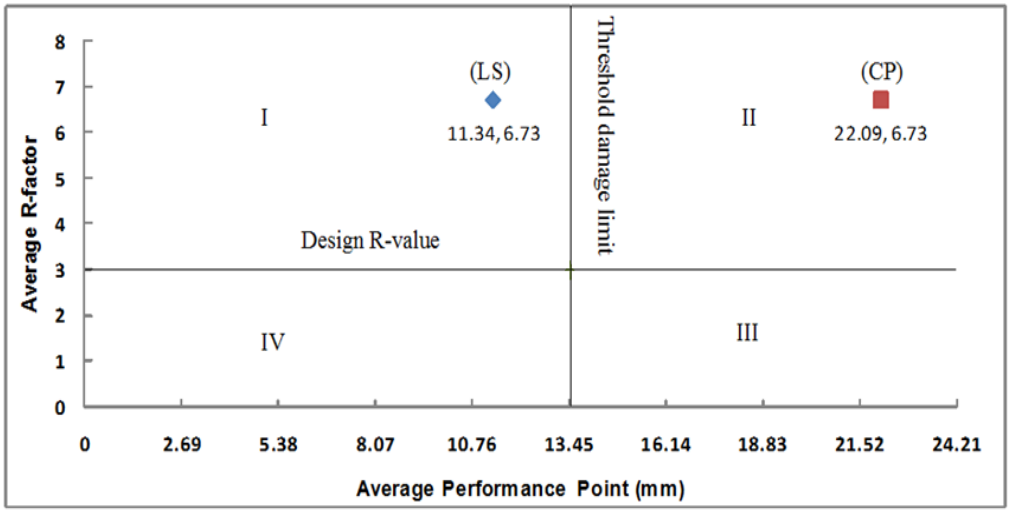

Figure 6.15 Average R-factor versus average performance point graph of model-1

Figure 6.15 shows the average R-factor versus average performance point graph of model-1. The point of intersection of R-factor and performance point for collapse prevention is located in IInd quadrant so there is a need to retrofit the building according to the "Quadrants assessment method".

6.3.2 Seismic investigation of model-2

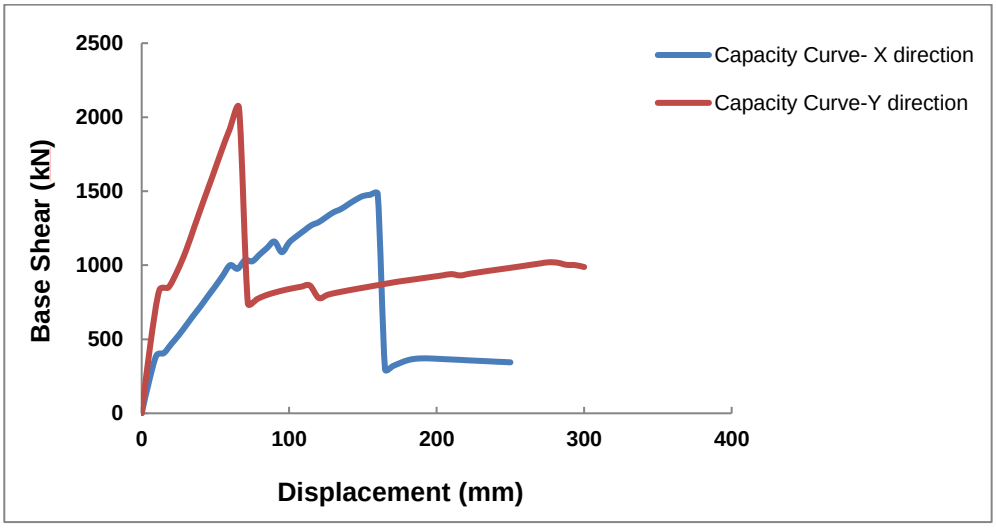

Figure 6.16 Capacity curves of model-2

As shown in Figure 6.16, the ultimate capacity of the building is higher in the Y direction as compared to X direction due to the structural configuration of building, and the remaining

parameters are discussed in Table 6.5. The performance points of model-2 in X and Y direction are shown in Table 6.6 for life safety and collapse prevention purpose.

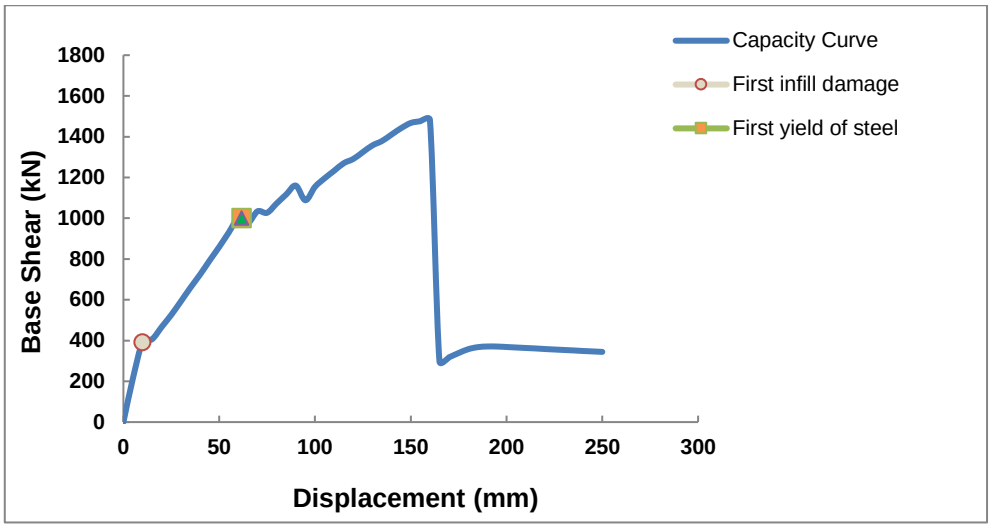

Figure 6.17 Damage pattern of Model-2 in the X direction

Figure 6.17 shows the damage pattern of model-2 in the X direction. The first infill damage occurred at a base shear 390.85 kN and displacement of 9.90 mm. The first yielding of steel occurred at a base shear 1000.78 kN and displacement of 61.76 mm and the first crushing of the unconfined concrete column occurred at base shear 1000.78 kN and displacement of 61.76 mm.

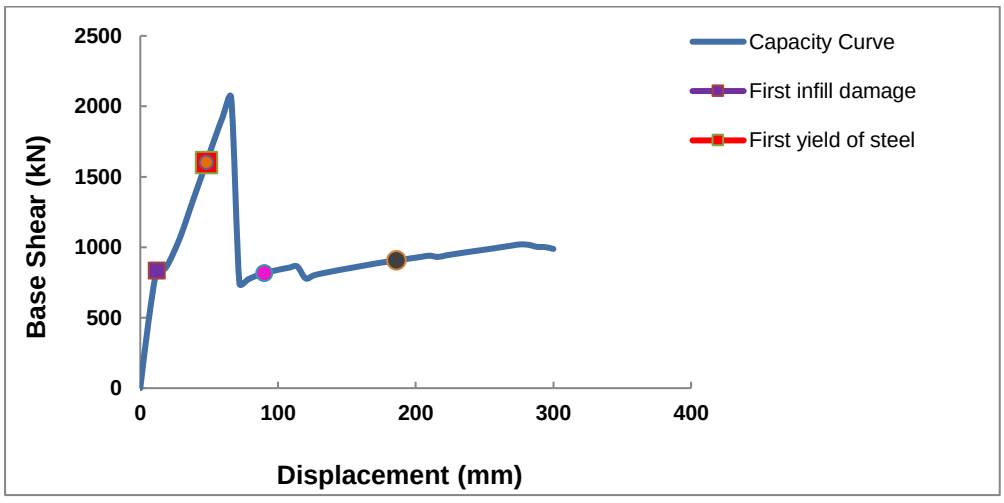

Figure 6.18 Damage pattern of Model-2 in the Y direction

Figure 6.18 shows the damage pattern of model-2 in the y direction. The first infill damage occurred at a base shear 833.03 kN and displacement of 12 mm. The first yielding of steel & the first crushing of the unconfined concrete column occurred at a base shear 1601.07 kN and displacement of 48 mm. The first crush of confined concrete occurred at base shear 814.94 kN and displacement of 90 mm and first fracture of steel occurred at base shear 906.21 kN and displacement of 186 mm.

Table 6.5 Comparison of different parameters of Model-2

Parameters			Remarks
	In X-axis	In Y-axis	
Ultimate capacity(kN)	1482.71	2060.55	The ultimate capacity is increasedby 1.38 times in Y-axis as compared to X-axis
Yield displacement (mm)	63.85	47.69	The yield displacementis decreased by 25.30% in Y-axis as compared to X-axis
Maximum Displacement (mm)	160	66.00	The maximum displacement is decreased by 58.75 % in Y-axis as compared to X-axis
Ductility	2.51	1.38	The ductility is decreased by 45.02 % in Y-axis as compared to X-axis
Ductility Reduction Factor	2.00	1.33	The ductility reduction factor is decreased by 33.5 % in Y-axis as compared to X-axis
Overstrength factor	5.26	7.31	The overstrength factor is increased by 38.97 % in Y-axis as compared to X-axis
Time Period (sec)	0.41	0.41	The time period is same in X and Y direction
R-factor	5.26	4.86	The R-factor is increased by 8.23 % in X-axis as compared to Y-axis

Table 6.6 Performance points of Model-2 in X and Y direction				
Performance level	Displacement (mm)		Corresponding Base Shear (kN)	
	X direction	Y direction	X direction	Y direction
Life Safety	16.5	14.49	424.58	839.58
Collapse Prevention	27.13	23.44	554.19	947.49

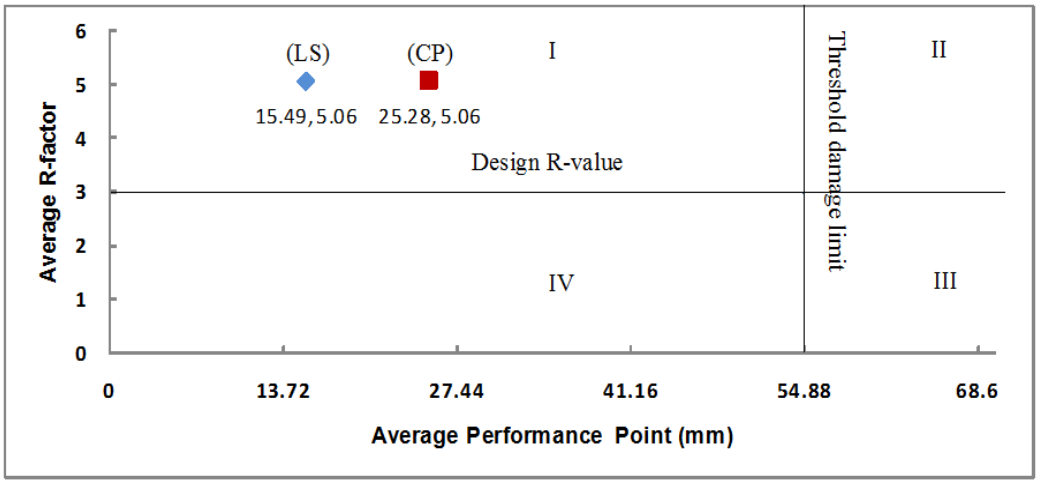

Figure 6.19 Average R-factor versus average performance point graph of model-2

Figure 6.19 shows the average R-factor versus average performance point graph of model-2. The point of intersection of R-factor and performance point for life safety & collapse prevention is located in Ist quadrant so there is no need to retrofit the building according to the "Quadrants assessment method".

6.3.3 Seismic investigation of model-3

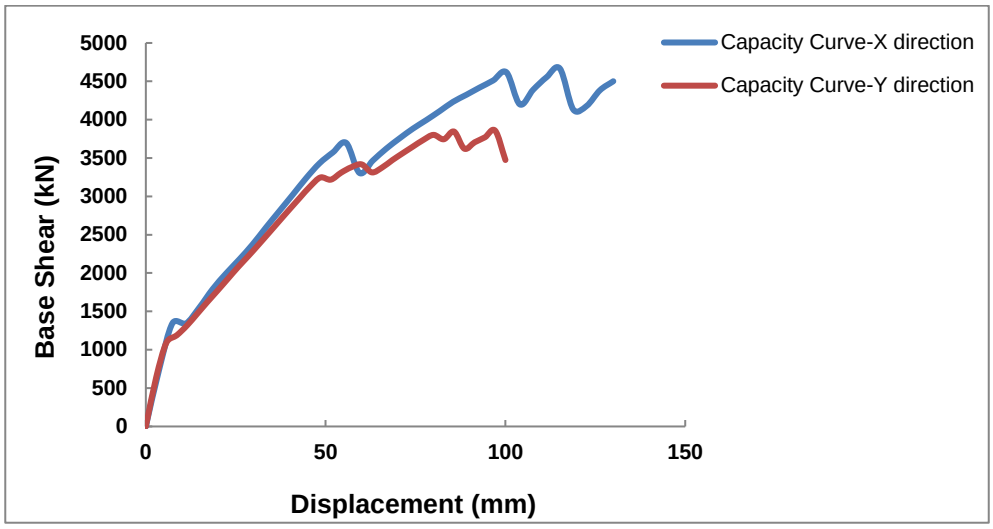

Figure 6.20 Capacity curves of model-3

As shown in Figure 6.20, the ultimate capacity of the building is higher in the X direction as compared to Y direction due to the structural configuration of building, and the remaining parameters are discussed in Table 6.7. The performance points of model-3 in X and Y direction are shown in Table 6.8 for life safety and collapse prevention purpose.

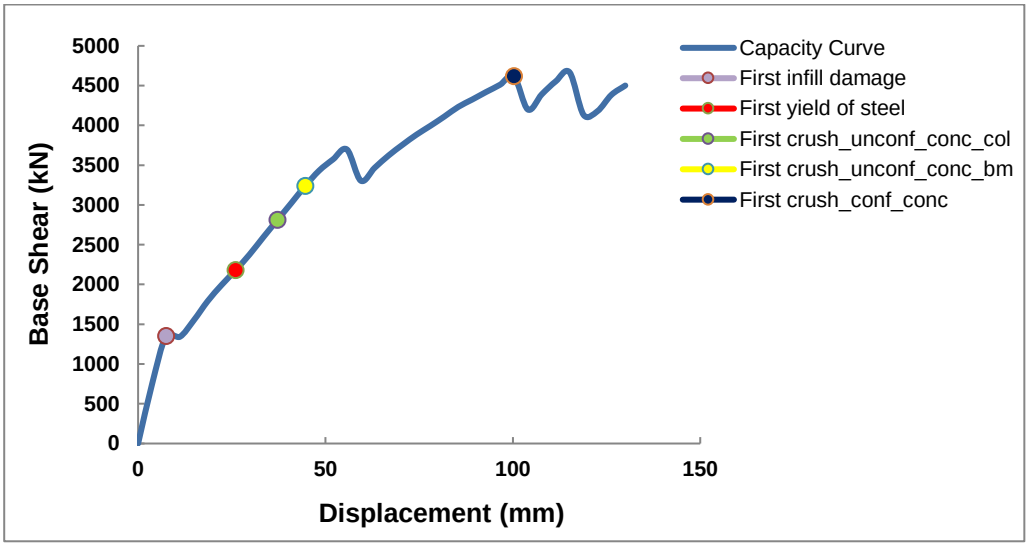

Figure 6.21 Damage pattern of Model-3 in the X direction

Figure 6.21 shows the damage pattern of model-3 in the X direction. The first infill damage occurred at a base shear 1348.41kN and displacement of 7.43 mm. The first yielding of steel occurred at a base shear 2178.67 kN and displacement of 26 mm. The first crushing of the unconfined concrete column occurred at base shear 2809.10 kN and displacement of 37.14 mm. The first crushing of the unconfined concrete beam occurred at base shear 3237.65 kN and displacement of 44.57 mm, and the first crushing of confined concrete occurred at base shear 4618.11 kN and displacement of 100.29 mm.

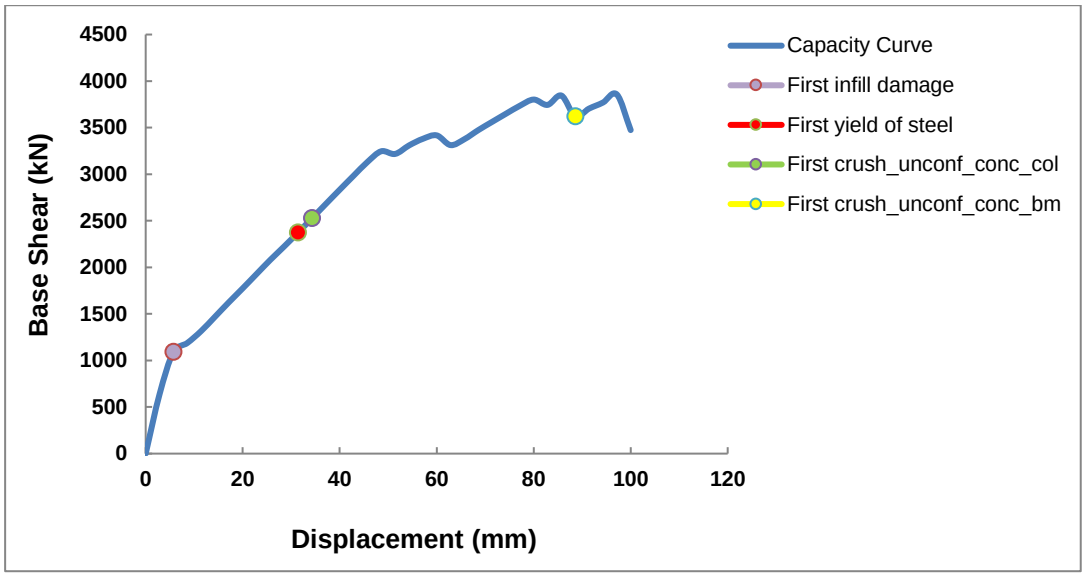

Figure 6.22 Damage pattern of Model-3 in the Y direction

Figure 6.22 shows the damage pattern of model-3 in the Y direction. The first infill damage occurred at a base shear 1091.62 kN and displacement of 5.71 mm. The first yielding of steel occurred at a base shear 2374.34 kN and displacement of 31.43 mm. The first crushing of the unconfined concrete column occurred at base shear 2527.10 kN and displacement of 34.29 mm, and the first crushing of the unconfined concrete beam occurred at base shear 3621.97 kN and displacement of 88.57 mm.

Table 6.7 Comparison of different parameters of Model-3			
Parameters			Remarks
	In X-axis	In Y-axis	
Ultimate capacity(kN)	4667.1	3857.04	The ultimate capacity increases by 1.21 times in X-axis as compared to Y-axis
Yield displacement (mm)	43.50	40.14	The yield displacement decreases by 7.72 % in Y-axis as compared to X-axis
Maximum Displacement (mm)	115.14	97.14	The maximum displacement decreases by 15.63 % in Y-axis as compared to X-axis
Ductility	2.65	2.42	The ductility decreases by 8.67 % in Y-axis as compared to X-axis
Ductility Reduction Factor	2.07	1.96	The ductility reduction factor decreases by 5.31 % in Y-axis as compared to X-axis
Overstrength factor	6.11	5.05	The overstrength factor increases by 21% in X-axis as compared to Y-axis
Time Period (sec)	0.36	0.36	The time period is same in X and Y direction
R-factor	6.32	4.95	The R-factor increases by 27.67 % in X-axis as compared to Y-axis

Table 6.8 Performance points of Model-3 in X and Y direction				
Performance level	Displacement (mm**)**		Corresponding Base Shear (kN)	
	X direction	Y direction	X direction	Y direction
Life Safety	11.52	11.61	1342.10	1316
Collapse Prevention	20.02	20.73	1870.09	1813.71

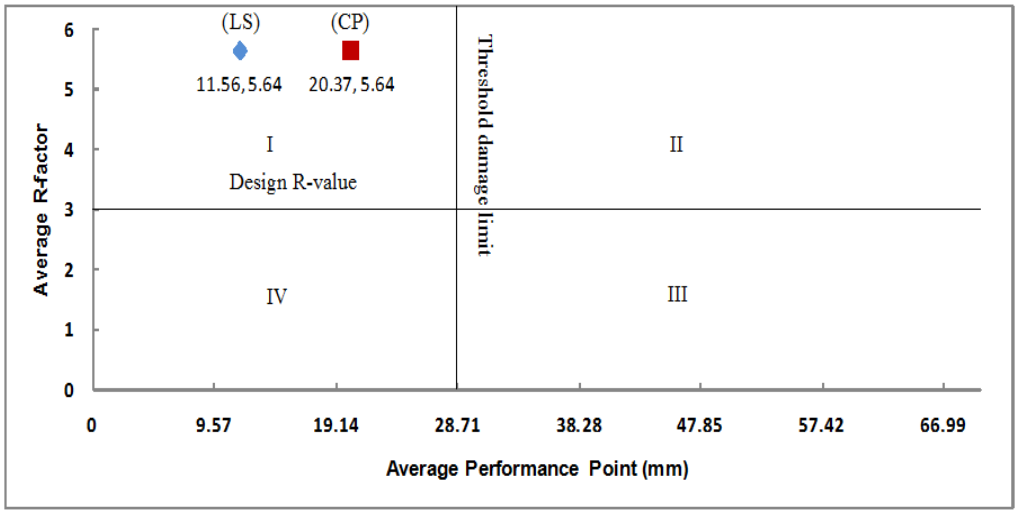

Figure 6.23 Average R-factor versus average performance point graph of model-3

Figure 6.23 shows the average R-factor versus average performance point graph of model-3. The point of intersection of R-factor and performance point for life safety & collapse prevention is located in Ist quadrant so there is no need to retrofit the building according to the "Quadrants assessment method".

6.3.4 Seismic investigation of model-4

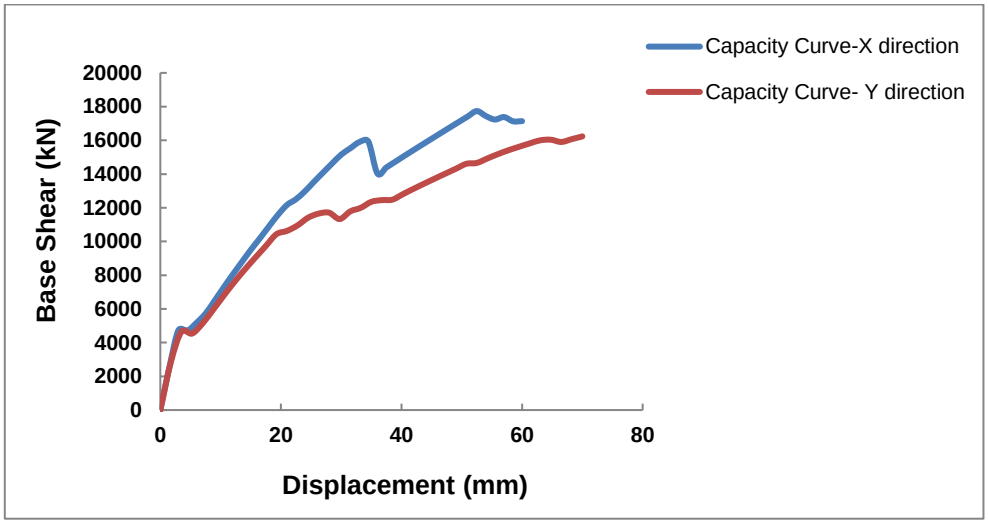

Figure 6.24 Capacity curves of model-4

As shown in Figure 6.24, the ultimate capacity of the building is higher in the X direction as compared to the Y direction due to the structural configuration of the building, and the remaining parameters are discussed in Table 6.9. The performance points of model-4 in X and

Y direction are shown in Table 6.10 for life safety and collapse prevention purpose.

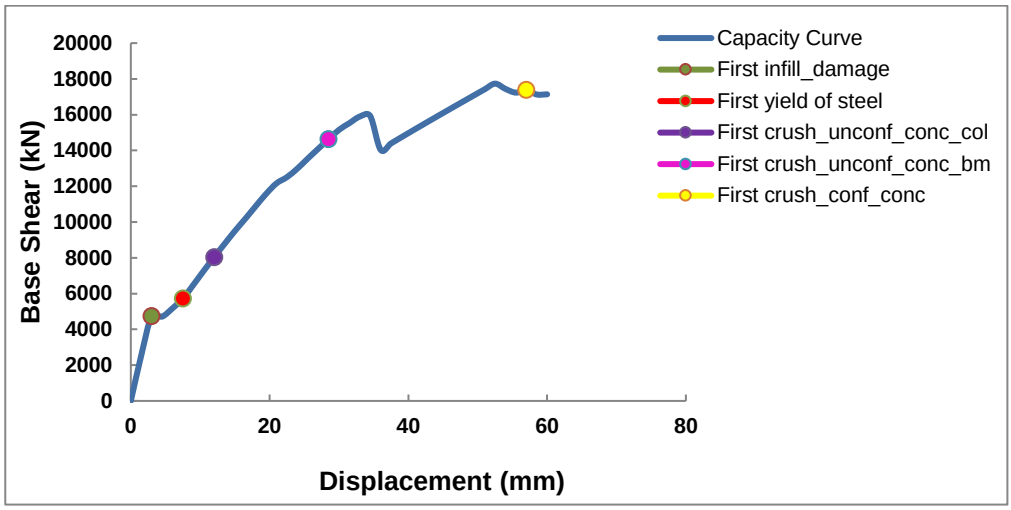

Figure 6.25 Damage pattern of Model-4 in the X direction

Figure 6.25 shows the damage pattern of model-4 in the X direction. The first infill damage occurred at a base shear 4734.32 kN and displacement of 3 mm. The first yielding of steel occurred at a base shear 5721.94 kN and displacement of 7.50 mm. The first crushing of the unconfined concrete column occurred at base shear 8030.94 kN and displacement of 12 mm. The first crushing of the unconfined concrete beam occurred at base shear 14629.58 kN and displacement of 28.50 mm, and the first crushing of confined concrete occurred at base shear 17381.19 kN and displacement of 57 mm.

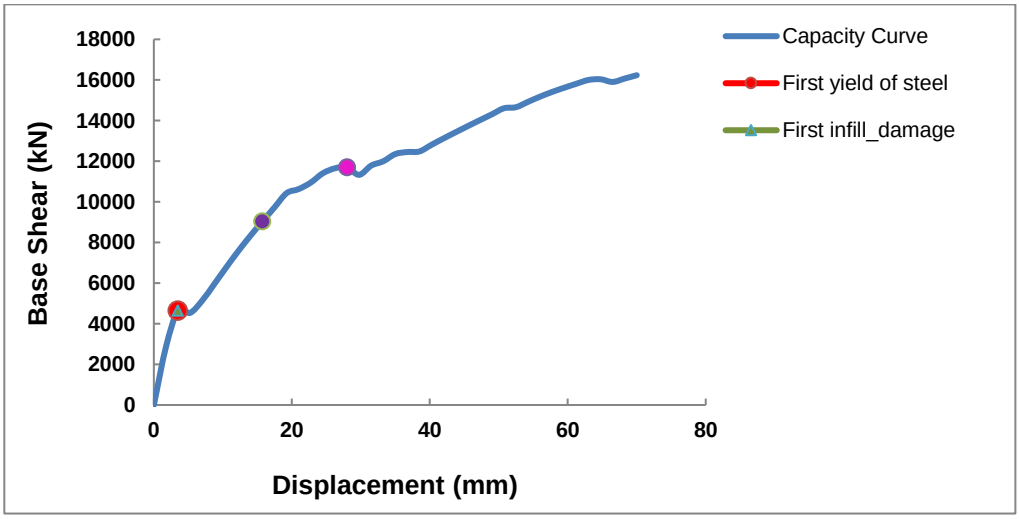

Figure 6.26 Damage pattern of Model-4 in the Y direction

Figure 6.26 shows the damage pattern of model-4 in the Y direction. The first infill damage & the first yielding of steel occurred at a base shear 4649.33 kN and displacement of 3.50 mm. The first crushing of the unconfined concrete column occurred at base shear 9040.66 kN and displacement of 15.75 mm, and the first crushing of the unconfined concrete beam occurred at base shear 11706.41 kN and displacement of 28 mm.

Table 6.9 Comparison of different parameters of Model-4

Parameters			Remarks
	In X-axis	In Y-axis	
Ultimate capacity(kN)	17735.47	16232.99	The ultimate capacity increases by 1.09 times in X-axis as compared to Y-axis
Yield displacement (mm)	23.01	19.76	The yield displacement decreases by 14.12% in Y-axis as compared to X-axis
Maximum Displacement (mm)	52.5	70	The maximum displacement increases by 33.33 % in Y-axis as compared to X-axis
Ductility	2.28	3.54	The ductility increases by 55.26% in Y-axis as compared to X-axis
Ductility Reduction Factor	1.00	1.00	The ductility reduction factor is same in X-axis and Y-axis
Overstrength factor	16.11	14.74	The overstrength factor decreases by 8.50% in Y-axis as compared to X-axis
Time period (sec)	0.13	0.13	The time period is same in X and Y direction
R-factor	8.05	7.37	The R-factor increases by 9.22% in X-axis as compared to Y-axis

Table 6.10 Performance points of model-4 in X and Y direction				
Performance level	Displacement (mm)		Corresponding Base Shear (kN)	
	X direction	Y direction	X direction	Y direction
Life Safety	1.88	1.87	3094.82	2969.42
Collapse Prevention	2.28	2.25	3680.36	3361.05

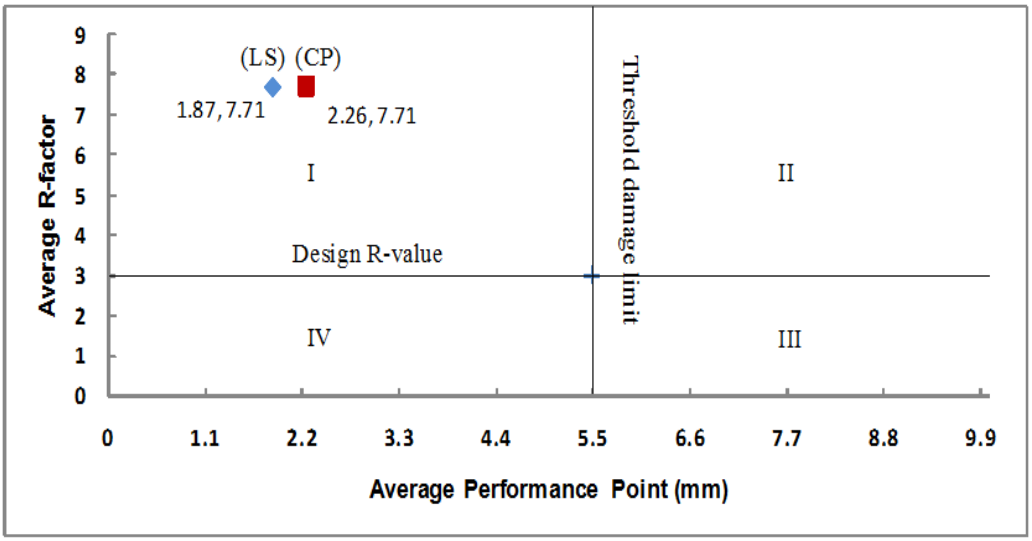

Figure 6.27 Average R-factor versus average performance point graph of model-4

Figure 6.27 shows the average R-factor versus average performance point graph of model-4. The point of intersection of R-factor and performance point for life safety & collapse prevention is located in Ist quadrant so there is no need to retrofit the building according to the "Quadrants assessment method".

6.3.5 Seismic investigation of model-5

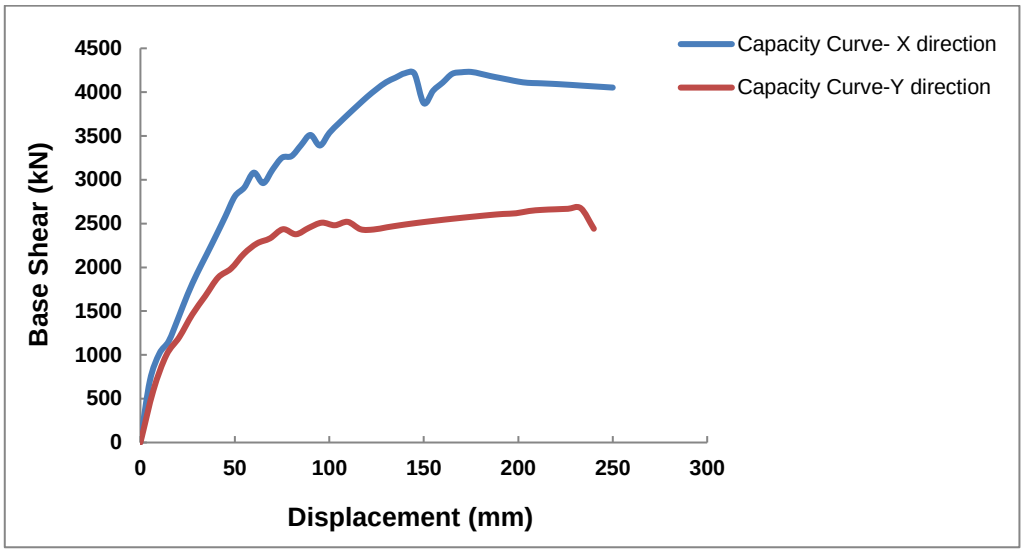

Figure 6.28 Capacity curves of model-5

As shown in Figure 6.28, the ultimate capacity of the building is higher in the X direction as compared to the Y direction due to the structural configuration of the building, and the remaining parameters are discussed in Table 6.11. The performance points of model-5 in X and Y direction are shown in Table 6.12 for life safety and collapse prevention purpose.

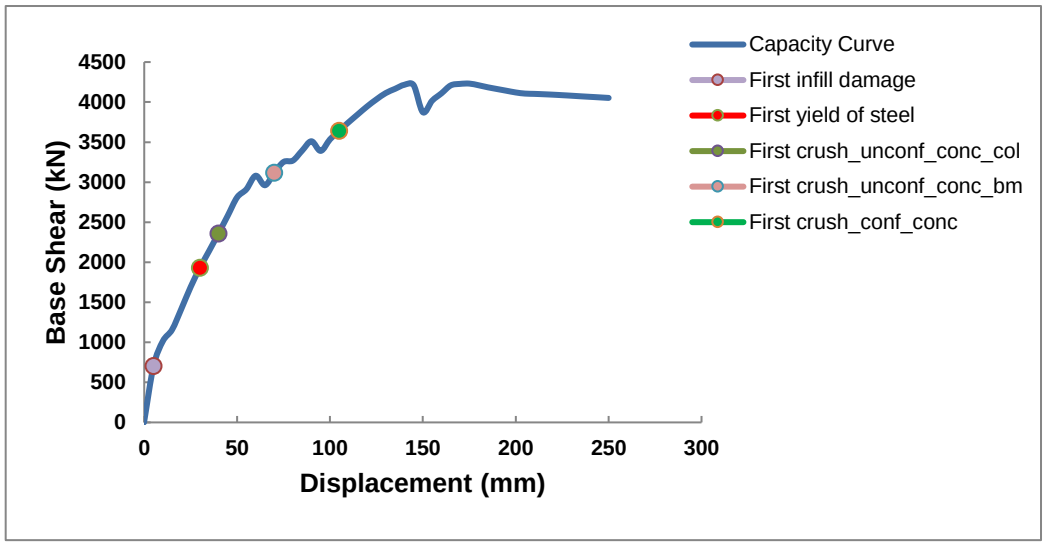

Figure 6.29 Damage pattern of Model-5 in the X direction

Figure 6.29 shows the damage pattern of model-5 in the X direction. The first infill damage occurred at a base shear 703.73 kN and displacement of 5 mm. The first yielding of steel occurred at a base shear 1930.38 kN and displacement of 30 mm. The first crushing of the unconfined concrete column occurred at base shear 2360.74 kN and displacement of 40 mm. The first crushing of the unconfined concrete beam occurred at base shear 3117.11kN and displacement of 70 mm, and the first crushing of confined concrete occurred at base shear 3643.89 kN and displacement of 105 mm.

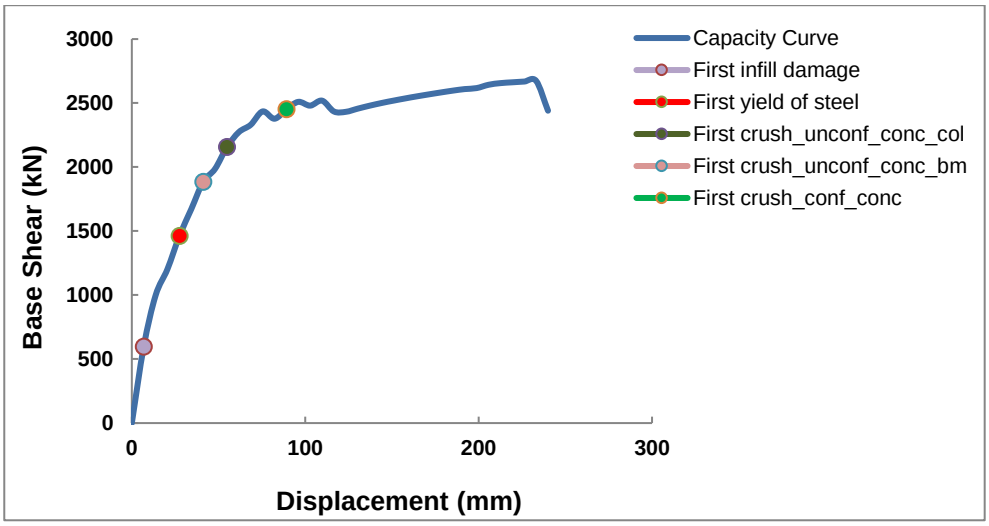

Figure 6.30 Damage pattern of Model-5 in the Y direction

Figure 6.30 shows the damage pattern of model-5 in the Y direction. The first infill damage occurred at a base shear 596.04 kN and displacement of 6.86 mm. The first yielding of steel occurred at a base shear 1460.93 kN and displacement of 27.43 mm. The first crushing of the unconfined concrete column occurred at base shear 2156.34 kN and displacement of 54.86 mm. The first crushing of the unconfined concrete beam occurred at base shear 1884.37 kN and displacement of 41.14 mm, and the first crushing of confined concrete occurred at base shear 2450.70 kN and displacement of 89.14 mm.

Table 6.11 Comparison of different parameters of Model-5			
Parameters			Remarks
	In X-axis	In Y-axis	
Ultimate capacity(kN)	4231.01	2673.60	The ultimate capacity increases by 1.58 times in X-axis as compared to Y-axis
Yield displacement (mm)	53.55	42.62	The yield displacement decreases by 20.41% in Y-axis as compared to X-axis
Maximum Displacement (mm)	175.00	233.14	The maximum displacement increases by 33.22 % in Y-axis as compared to X-axis
Ductility	3.27	5.47	The ductility increases by 67.27% in Y-axis as compared to X-axis
Ductility Reduction Factor	2.35	3.15	The ductility reduction factor increases by 34.04 % in Y-axis as compared to X-axis
Overstrength factor	8.07	5.10	The overstrength factor decreases by 36.80 % in Y-axis as compared to X-axis
Time period (sec)	0.33	0.33	The time period is same in X and Y direction
R-factor	9.48	8.03	The R-factor increases by 18.05 % in X-axis as compared to Y-axis

Table 6.12 Performance points of model-5 in X and Y direction				
Performance level	Displacement (mm**)**		Corresponding Base Shear (kN)	
	X direction	Y direction	X direction	Y direction
Life Safety	8.04	5.97	892.18	518.93
Collapse Prevention	14.10	12.78	1132.02	942.79

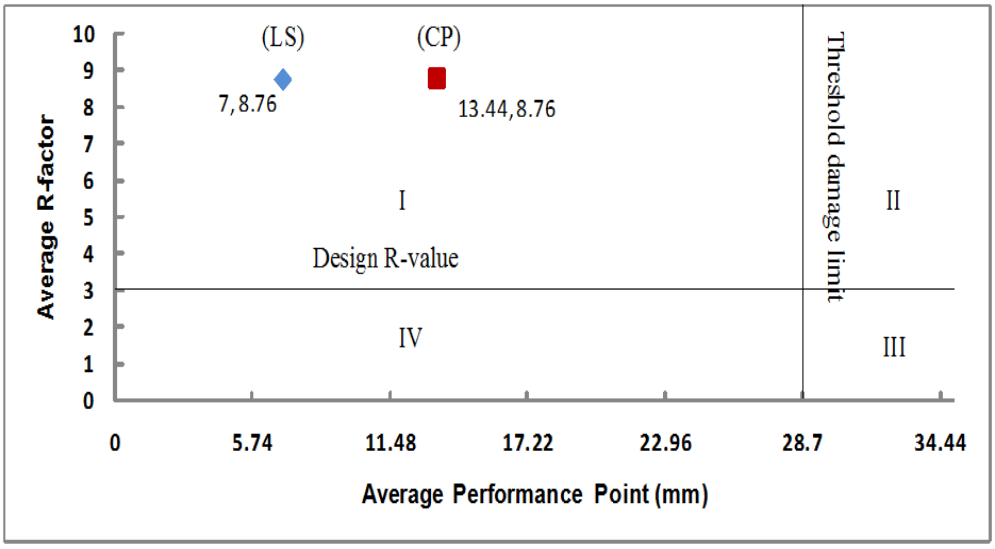

Figure 6.31 Average R-factor versus average performance point graph of model-5

Figure 6.31 shows the average R-factor versus average performance point graph of model-5. The point of intersection of R-factor and performance point for life safety & collapse prevention is located in Ist quadrant so there is no need to retrofit the building according to the "Quadrants assessment method".

6.3.6 Seismic investigation of model-6

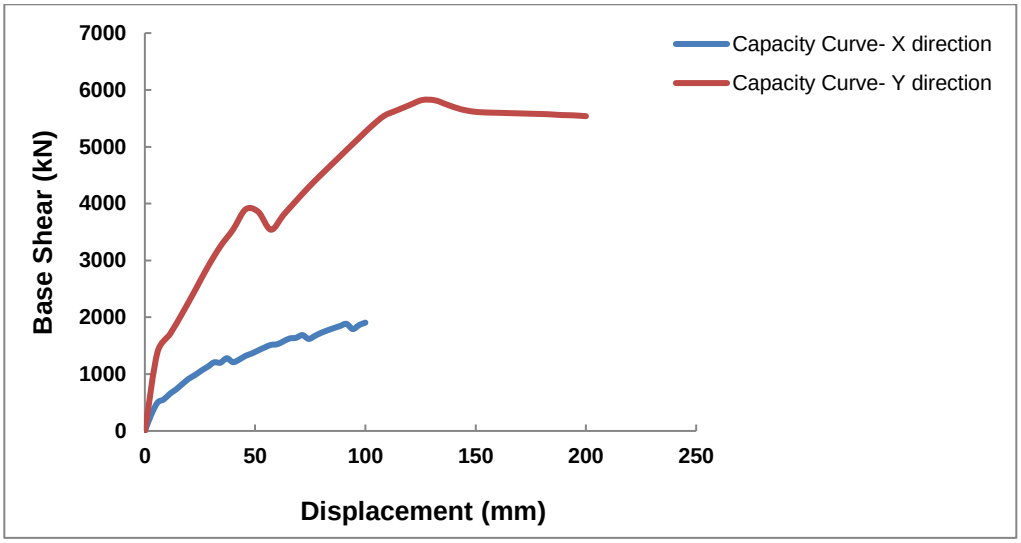

Figure 6.32 Capacity curves of model-6

As shown in Figure 6.32, the ultimate capacity of the building is higher in the Y direction as compared to the X direction due to the structural configuration of the building, and the remaining parameters are discussed in Table 6.13. The performance points of model-6 in X and Y direction are shown in Table 6.14 for life safety and collapse prevention purpose.

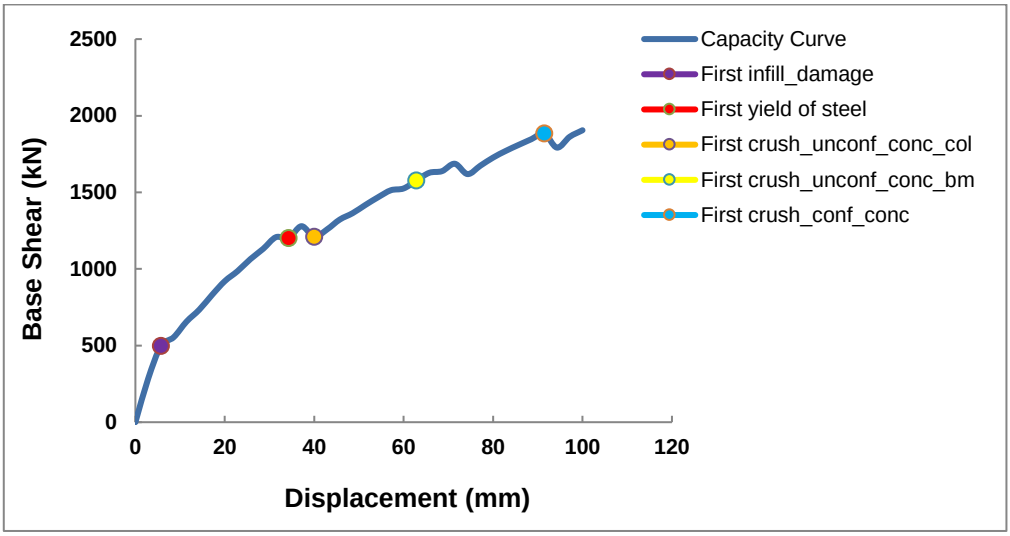

Figure 6.33 Damage pattern of Model-6 in the X direction

Figure 6.33 shows the damage pattern of model-6 in the X direction. The first infill damage occurred at a base shear 497.21kN and displacement of 5.71 mm. The first yielding of steel occurred at a base shear 1200.83 kN and displacement of 34.29 mm. The first crushing of the unconfined concrete column occurred at base shear 1209.32 kN and displacement of 40 mm. The first crushing of the unconfined concrete beam occurred at base shear 1577.12 kN and displacement of 62.86 mm, and the first crushing of confined concrete occurred at base shear 1884.38 kN and displacement of 91.43 mm.

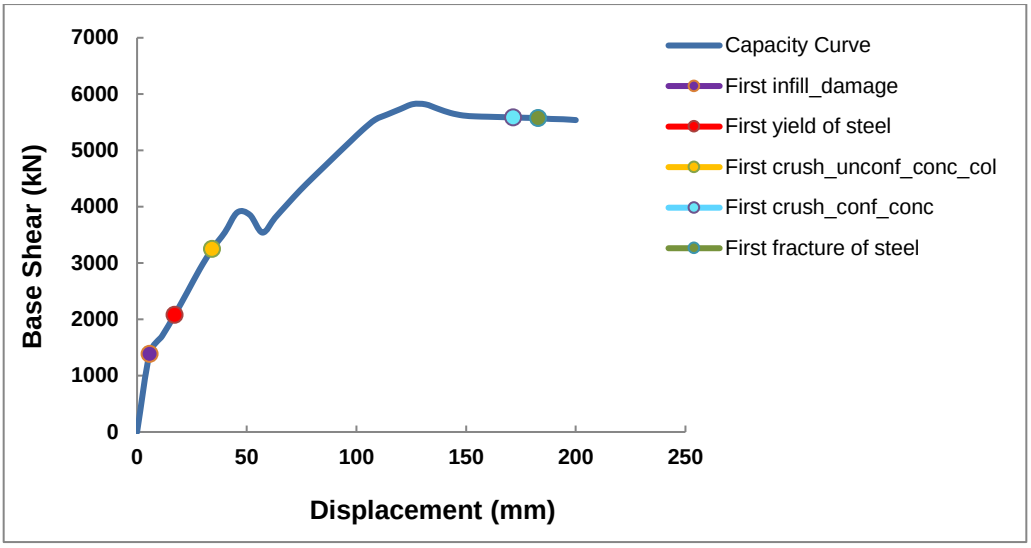

Figure 6.34 Damage pattern of Model-6 in the Y direction

Figure 6.34 shows the damage pattern of model-6 in the Y direction. The first infill damage occurred at a base shear 1384.37 kN and displacement of 5.71 mm. The first yielding of steel occurred at a base shear 2080.83 kN and displacement of 17.14 mm. The first crushing of the unconfined concrete column occurred at base shear 3250.53 kN and displacement of 34.29 mm. First crushing of confined concrete occurred at base shear 5585.46 kN and displacement of 171.43mm. And, the first fracture of steel occurred at a base shear 5572.67 kN and displacement of 182.86 mm.

Table 6.13 Comparison of different parameters of Model-6			
Parameters			Remarks
	In X-axis	In Y-axis	
Ultimate capacity(kN)	1905.09	5821.58	The ultimate capacity increases by 3.05 times in Y-axis as compared to X-axis
Yield displacement (mm)	25.65	30.77	The yield displacement decreases by 16.63% in X-axis as compared to Y-axis
Maximum Displacement (mm)	100.00	125.71	The maximum displacement increases by 25.71% in Y-axis as compared to X-axis
Ductility	3.90	4.09	The ductility increases by 4.87% in Y-axis as compared to X-axis
Ductility Reduction Factor	2.60	2.67	The ductility reduction factor increases by 2.69% in Y-axis as compared to X-axis
Overstrength factor	6.11	18.67	The overstrength factor decreases by 67.27% in X-axis as compared to Y-axis
Time period (sec)	0.33	0.33	The time period is same in X and Y direction
R-factor	7.94	24.92	The R-factor increases by 213.85 % in Y-axis as compared to X-axis

Table 6.14 Performance points of model-6 in X and Y direction				
Performance level	Displacement (mm**)**		Corresponding Base Shear (kN)	
	X direction	Y direction	X direction	Y direction
Life Safety	7.41	3.67	531.28	889.11
Collapse Prevention	15.07	6.91	760.63	1451.38

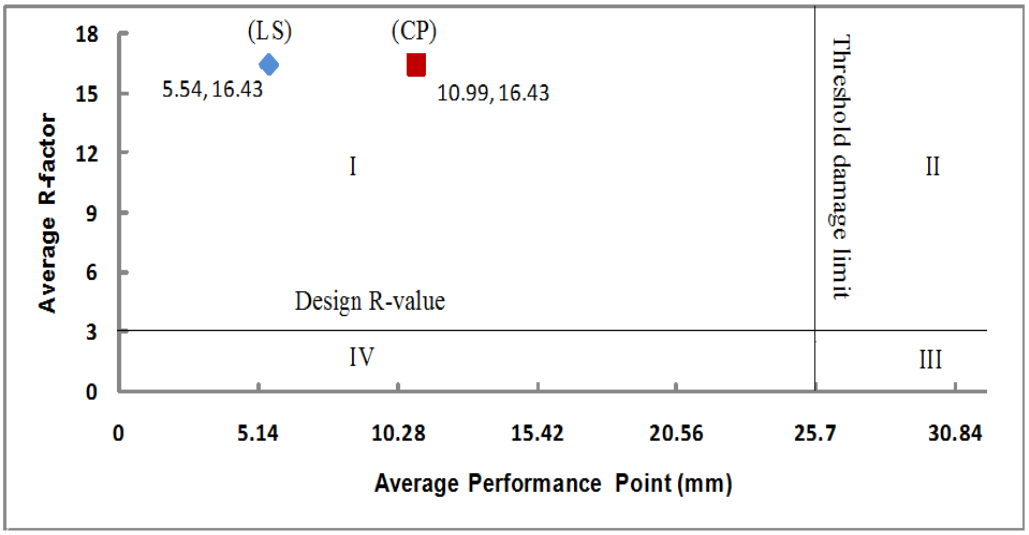

Figure 6.35 Average R-factor versus average performance point graph of model-6

Figure 6.35 shows the average R-factor versus average performance point graph of model-6. The point of intersection of R-factor and performance point for life safety & collapse prevention is located in Ist quadrant so there is no need to retrofit the building according to the "Quadrants assessment method".

6.3.7 Seismic investigation of model-7

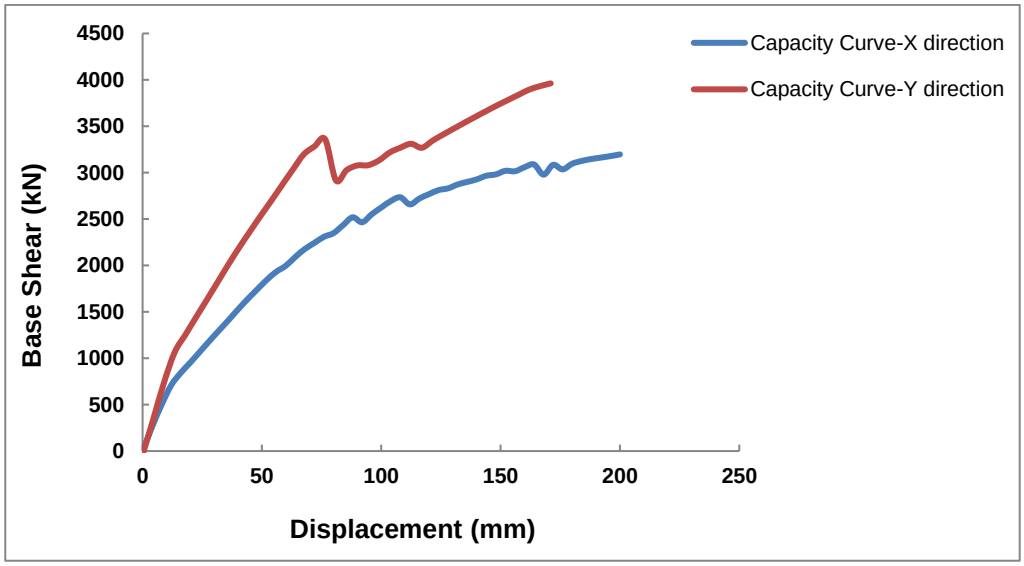

Figure 6.36 Capacity curves of model-7

As shown in Figure 6.36, the ultimate capacity of the building is higher in the Y direction as compared to the X direction due to the structural configuration of the building, and the remaining parameters are discussed in Table 6.15. The performance points of model-7 in X and Y direction are shown in Table 6.16 for life safety and collapse prevention purpose.

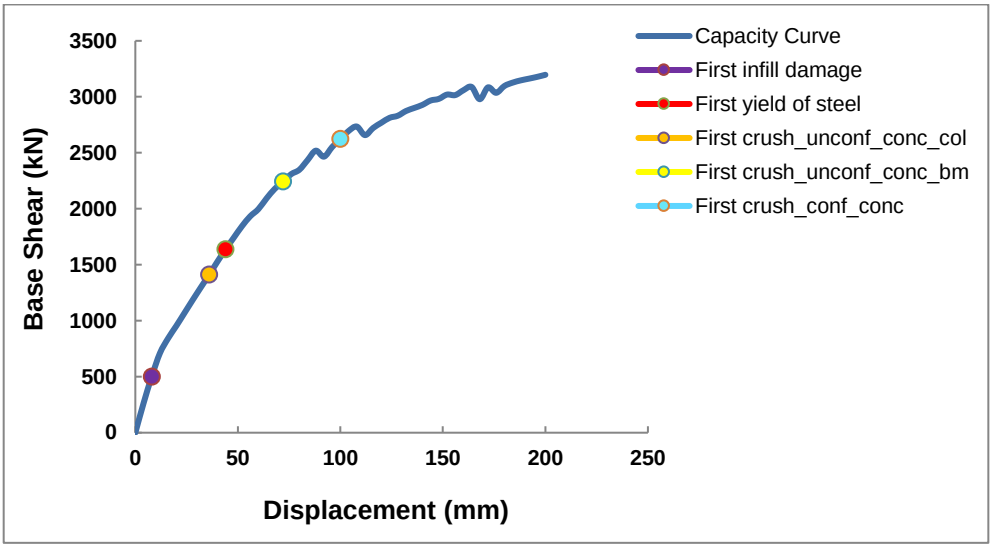

Figure 6.37 Damage pattern of Model-7 in the X direction

Figure 6.37 shows the damage pattern of model-7 in the X direction. The first infill damage occurred at a base shear 501.22 kN and displacement of 8.00 mm. The first yielding of steel occurred at a base shear 1637.40 kN and displacement of 44.00 mm. The first crushing of the unconfined concrete column occurred at base shear 1410.76 kN and displacement of 36 mm. The first crushing of the unconfined concrete beam occurred at base shear 2243.40 kN and displacement of 72 mm, and the first crushing of confined concrete occurred at base shear 2624.46 kN and displacement of 100 mm.

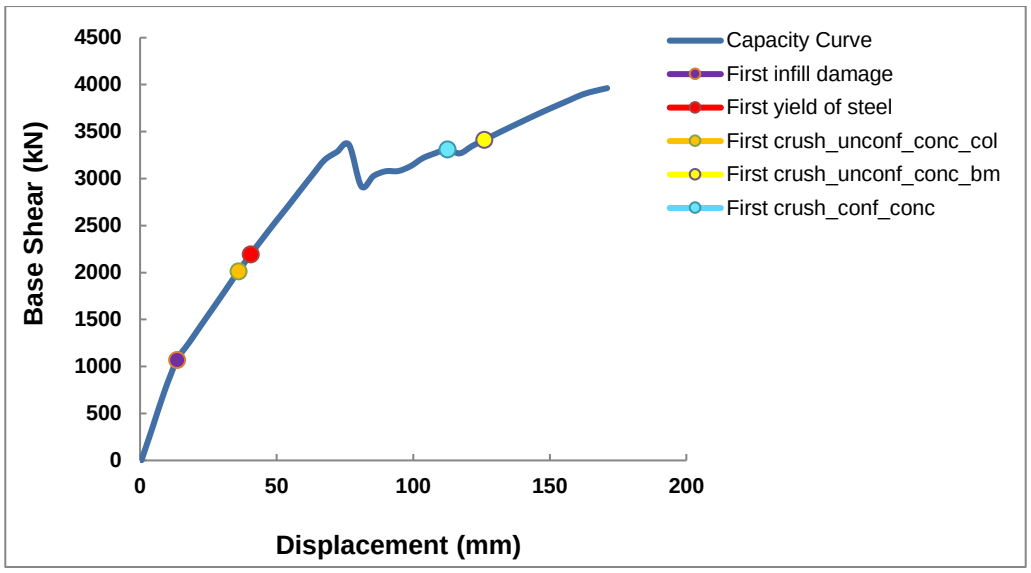

Figure 6.38 Damage pattern of Model-7 in the Y direction

Figure 6.38 shows the damage pattern of model-7 in the Y direction. The first infill damage occurred at a base shear 1067.69 kN and displacement of 13.5 mm. The first yielding of steel occurred at a base shear 2194.26 kN and displacement of 40.50 mm. The first crushing of the unconfined concrete column occurred at base shear 2013.16 kN and displacement of 36 mm. The first crushing of the unconfined concrete beam occurred at base shear 3411.82 kN and displacement of 126 mm, and the first crushing of confined concrete occurred at base shear 3311.23 kN and displacement of 112.50 mm.

Table 6.15 Comparison of different parameters of Model-7			
Parameters			Remarks
	In X-axis	In Y-axis	
Ultimate capacity(kN)	3196.64	3962.29	The ultimate capacity increases by 1.23times in Y-axis as compared to X-axis
Yield displacement (mm)	69.37	53.04	The yield displacement decreases by 23.54% in Y-axis as compared to X-axis
Maximum Displacement (mm)	200.00	171.00	The maximum displacement increases by 16.95% in X-axis as compared to Y-axis
Ductility	2.88	3.22	The ductility increases by 11.80% in Y-axis as compared to X-axis
Ductility Reduction Factor	2.88	3.22	The ductility reduction factor increases by 11.80 % in Y-axis as compared to X-axis
Overstrength factor	3.83	4.74	The overstrength factor decreases by 19.19% in X-axis as compared to Y-axis
Time period (sec)	0.59	0.59	The time period is same in X and Y direction
R-factor	5.51	7.63	The R-factor increases by 38.47% in Y-axis as compared to X-axis

Table 6.16 Performance points of model-7 in X and Y direction				
Performance level	Displacement (mm**)**		Corresponding Base Shear (kN)	
	X direction	Y direction	X direction	Y direction
Life Safety	22.95	21.51	1039.51	1404.25
Collapse Prevention	36.69	34.29	1430.74	1940.82

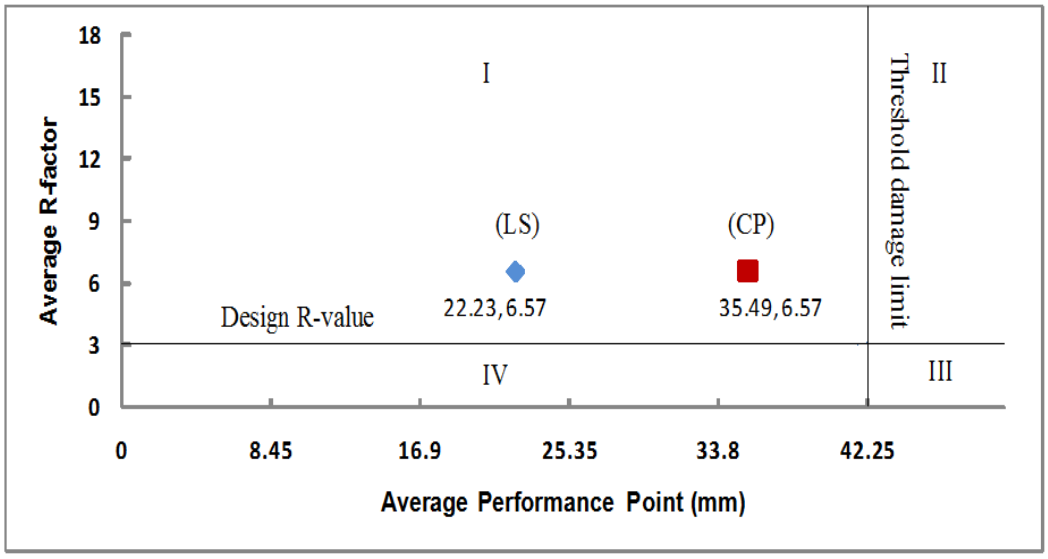

Figure 6.39 Average R-factor versus average performance point graph of model-7

Figure 6.39 shows the average R-factor versus average performance point graph of model-7. The point of intersection of R-factor and performance point for life safety & collapse prevention is located in Ist quadrant so there is no need to retrofit the building according to the "Quadrants assessment method".

6.3.8 Seismic investigation of model-8

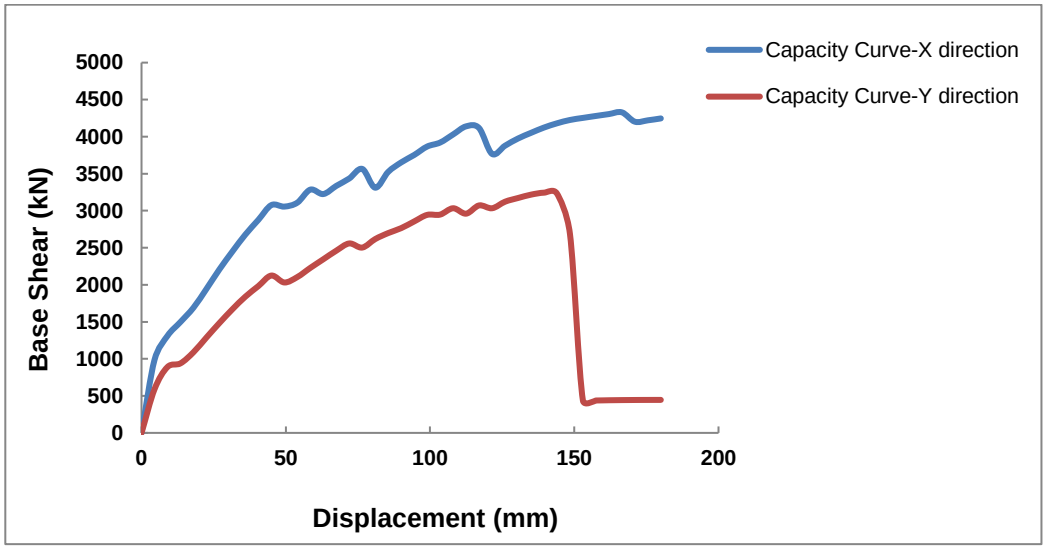

Figure 6.40 Capacity curves of model-8

As shown in Figure 6.40, the ultimate capacity of the building is higher in the X direction as compared to the Y direction due to the structural configuration of the building, and the remaining parameters are discussed in Table 6.17. The performance points of model-8 in X and Y direction are shown in Table 6.18 for life safety and collapse prevention purpose.

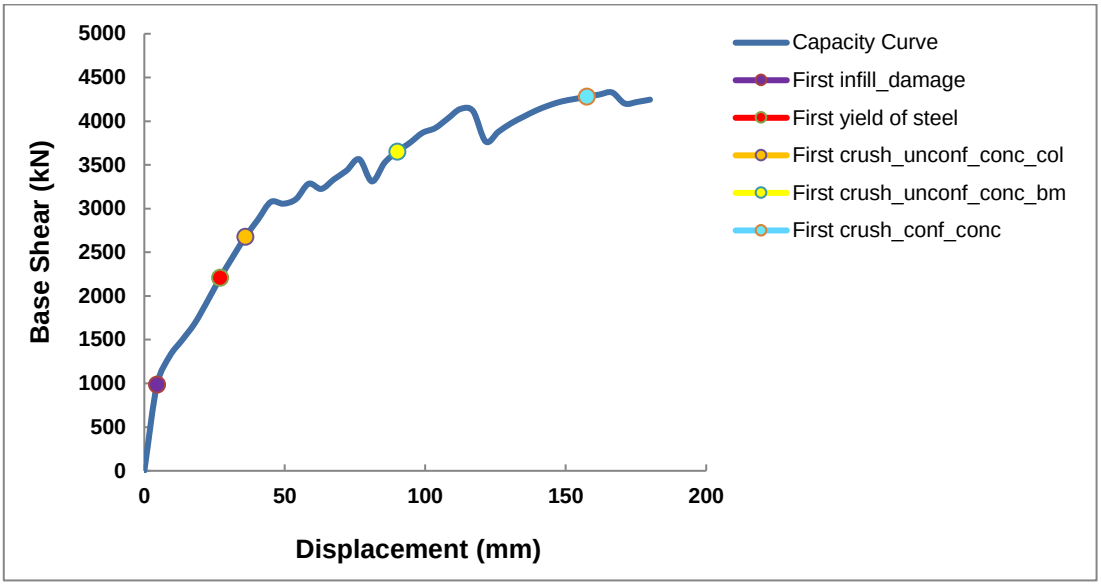

Figure 6.41 Damage pattern of Model-8 in the X direction

Figure 6.41 shows the damage pattern of model-8 in the X direction. The first infill damage occurred at a base shear 985.39 kN and displacement of 4.5 mm. The first yielding of steel occurred at a base shear 2207.74kN and displacement of 27 mm. The first crushing of the unconfined concrete column occurred at base shear 2678.26 kN and displacement of 36 mm. The first crushing of the unconfined concrete beam occurred at base shear 3652.38 kN and displacement of 90 mm, and the first crushing of confined concrete occurred at base shear 4279.58 kN and displacement of 157.5 mm.

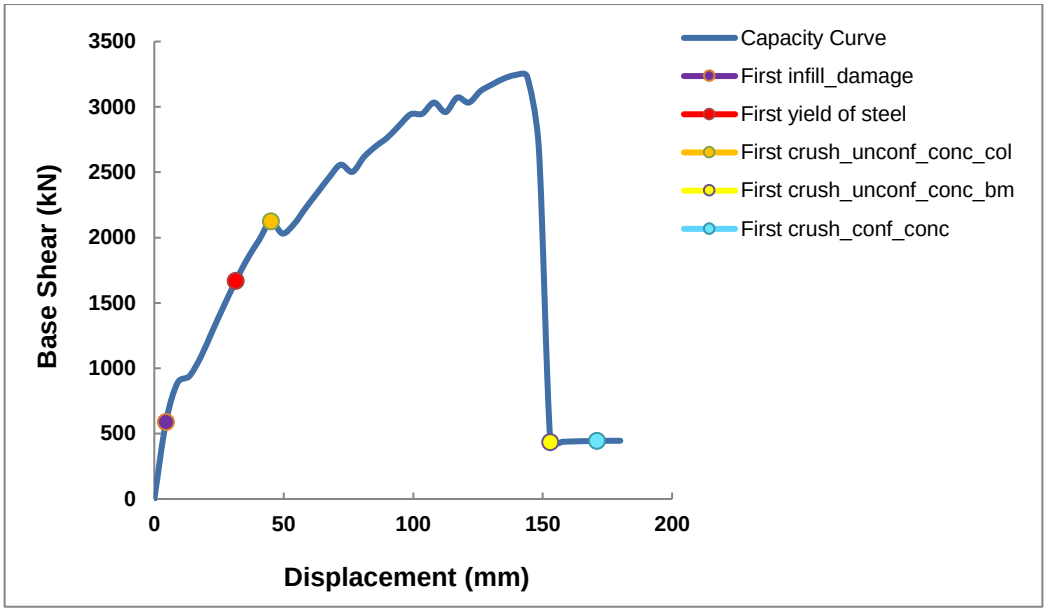

Figure 6.42 Damage pattern of Model-8 in the Y direction

Figure 6.42 shows the damage pattern of model-8 in the Y direction. The first infill damage occurred at a base shear 589.28 kN and displacement of 4.5 mm. The first yielding of steel occurred at a base shear 1669.24 kN and displacement of 31.5 mm. The first crushing of the unconfined concrete column occurred at base shear 2124.61kN and displacement of 45 mm. The first crushing of the unconfined concrete beam occurred at base shear 435.63kN and displacement of 153 mm, and the first crushing of confined concrete occurred at base shear 444.32 kN and displacement of 171 mm.

Table 6.17 Comparison of different parameters of Model-8			
Parameters			Remarks
	In X-axis	In Y-axis	
Ultimate capacity(kN)	4328.57	3243.55	The ultimate capacity increases by 1.33 times in X-axis as compared to Y-axis
Yield displacement (mm)	37.08	47.93	The yield displacement decreases by 22.63 % in X-axis as compared to Y-axis
Maximum Displacement (mm)	166.50	139.50	The maximum displacement increases by 19.35 % in X-axis as compared to Y-axis
Ductility	4.49	2.91	The ductility increases by 54.29% in X-axis as compared to Y-axis
Ductility Reduction Factor	2.82	2.91	The ductility reduction factor increases by 3.19 % in Y-axis as compared to X-axis
Overstrength factor	8.54	6.40	The overstrength factor decreases by 25.05% in Y-axis as compared to X-axis
Time period (sec)	0.31	0.31	The time period is same in X and Y direction
R-factor	12.04	9.31	The R-factor increases by 29.32% in X-axis as compared to Y-axis

Table 6.18 Performance points of model-8 in X and Y direction				
Performance level	Displacement (mm**)**		Corresponding Base Shear (kN)	
	X direction	Y direction	X direction	Y direction
Life Safety	7.72	9.07	1217.88	889.60
Collapse Prevention	14.25	16.56	1529.74	1040.77

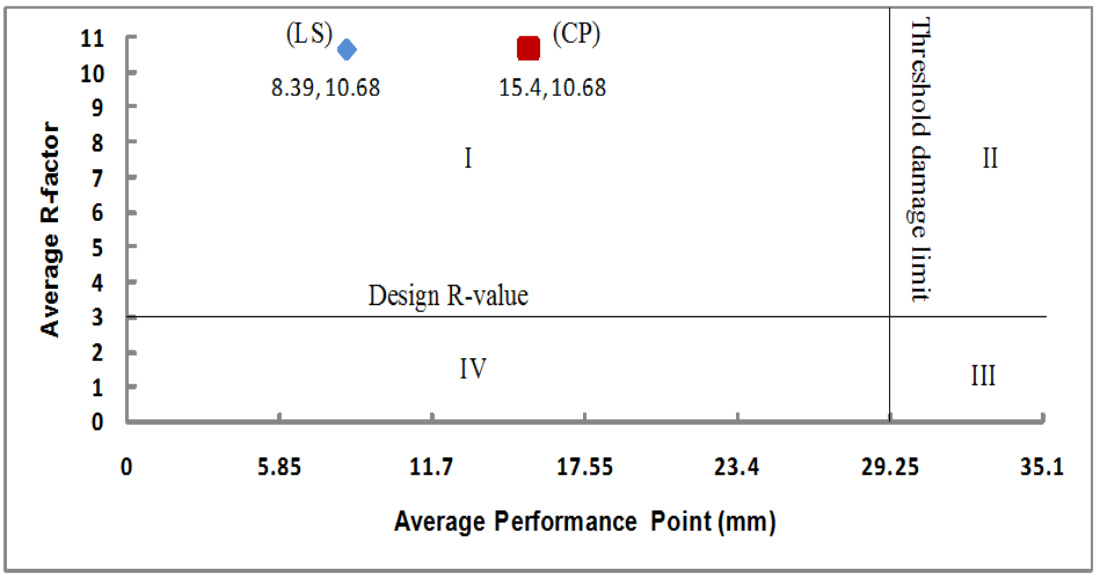

Figure 6.43 Average R-factor versus average performance point graph of model-8

Figure 6.43 shows the average R-factor versus average performance point graph of model-8. The point of intersection of R-factor and performance point for life safety & collapse prevention is located in Ist quadrant so there is no need to retrofit the building according to the "Quadrants assessment method".

6.3.9 Seismic investigation of model-9

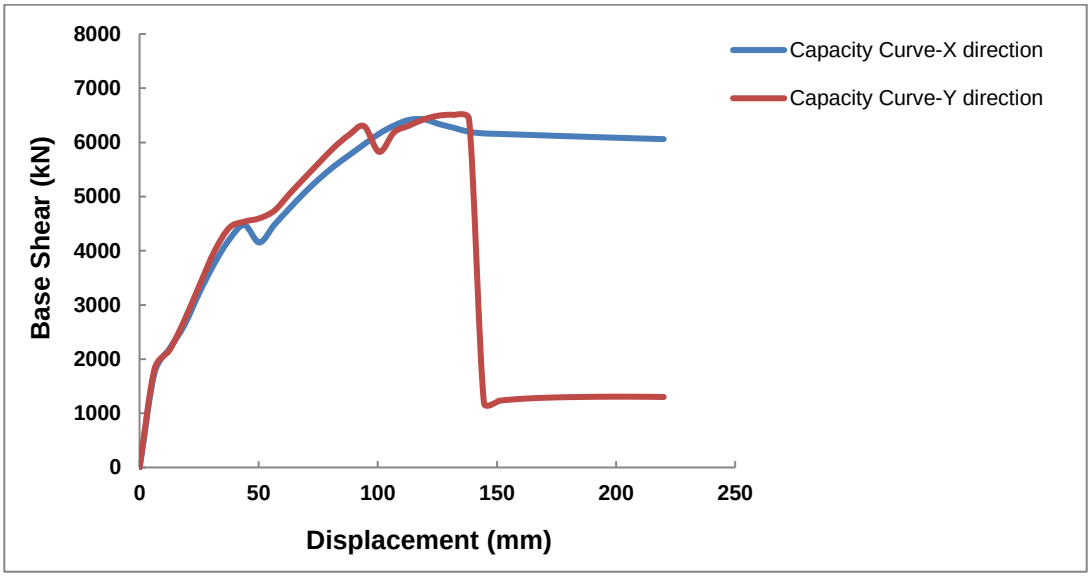

Figure 6.44 Capacity curves of model-9

As shown in Figure 6.44, the ultimate capacity of the building is higher in the Y direction as compared to the X direction due to the structural configuration of the building, and the remaining parameters are discussed in Table 6.19. The performance points of model-9 in X and Y direction are shown in Table 6.20 for life safety and collapse prevention purpose.

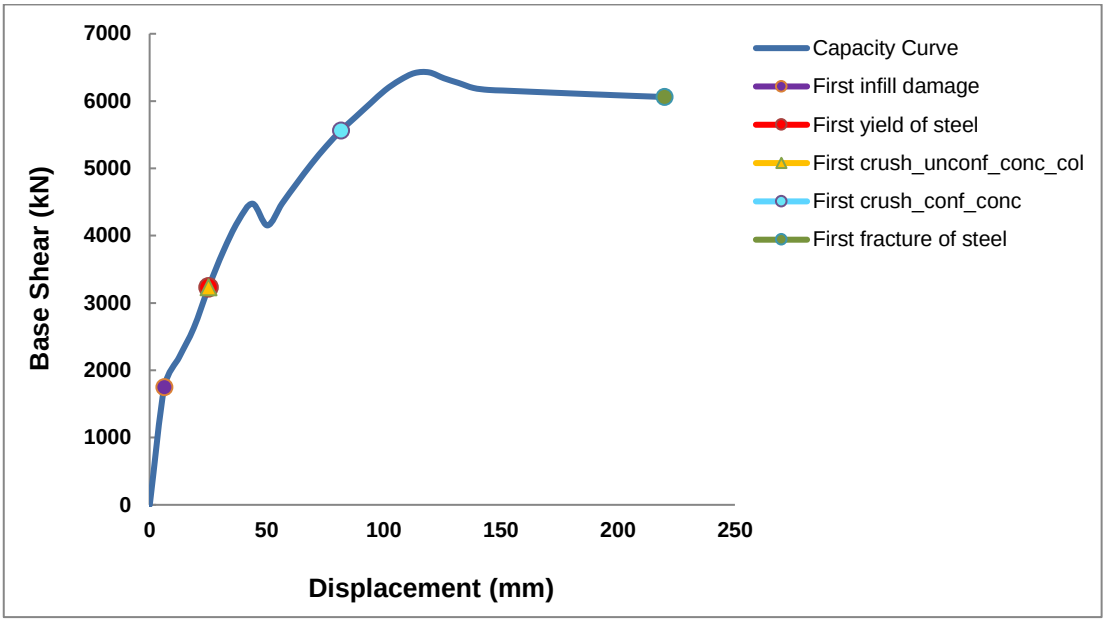

Figure 6.45 Damage pattern of Model-9 in the X direction

Figure 6.45 shows the damage pattern of model-9 in the X direction. The first infill damage occurred at a base shear 1746.98kN and displacement of 6.29 mm. The first yielding of steel & the first crushing of the unconfined concrete column occurred at a base shear 3228.91kN and displacement of 25.14 mm. The first crushing of confined concrete occurred at base shear 5561.53 kN and displacement of 81.71mm. And the first fracture of steel occurred at base shear 6060.01 kN and displacement of 220 mm.

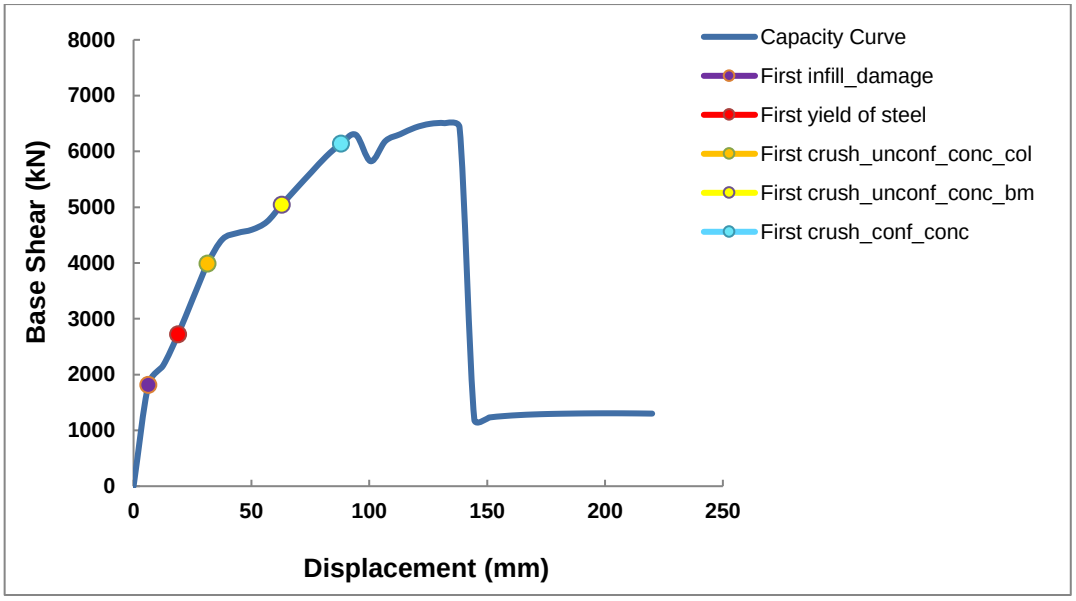

Figure 6.46 Damage pattern of Model-9 in the Y direction

Figure 6.46 shows the damage pattern of model-9 in the Y direction. The first infill damage occurred at a base shear 1815.46 kN and displacement of 6.29 mm. The first yielding of steel occurred at a base shear 2719.86 kN and displacement of 18.86 mm. The first crushing of the unconfined concrete column occurred at base shear 3989.00 kN and displacement of 31.43 mm. The first crushing of the unconfined concrete beam occurred at base shear 5044.75 kN and displacement of 62.86 mm, and the first crushing of confined concrete occurred at base shear 6141.05 kN and displacement of 88 mm.

Table 6.19 Comparison of different parameters of Model-9			
Parameters			Remarks
	In X-axis	In Y-axis	
Ultimate capacity(kN)	6425.65	6506.65	The ultimate capacity increases by 1.01 times in Y-axis as compared to X-axis
Yield displacement (mm)	34.30	37.09	The yield displacement decreases by 7.52 % in X-axis as compared to Y-axis
Maximum Displacement (mm)	119.43	132.00	The maximum displacement increases by 10.52 % in Y-axis as compared to X-axis
Ductility	3.48	3.56	The ductility increases by 2.29 % in Y-axis as compared to X-axis
Ductility Reduction Factor	2.44	2.47	The ductility reduction factor increases by 1.22 % in Y-axis as compared to X-axis
Overstrength factor	15.68	15.88	The overstrength factor increases by 1.27 % in Y-axis as compared to X-axis
Time period (sec)	0.21	0.21	The time period is same in X and Y direction
R-factor	19.12	19.61	The R-factor increases by 2.56 % in Y-axis as compared to X-axis

Table 6.20 Performance points of model-9 in X and Y direction				
Performance level	Displacement (mm**)**		Corresponding Base Shear (kN)	
	X direction	Y direction	X direction	Y direction
Life Safety	5.62	5.73	1560.89	1655.14
Collapse Prevention	6.91	7.06	1790.75	1858.33

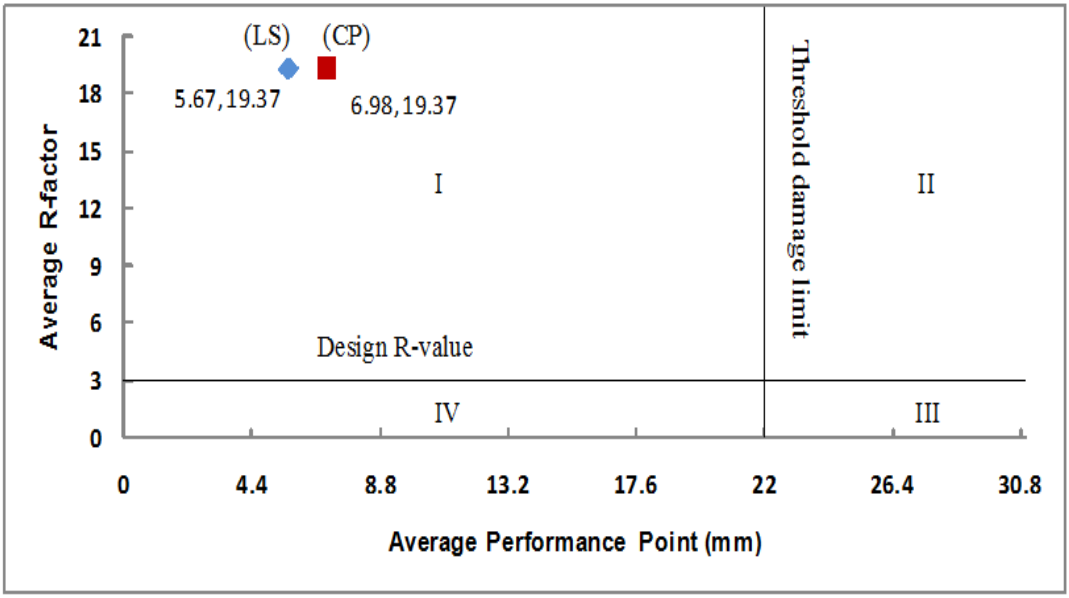

Figure 6.47 Average R-factor versus average performance point graph of model-9

Figure 6.47 shows the average R-factor versus average performance point graph of model-9. The point of intersection of R-factor and performance point for life safety & collapse prevention is located in Ist quadrant so there is no need to retrofit the building according to the "Quadrants assessment method".

6.3.10 Seismic investigation of model-10

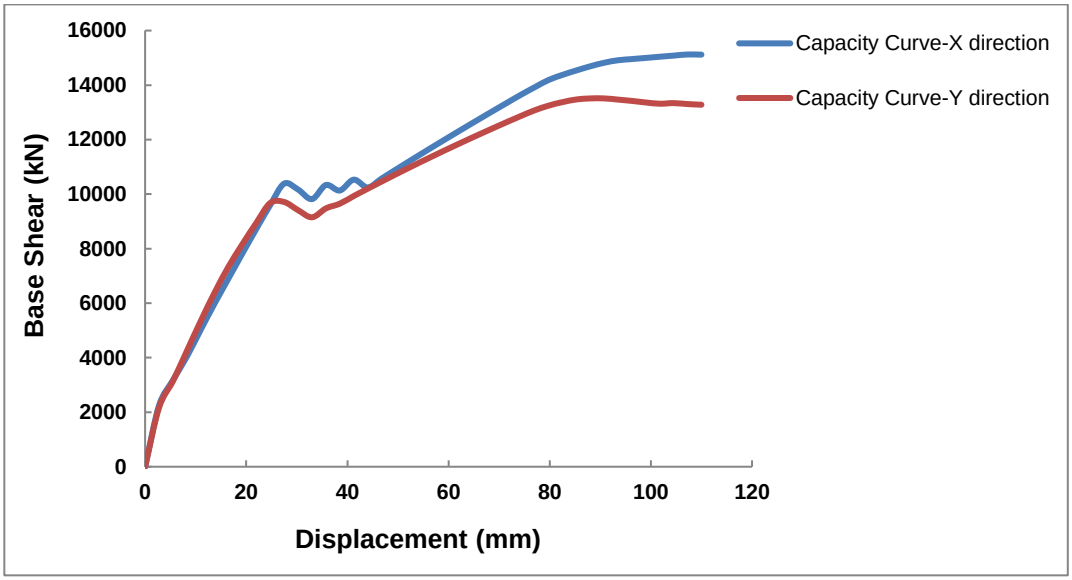

Figure 6.48 Capacity curves of model-10

As shown in Figure 6.48, the ultimate capacity of the building is higher in the X direction as compared to the Y direction due to the structural configuration of the building, and the remaining parameters are discussed in Table 6.21. The performance points of model-10 in X and Y direction are shown in Table 6.22 for life safety and collapse prevention purpose.

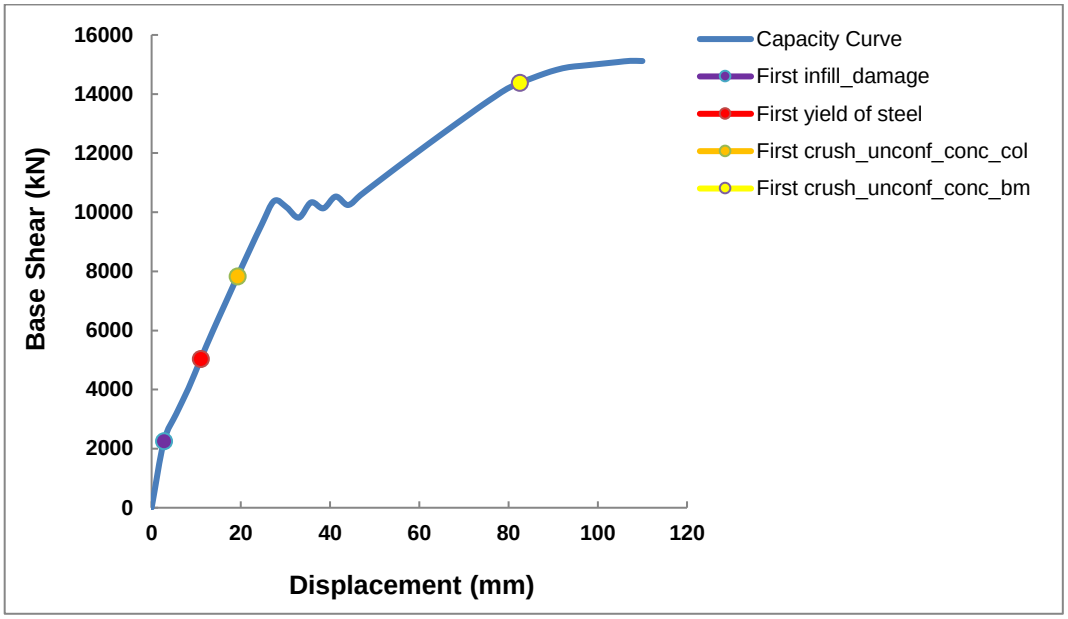

Figure 6.49 Damage pattern of Model-10 in the X direction

Figure 6.49 shows the damage pattern of model-10 in the X direction. The first infill damage occurred at a base shear 2247.03 kN and displacement of 2.75 mm. The first yielding of steel occurred at a base shear 5028.42 kN and displacement of 11 mm. The first crushing of the unconfined concrete column occurred at a base shear 7829.76 kN and displacement of 19.25 mm. The first crushing of the unconfined concrete beam occurred at a base shear 14373.65 kN and displacement of 82.5 mm.

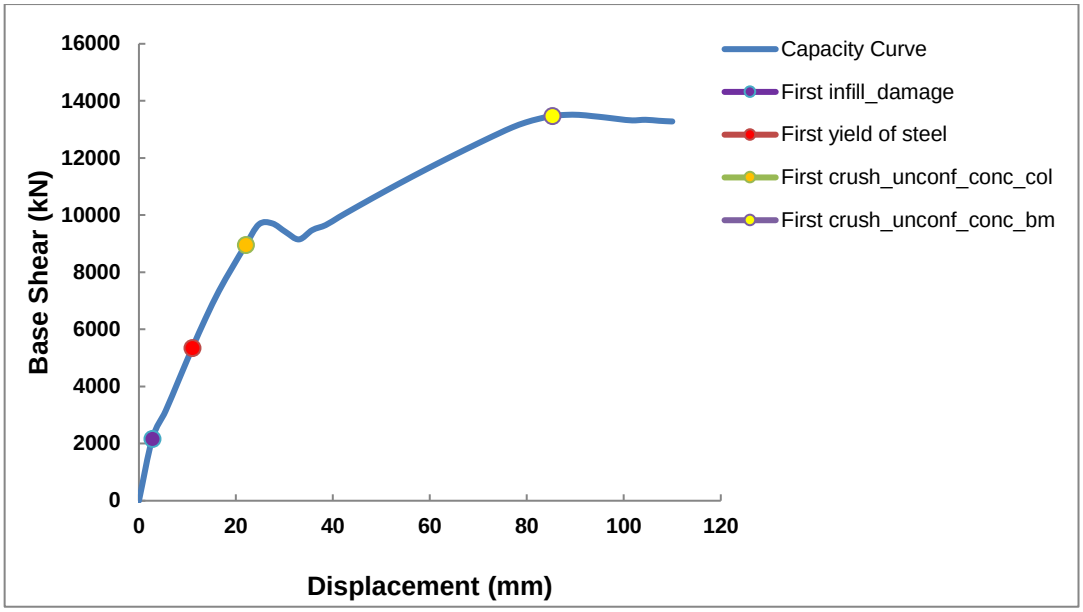

Figure 6.50 Damage pattern of Model-10 in the Y direction

Figure 6.50 shows the damage pattern of model-10 in the Y direction. The first infill damage occurred at a base shear 2165.36 kN and displacement of 2.75 mm. The first yielding of steel occurred at a base shear 5345.67 kN and displacement of 11 mm. The first crushing of the unconfined concrete column occurred at base shear 8948.90 kN and displacement of 22 mm. The first crushing of the unconfined concrete beam occurred at base shear 13472.10 kN and displacement of 85.25 mm.

Table 6.21 Comparison of different parameters of Model-10			
Parameters			Remarks
	In X-axis	In Y-axis	
Ultimate capacity(kN)	15122.63	13511.48	The ultimate capacity increases by 1.12 times in X-axis as compared to Y-axis
Yield displacement (mm)	26.83	20.90	The yield displacement decreases by 22.10 % in Y-axis as compared to X-axis
Maximum Displacement (mm)	107.25	90.75	The maximum displacement increases by 18.18 % in X-axis as compared to Y-axis
Ductility	4.00	4.34	The ductility increases by 8.5 % in Y-axis as compared to X-axis
Ductility Reduction Factor	1.00	1.00	The ductility reduction factor is same in X and Y direction
Overstrength factor	21.19	18.93	The overstrength factor increases by 11.93 % in X-axis as compared to Y-axis
Time period (sec)	0.12	0.12	The time period is same in X and Y direction
R-factor	10.59	9.46	The R-factor increases by 11.94 % in X-axis as compared to Y-axis

Table 6.22 Performance points of model-10 in X and Y direction				
Performance level	Displacement (mm**)**		Corresponding Base Shear (kN)	
	X direction	Y direction	X direction	Y direction
Life Safety	1.27	0.99	1037.71	779.52
Collapse Prevention	1.55	1.20	1266.50	944.88

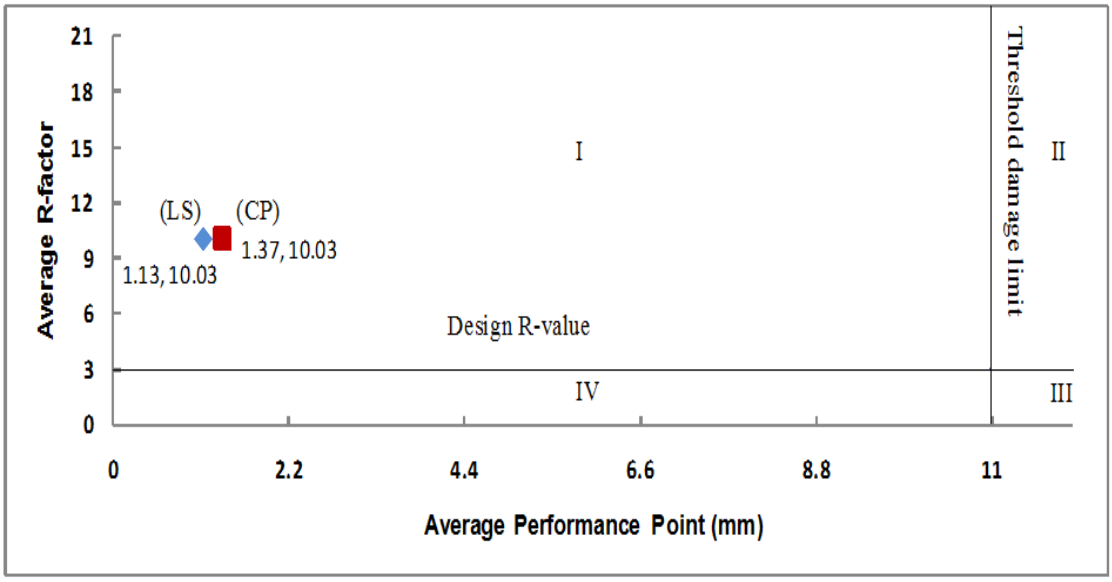

Figure 6.51 Average R-factor versus average performance point graph of model-10

Figure 6.51 shows the average R-factor versus average performance point graph of model-10. The point of intersection of R-factor and performance point for life safety & collapse prevention is located in Ist quadrant so there is no need to retrofit the building according to the "Quadrants assessment method".

6.3.11 Seismic investigation of model-11

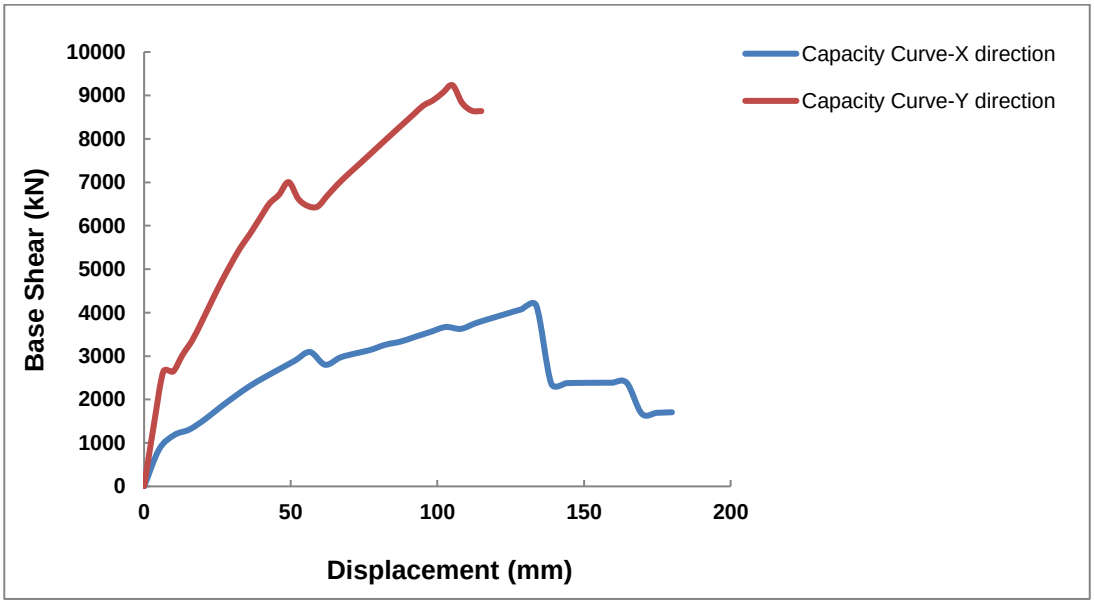

Figure 6.52 Capacity curves of model-11

As shown in Figure 6.52, the ultimate capacity of the building is higher in the Y direction as compared to the X direction due to the structural configuration of the building, and the remaining parameters are discussed in Table 6.23. The performance points of model-11 in X and Y direction are shown in Table 6.24 for life safety and collapse prevention purpose.

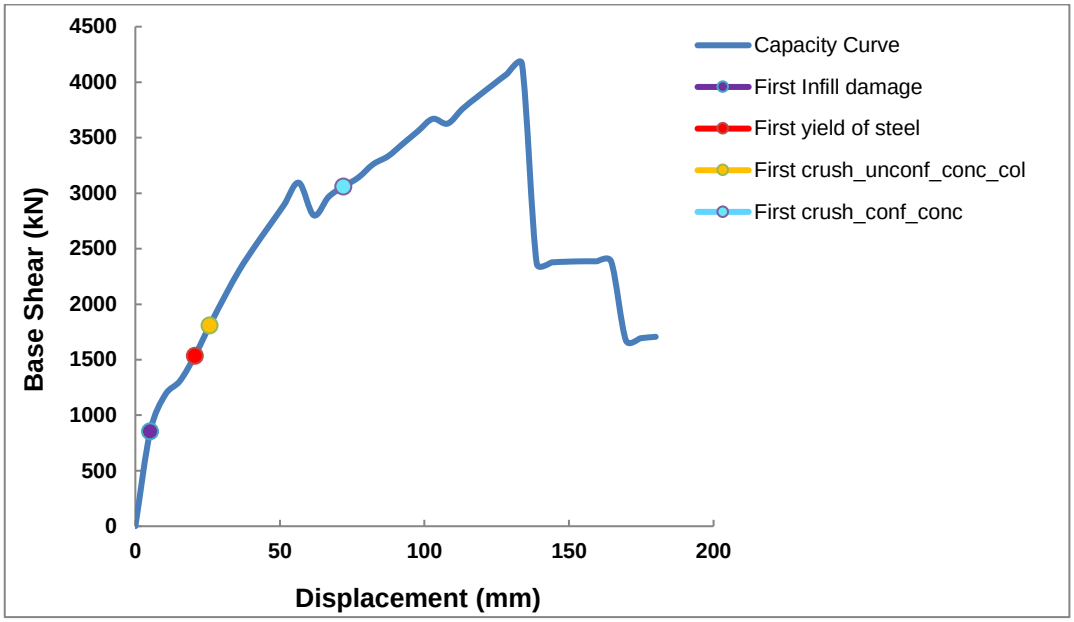

Figure 6.53 Damage pattern of Model-11 in the X direction

Figure 6.53 shows the damage pattern of model-11 in the X direction. The first infill damage occurred at a base shear 855.61 kN and displacement of 5.14 mm. The first yielding of steel occurred at a base shear 1535.13 kN and displacement of 20.57 mm. The first crushing of the unconfined concrete column occurred at a base shear 1808.87 kN and displacement of 25.71 mm. The first crushing of confined concrete occurred at a base shear 3060.09 kN and displacement of 72 mm.

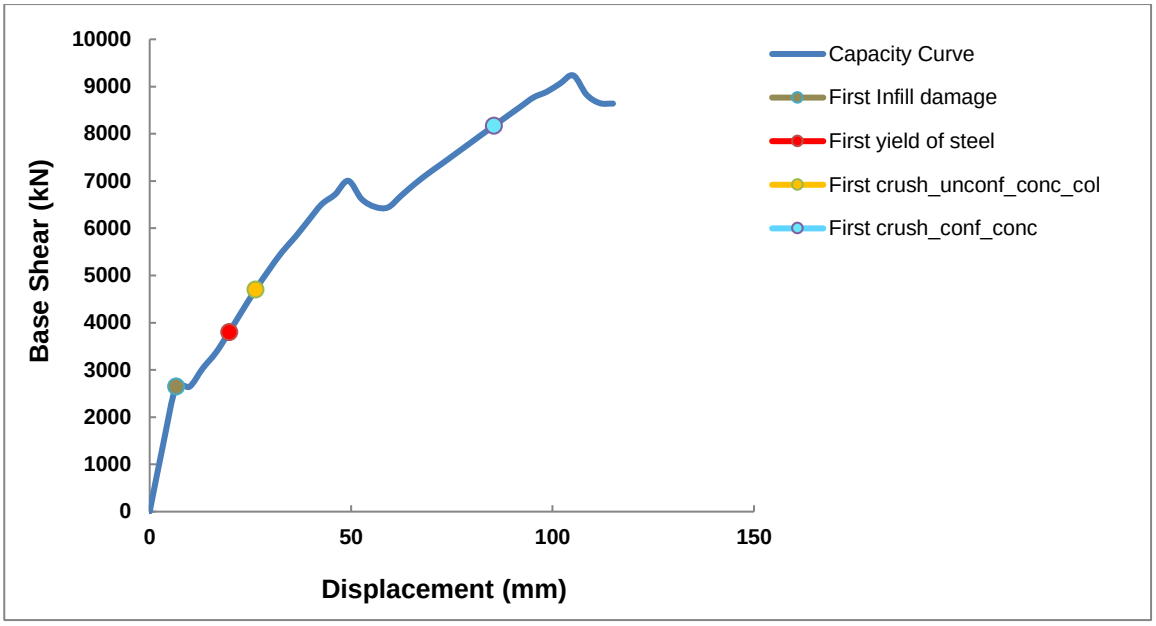

Figure 6.54 Damage pattern of Model-11 in the Y direction

Figure 6.54 shows the damage pattern of model-11 in the Y direction. The first infill damage occurred at a base shear 2646.09 kN and displacement of 6.57 mm. The first yielding of steel occurred at a base shear 3799.54 kN and displacement of 19.71 mm. The first crushing of the unconfined concrete column occurred at a base shear 4701.38 kN and displacement of 26.29 mm. The first crushing of confined concrete occurred at a base shear 8168.32 kN and displacement of 85.43 mm.

Table 6.23 Comparison of different parameters of Model-11			
Parameters			Remarks
	In X-axis	In Y-axis	
Ultimate capacity(kN)	4165.74	9235.29	The ultimate capacity increases by 2.21times in Y-axis as compared to X-axis
Yield displacement (mm)	45.86	31.07	The yield displacement decreases by 32.25 % in Y-axis as compared to X-axis
Maximum Displacement (mm)	133.71	105.14	The maximum displacement increases by 27.17 % in X-axis as compared to Y-axis
Ductility	2.92	3.38	The ductility increases by 15.75 % in Y-axis as compared to X-axis
Ductility Reduction Factor	2.20	2.40	The ductility reduction factor increases by 9.09 % in Y-axis as compared to X-axis
Overstrength factor	4.77	10.57	The overstrength factor increases by 121.59 % in Y-axis as compared to X-axis
Time period (sec)	0.4	0.4	The time period is same in X and Y direction
R-factor	5.24	12.68	The R-factor increases by 141.98 % in Y-axis as compared to X-axis

Table 6.24 Performance points of model-11 in X and Y direction				
Performance level	Displacement (mm**)**		Corresponding Base Shear (kN)	
	X direction	Y direction	X direction	Y direction
Life Safety	12.73	10.62	1242.65	2733.08
Collapse Prevention	18.90	17.29	1461.68	3480.26

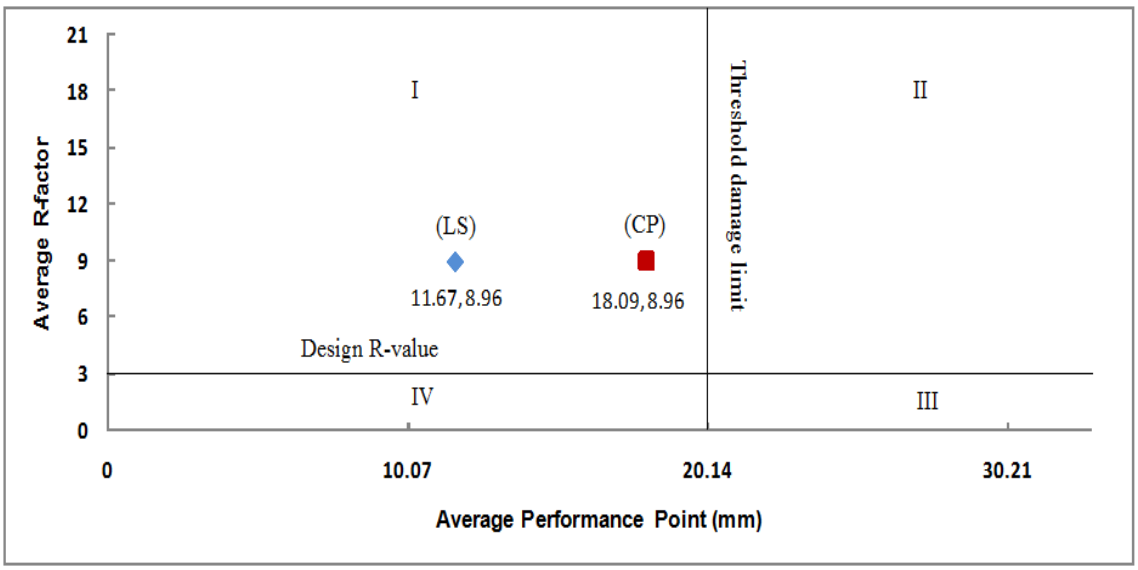

Figure 6.55 Average R-factor versus average performance point graph of model-11

Figure 6.55 shows the average R-factor versus average performance point graph of model-11. The point of intersection of R-factor and performance point for life safety & collapse prevention is located in Ist quadrant so there is no need to retrofit the building according to the "Quadrants assessment method".

6.3.12 Seismic investigation of model-12

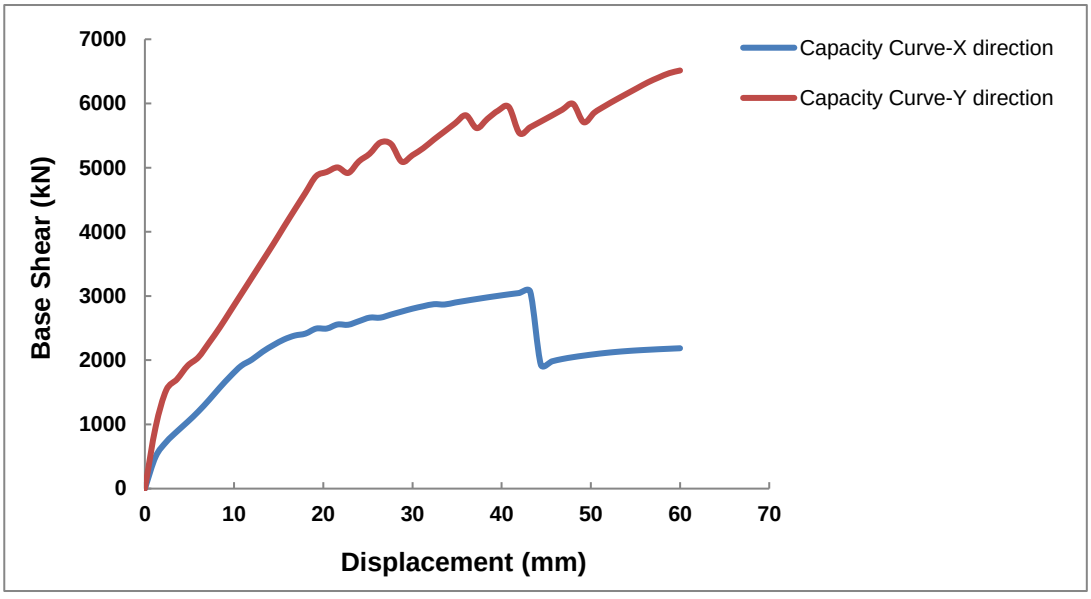

Figure 6.56 Capacity curves of model-12

As shown in Figure 6.56, the ultimate capacity of the building is higher in the Y direction as compared to the X direction due to the structural configuration of the building, and the remaining parameters are discussed in Table 6.25. The performance points of model-12 in X and Y direction are shown in Table 6.26 for life safety and collapse prevention purpose.

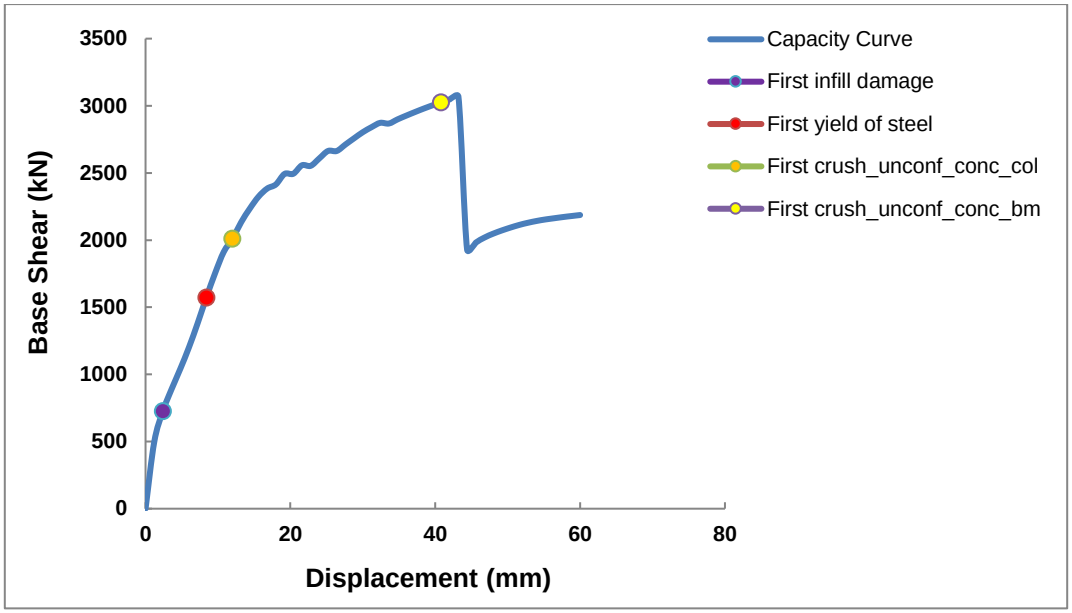

Figure 6.57 Damage pattern of Model-12 in the X direction

Figure 6.57 shows the damage pattern of model-12 in the X direction. The first infill damage occurred at a base shear 727.50 kN and displacement of 2.4 mm. The first yielding of steel occurred at a base shear 1573.13 kN and displacement of 8.4 mm. The first crushing of the unconfined concrete column occurred at a base shear 2009.61 kN and displacement of 12 mm. The first crushing of the unconfined concrete beam occurred at a base shear 3026.30 kN and displacement of 40.8 mm.

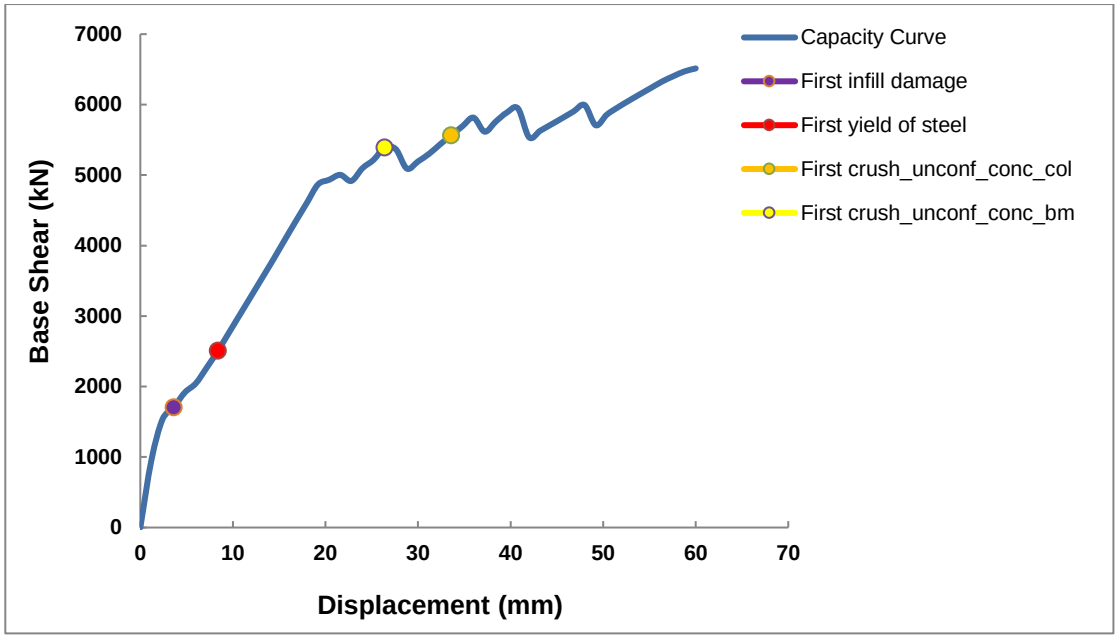

Figure 6.58 Damage pattern of Model-12 in the Y direction

Figure 6.58 shows the damage pattern of model-12 in the Y direction. The first infill damage occurred at a base shear 1703.63 kN and displacement of 3.6 mm. The first yielding of steel occurred at a base shear 2510.27 kN and displacement of 8.4 mm. The first crushing of the unconfined concrete column occurred at a base shear 5564.56 kN and displacement of 33.6 mm. The first crushing of the unconfined concrete beam occurred at a base shear 5391.99 kN and displacement of 26.4 mm.

Table 6.25 Comparison of different parameters of Model-12			
Parameters			Remarks
	In X-axis	In Y-axis	
Ultimate capacity(kN)	3068.38	6513.54	The ultimate capacity increases by 2.12 times in Y-axis as compared to X-axis
Yield displacement (mm)	13.07	18.85	The yield displacement decreases by 30.66 % in X-axis as compared to Y-axis
Maximum Displacement (mm)	43.20	60.00	The maximum displacement increases by 38.88 % in Y-axis as compared to X-axis
Ductility	3.30	3.18	The ductility increases by 3.77 % in X-axis as compared to Y-axis
Ductility Reduction Factor	1.00	1.00	The ductility reduction factor is same in X and Y direction
Overstrength factor	9.05	19.21	The overstrength factor increases by 112.26 % in Y-axis as compared to X-axis
Time period (sec)	0.13	0.13	The time period is same in X and Y direction
R-factor	4.52	9.6	The R-factor increases by 112.38 % in Y-axis as compared to X-axis

Table 6.26 Performance points of model-12 in X and Y direction				
Performance level	Displacement (mm**)**		Corresponding Base Shear (kN)	
	X direction	Y direction	X direction	Y direction
Life Safety	0.57	0.69	235.85	549.89
Collapse Prevention	0.69	0.85	285.50	677.40

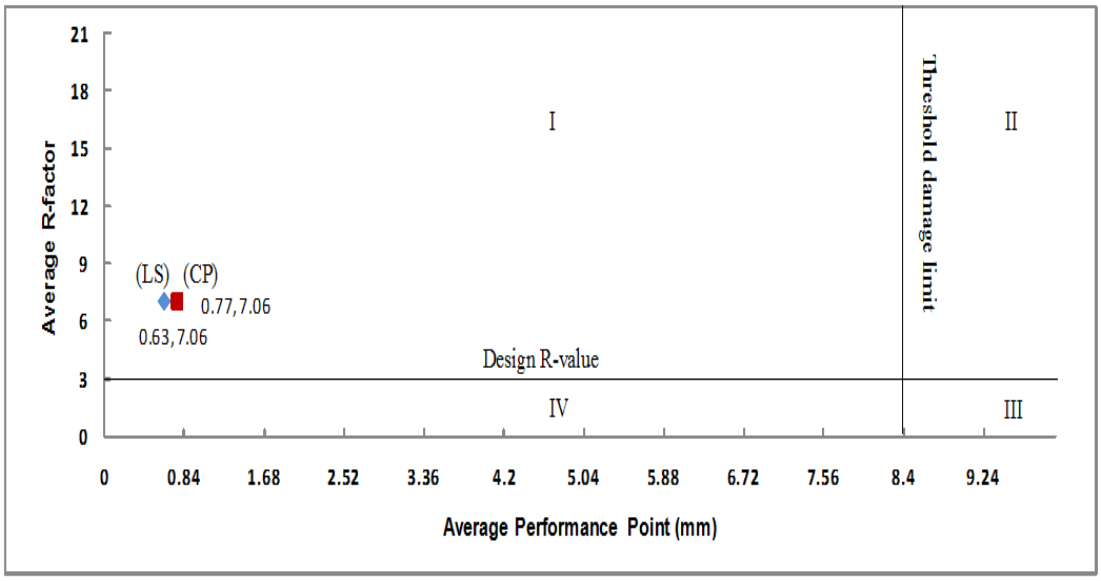

Figure 6.59 Average R-factor versus average performance point graph of model-12

Figure 6.59 shows the average R-factor versus average performance point graph of model-12. The point of intersection of R-factor and performance point for life safety & collapse prevention is located in Ist quadrant so there is no need to retrofit the building according to the "Quadrants assessment method".

6.3.13 Seismic investigation of model-13

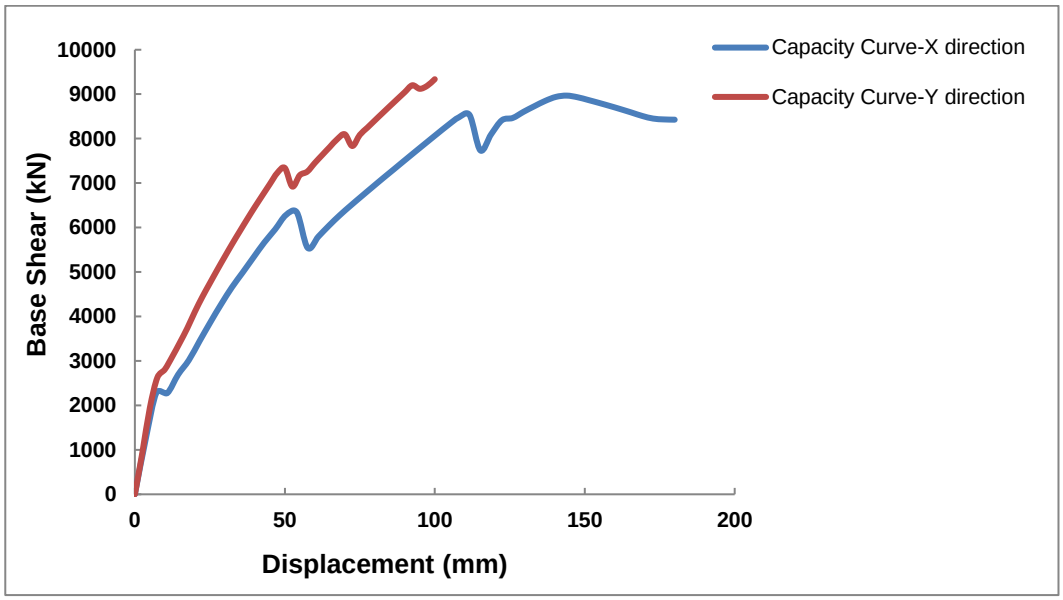

Figure 6.60 Capacity curves of model-13

As shown in Figure 6.60, the ultimate capacity of the building is higher in the Y direction as compared to the X direction due to the structural configuration of the building, and the remaining parameters are discussed in Table 6.27. The performance points of model-13 in X and Y direction are shown in Table 6.28 for life safety and collapse prevention purpose.

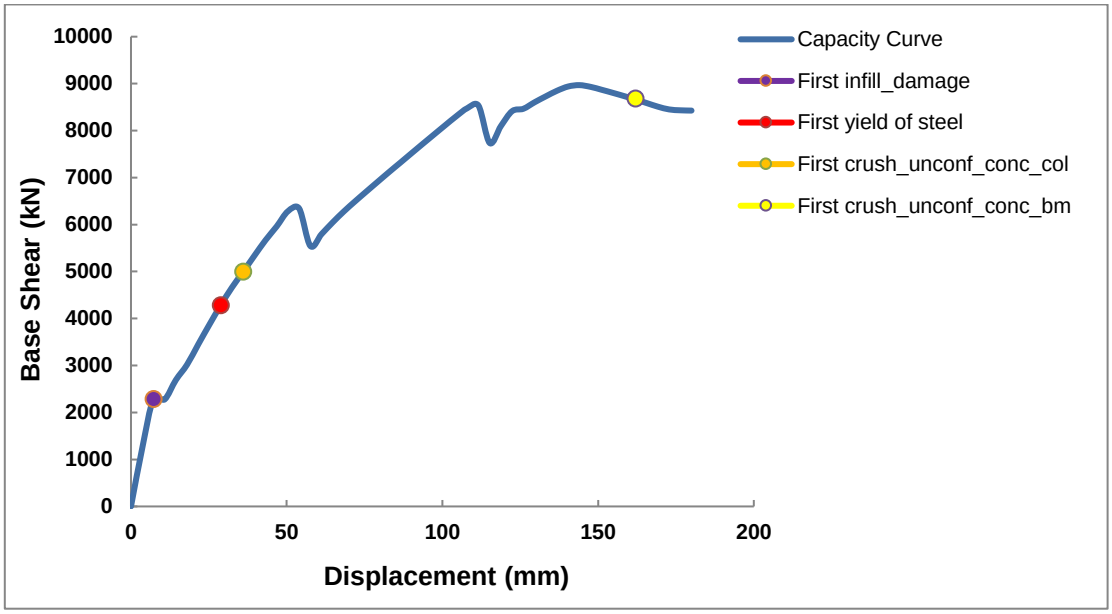

Figure 6.61 Damage pattern of Model-13 in the X direction

Figure 6.61 shows the damage pattern of model-13 in the X direction. The first infill damage occurred at a base shear 2288.14 kN and displacement of 7.2 mm. The first yielding of steel occurred at a base shear 4280.14 kN and displacement of 28.8 mm. The first crushing of the unconfined concrete column occurred at a base shear 4993.66 kN and displacement of 36 mm. The first crushing of the unconfined concrete beam occurred at a base shear 8681.57 kN and displacement of 162 mm.

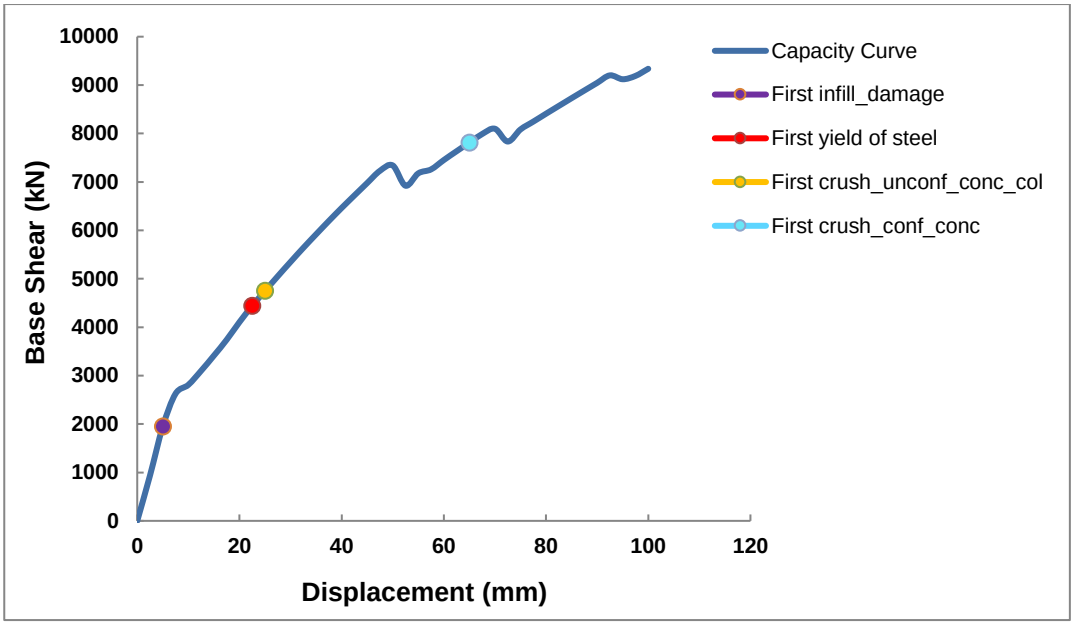

Figure 6.62 Damage pattern of Model-13 in the Y direction

Figure 6.62 shows the damage pattern of model-13 in the Y direction. The first infill damage occurred at a base shear 1945.87 kN and displacement of 5 mm. The first yielding of steel occurred at a base shear 4440.34 kN and displacement of 22.5 mm. The first crushing of the unconfined concrete column occurred at a base shear 4748.58 kN and displacement of 25 mm. The first crushing of confined concrete occurred at a base shear 7812.86 kN and displacement of 65 mm.

Table 6.27 Comparison of different parameters of Model-13			
Parameters			Remarks
	In X-axis	In Y-axis	
Ultimate capacity(kN)	8968.35	9336.88	The ultimate capacity increases by 1.04 times in Y-axis as compared to X-axis
Yield displacement (mm)	46.65	36.60	The yield displacement decreases by 21.54 % in Y-axis as compared to X-axis
Maximum Displacement (mm)	144.00	100.00	The maximum displacement increases by 44 % in X-axis as compared to Y-axis
Ductility	3.09	2.73	The ductility increases by 13.18 % in X-axis as compared to Y-axis
Ductility Reduction Factor	2.27	2.11	The ductility reduction factor increases by 7.58 % in X axis as compared to Y-axis
Overstrength factor	4.62	4.81	The overstrength factor increases by 4.11 % in Y-axis as compared to X-axis
Time period (sec)	0.35	0.35	The time period is same in X and Y direction
R-factor	5.24	5.07	The R-factor increases by 3.35 % in X-axis as compared to Y-axis

Table 6.28 Performance points of model-13 in X and Y direction				
Performance level	Displacement (mm**)**		Corresponding Base Shear (kN)	
	X direction	Y direction	X direction	Y direction
Life Safety	10.65	8.32	2276.04	2686.16
Collapse Prevention	18.43	15.13	3069.05	3412.43

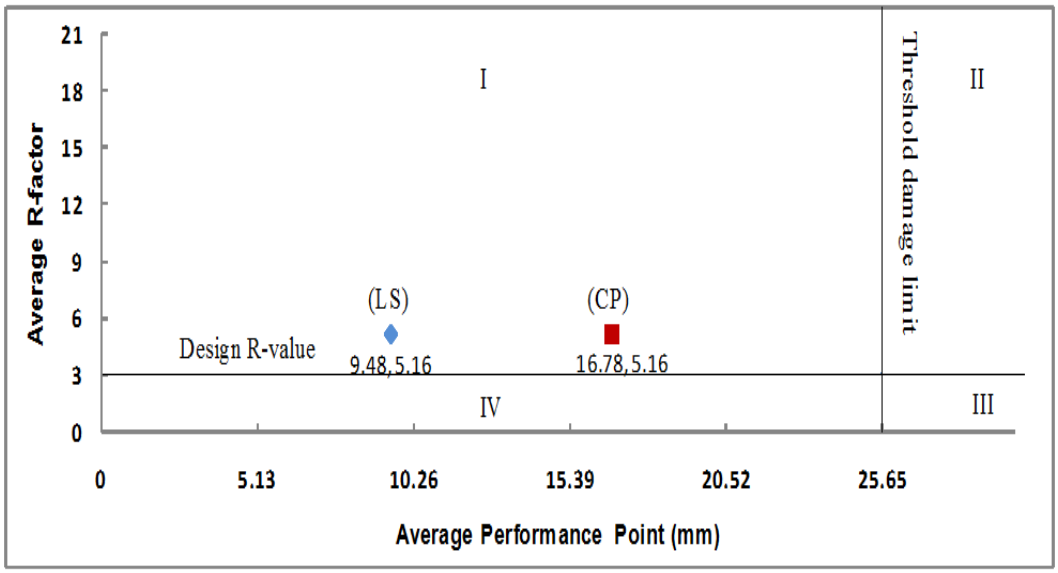

Figure 6.63 Average R-factor versus average performance point graph of model-13

Figure 6.63 shows the average R-factor versus average performance point graph of model-13. The point of intersection of R-factor and performance point for life safety & collapse prevention is located in Ist quadrant so there is no need to retrofit the building according to the "Quadrants assessment method".

6.3.14 Seismic investigation of model-14

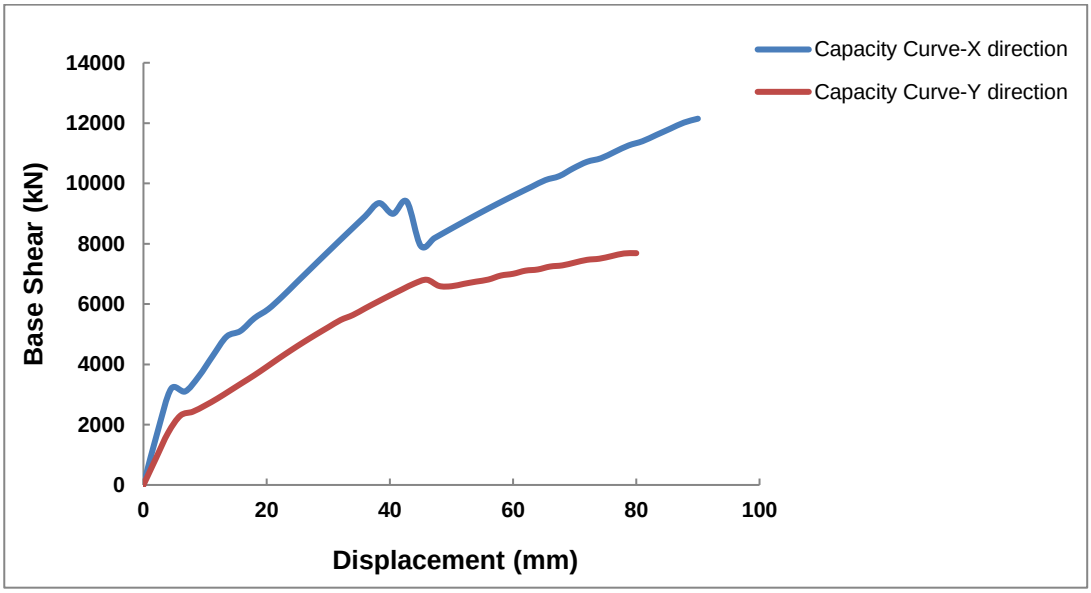

Figure 6.64 Capacity curves of model-14

As shown in Figure 6.64, the ultimate capacity of the building is higher in the X direction as compared to the Y direction due to the structural configuration of the building, and the remaining parameters are discussed in Table 6.29. The performance points of model-14 in X and Y direction are shown in Table 6.30 for life safety and collapse prevention purpose.

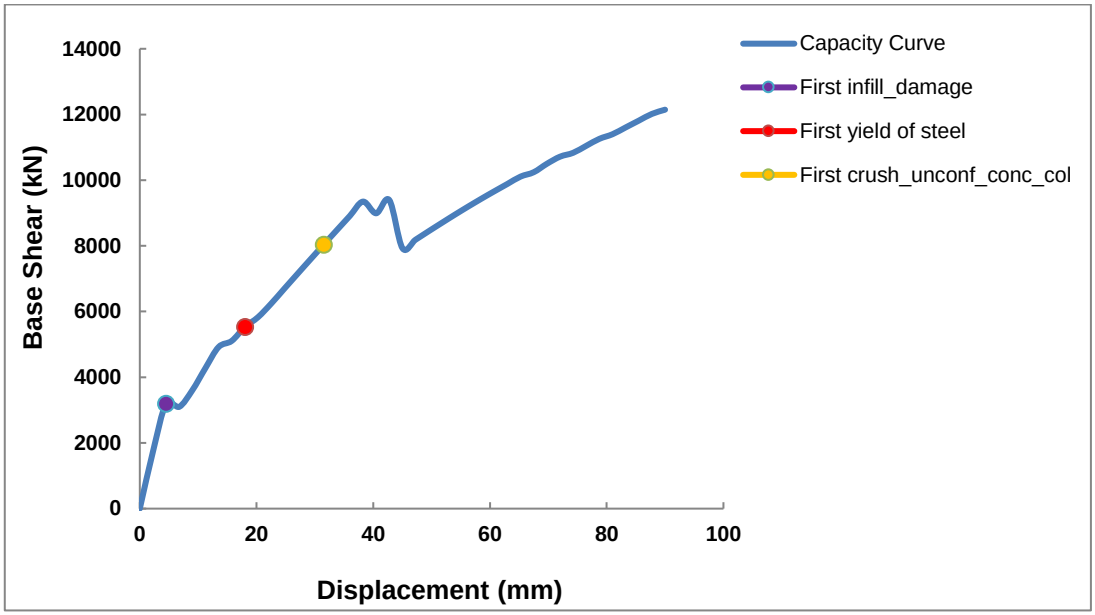

Figure 6.65 Damage pattern of Model-14 in the X direction

Figure 6.65 shows the damage pattern of model-14 in the X direction. The first infill damage occurred at a base shear 3193.12 kN and displacement of 4.5 mm. The first yielding of steel occurred at a base shear 5528.36 kN and displacement of 18 mm. The first crushing of the unconfined concrete column occurred at a base shear 8035.43 kN and displacement of 31.5 mm.

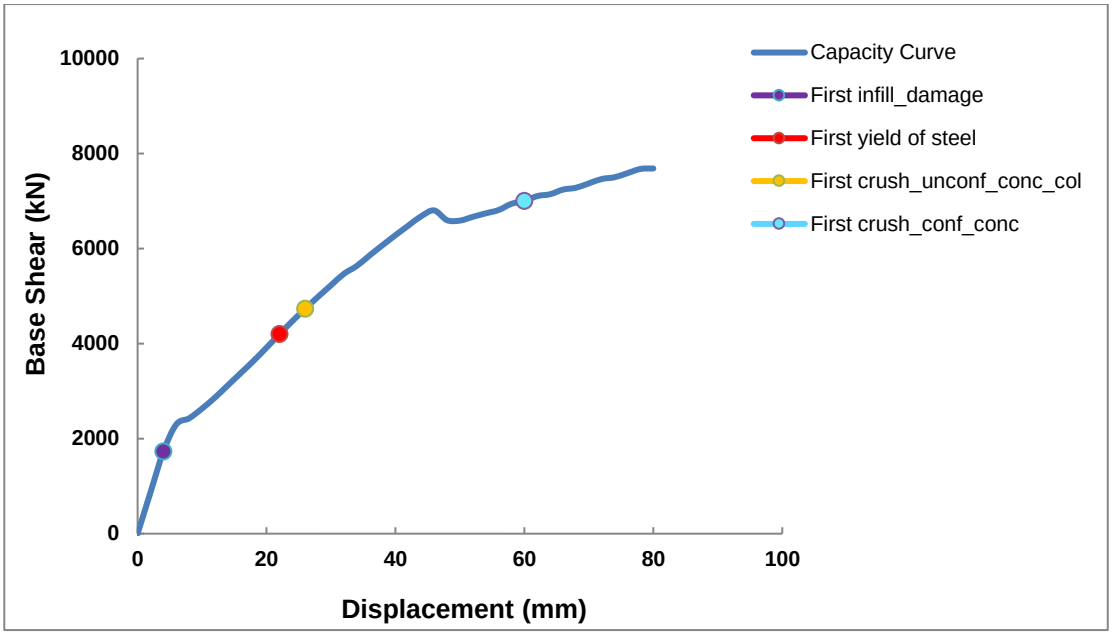

Figure 6.66 Damage pattern of Model-14 in the Y direction

Figure 6.66 shows the damage pattern of model-14 in the Y direction. The first infill damage occurred at a base shear 1729.1 kN and displacement of 4 mm. The first yielding of steel occurred at a base shear 4199.09 kN and displacement of 22 mm. The first crushing of the unconfined concrete column occurred at a base shear 4735.42 kN and displacement of 26 mm. The first crushing of confined concrete occurred at a base shear 7002.42 kN and displacement of 60 mm.

Table 6.29 Comparison of different parameters of Model-14			
Parameters			Remarks
	In X-axis	In Y-axis	
Ultimate capacity(kN)	12145.42	7686.58	The ultimate capacity increases by 1.58 times in X-axis as compared to Y-axis
Yield displacement (mm)	24.44	33.80	The yield displacement decreases by 27.69 % in X-axis as compared to Y-axis
Maximum Displacement (mm)	90.00	80.00	The maximum displacement increases by 12.5 % in X-axis as compared to Y-axis
Ductility	3.68	2.37	The ductility increases by 55.27 % in X-axis as compared to Y-axis
Ductility Reduction Factor	2.52	1.93	The ductility reduction factor increases by 30.56 % in X axis as compared to Y-axis
Overstrength factor	8.02	5.08	The overstrength factor increases by 57.87 % in X-axis as compared to Y-axis
Time period (sec)	0.26	0.26	The time period is same in X and Y direction
R-factor	10.1	4.9	The R-factor increases by 106.12 % in X-axis as compared to Y-axis

Table 6.30 Performance points of model-14 in X and Y direction				
Performance level	Displacement (mm**)**		Corresponding Base Shear (kN)	
	X direction	Y direction	X direction	Y direction
Life Safety	0.63	3.31	484.77	1433.10
Collapse Prevention	3.88	8.62	2790.32	2492.03

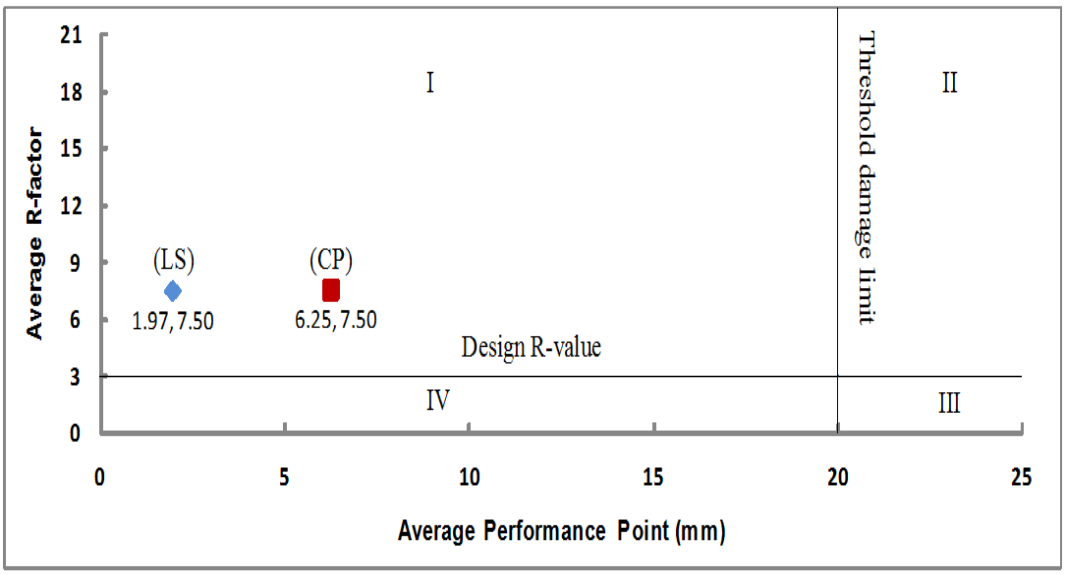

Figure 6.67 Average R-factor versus average performance point graph of model-14

Figure 6.67 shows the average R-factor versus average performance point graph of model-14. The point of intersection of R-factor and performance point for life safety & collapse prevention is located in Ist quadrant so there is no need to retrofit the building according to the "Quadrants assessment method".

6.3.15 Seismic investigation of model-15

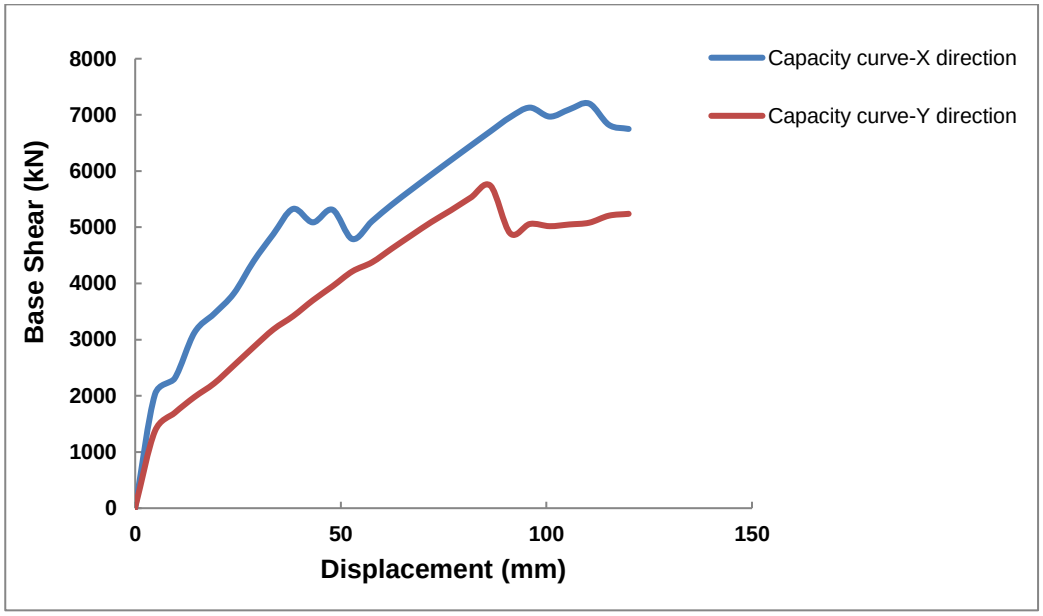

Figure 6.68 Capacity curves of model-15

As shown in Figure 6.68, the ultimate capacity of the building is higher in the X direction as compared to the Y direction due to the structural configuration of the building, and the remaining parameters are discussed in Table 6.31. The performance points of model-15 in X and Y direction are shown in Table 6.32 for life safety and collapse prevention purpose.

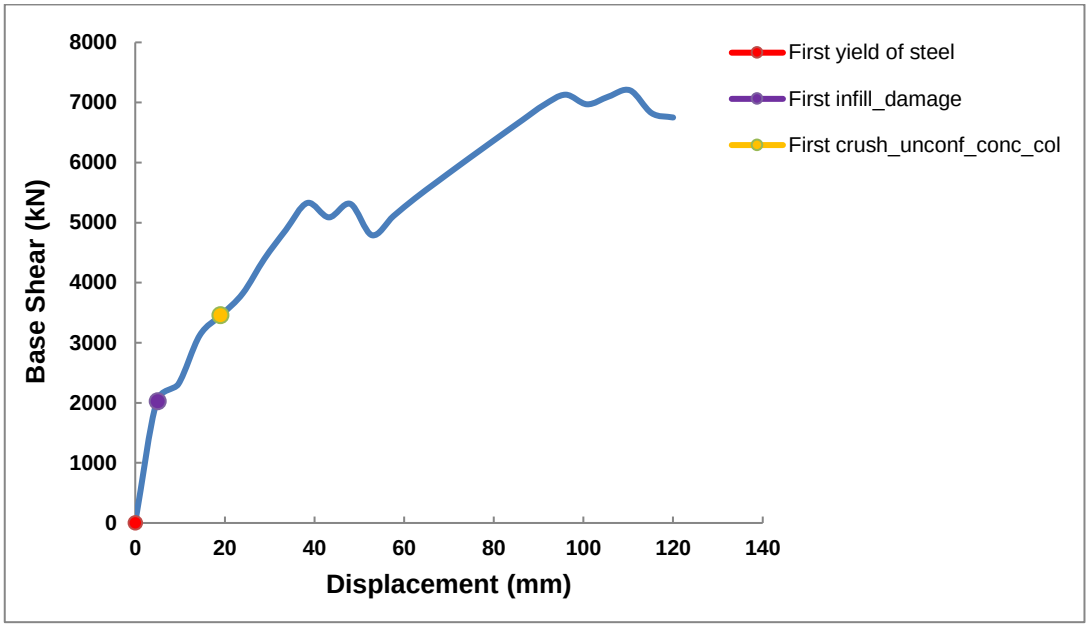

Figure 6.69 Damage pattern of Model-15 in the X direction

Figure 6.69 shows the damage pattern of model-15 in the X direction. The first yielding of steel occurred at a base shear 0 kN and displacement of 0 mm due to less steel. The first infill damage occurred at a base shear 2024.95 kN and displacement of 5 mm. The first crushing of the unconfined concrete column occurred at a base shear 3460.67 kN and displacement of 19 mm.

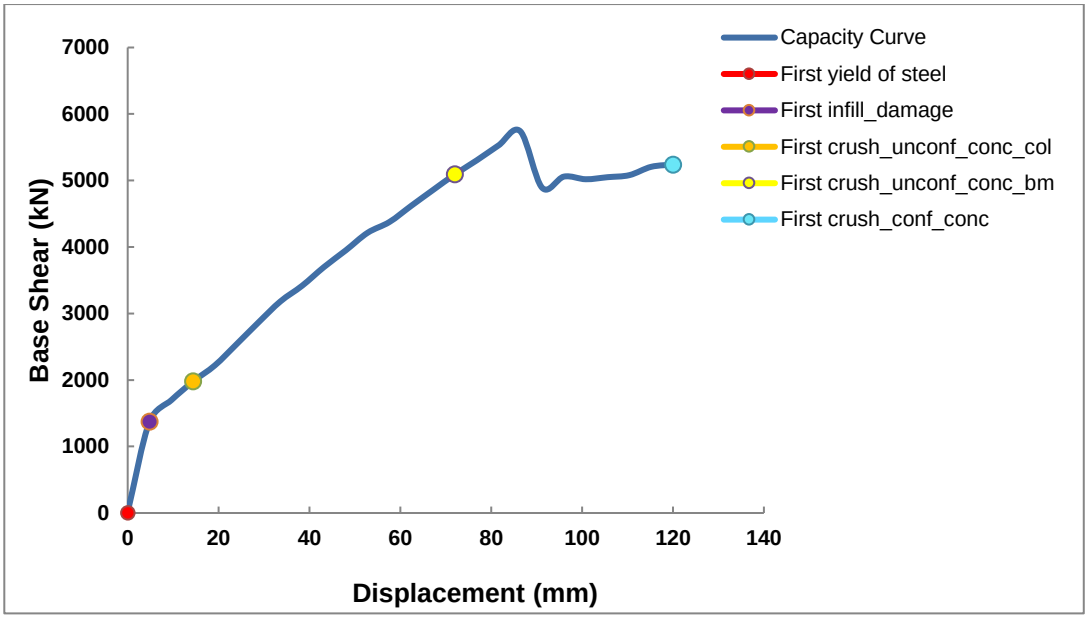

Figure 6.70 Damage pattern of Model-15 in the Y direction

Figure 6.70 shows the damage pattern of model-15 in the Y direction. The first yielding of steel occurred at a base shear 0 kN and displacement of 0 mm due to less steel. The first infill damage occurred at a base shear 1372.40 kN and displacement of 4.8 mm. The first crushing of the unconfined concrete column occurred at a base shear 1978.16 kN and displacement of 14.4 mm. The first crushing of the unconfined concrete beam occurred at a base shear 5091.98 kN and displacement of 72 mm. The first crushing of the confined concrete occurred at a base shear 5239.03 kN and displacement of 120 mm.

Table 6.31 Comparison of different parameters of Model-15			
Parameters			Remarks
	In X-axis	In Y-axis	
Ultimate capacity(kN)	7201.49	5739.61	The ultimate capacity increases by 1.25 times in X-axis as compared to Y-axis
Yield displacement (mm)	22.46	62.46	The yield displacement decreases by 64.04 % in X-axis as compared to Y-axis
Maximum Displacement (mm)	110.40	86.40	The maximum displacement increases by 27.77 % in X-axis as compared to Y-axis
Ductility	4.92	1.38	The ductility increases by 256.52 % in X-axis as compared to Y-axis
Ductility Reduction Factor	2.97	1.32	The ductility reduction factor increases by 125 % in X axis as compared to Y-axis
Overstrength factor	5.93	4.73	The overstrength factor increases by 25.36 % in X-axis as compared to Y-axis
Time period (sec)	0.3	0.30	The time period is same in X and Y direction
R-factor	8.8	3.12	The R-factor increases by 182.05 % in X-axis as compared to Y-axis

Table 6.32 Performance points of model-15 in X and Y direction				
Performance level	Displacement (mm**)**		Corresponding Base Shear (kN)	
	X direction	Y direction	X direction	Y direction
Life Safety	4.47	7.12	1885.78	1529.09
Collapse Prevention	10.2	13.18	2412.08	1906.58

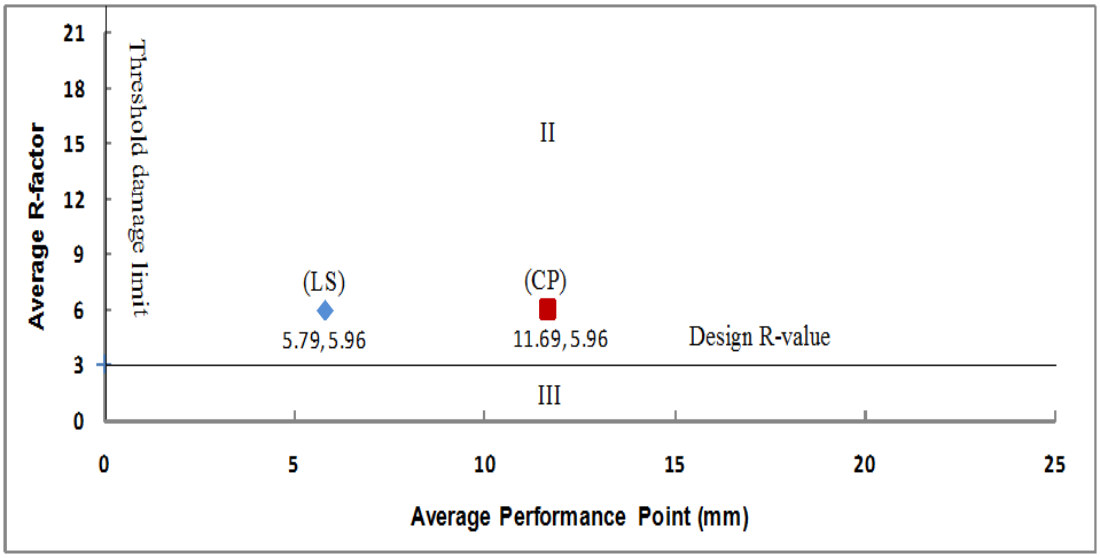

Figure 6.71 Average R-factor versus average performance point graph of model-15

Figure 6.71 shows the average R-factor versus average performance point graph of model-15. The point of intersection of R-factor and performance point for life safety & collapse prevention is located in IInd quadrant so there is need to retrofit the building according to the "Quadrants assessment method".

6.3.16 Seismic investigation of model-16

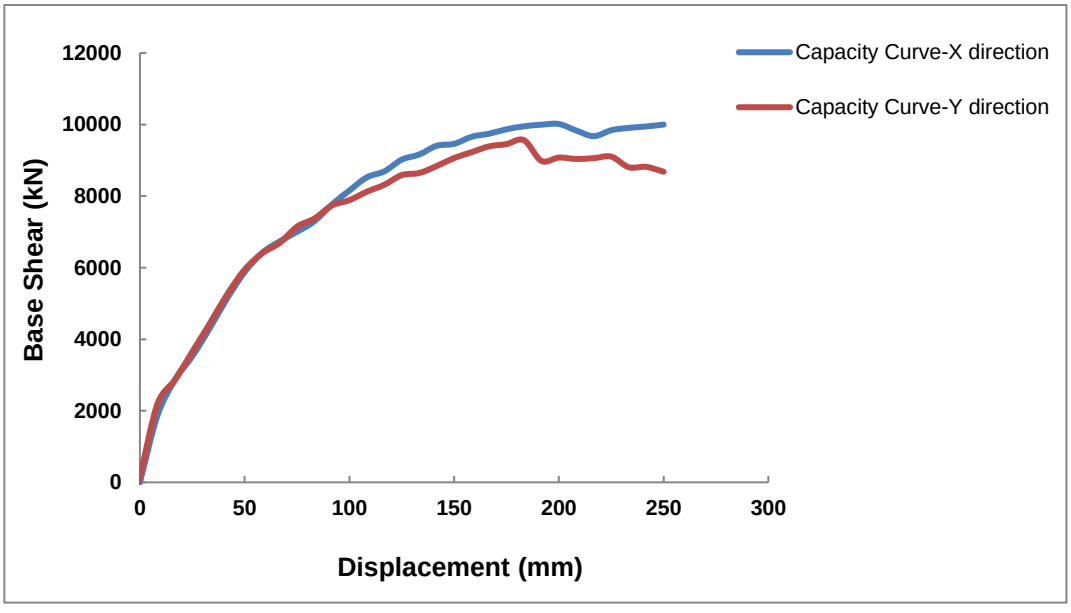

Figure 6.72 Capacity curves of model-16

As shown in Figure 6.72, the ultimate capacity of the building is higher in the X direction as compared to the Y direction due to the structural configuration of the building, and the remaining parameters are discussed in Table 6.33. The performance points of model-16 in X and Y direction are shown in Table 6.34 for life safety and collapse prevention purpose.

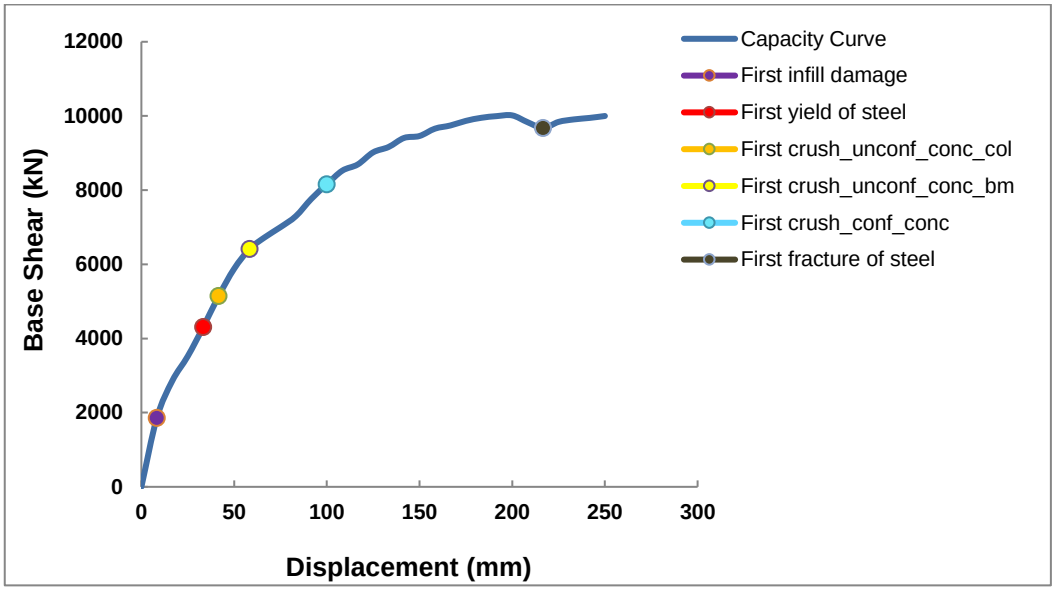

Figure 6.73 Damage pattern of Model-16 in the X direction

Figure 6.73 shows the damage pattern of model-16 in the X direction. The first infill damage occurred at a base shear 1858.26 kN and displacement of 8.33mm. The first yielding of steel occurred at a base shear 4305.61 kN and displacement of 33.33 mm. The first crushing of the unconfined concrete column occurred at a base shear 5142.88 kN and displacement of 41.66 mm. The first crushing of the unconfined concrete beam occurred at a base shear 6412.66 kN and displacement of 58.33 mm. The first crushing of the confined concrete occurred at a base shear 8156.22 kN and displacement of 100 mm. The first fracture of steel occurred at a base shear 9674.76 kN and displacement of 216.66 mm.

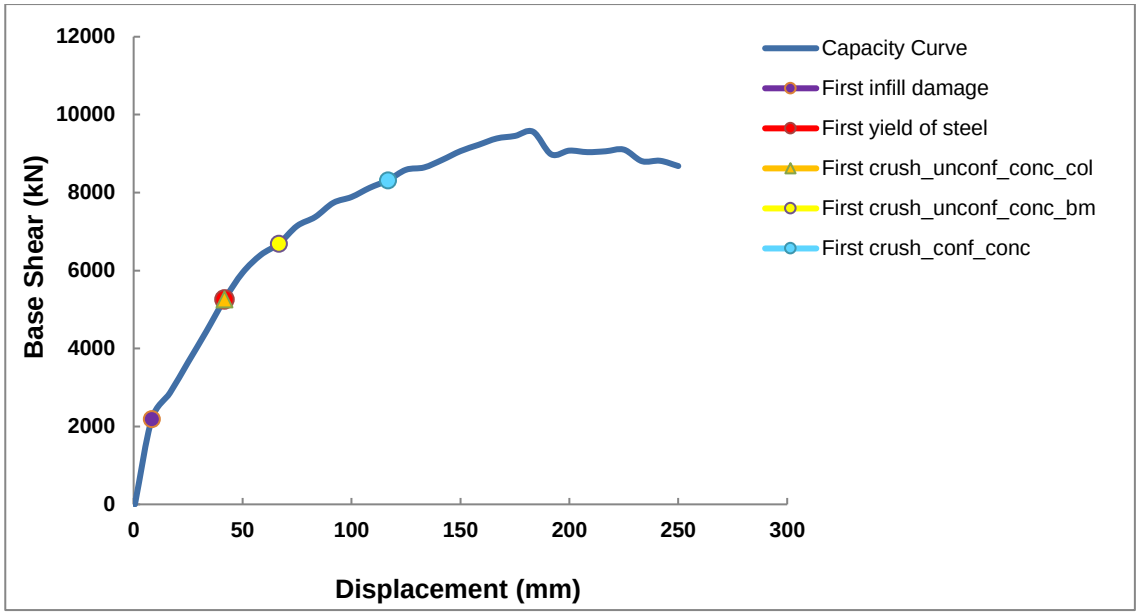

Figure 6.74 Damage pattern of Model-16 in the Y direction

Figure 6.74 shows the damage pattern of model-16 in the Y direction. The first infill damage occurred at a base shear 2186.78 kN and displacement of 8.33 mm. The first yielding of steel & first crushing of the unconfined concrete column occurred at a base shear 5254.79 kN and displacement of 41.67 mm. The first crushing of the unconfined concrete beam occurred at a base shear 6690.06 kN and displacement of 66.67 mm. The first crushing of the confined concrete occurred at a base shear 8315.30 kN and displacement of 116.67 mm.

Table 6.33 Comparison of different parameters of Model-16			
Parameters			Remarks
	In X-axis	In Y-axis	
Ultimate capacity(kN)	10014.52	9562.55	The ultimate capacity increases by 1.04 times in X-axis as compared to Y-axis
Yield displacement (mm)	65.80	57.89	The yield displacement decreases by 12.02 % in Y-axis as compared to X-axis
Maximum Displacement (mm)	200.00	183.33	The maximum displacement increases by 9.09 % in X-axis as compared to Y-axis
Ductility	3.04	3.17	The ductility increases by 4.27 % in Y-axis as compared to X-axis
Ductility Reduction Factor	2.25	2.31	The ductility reduction factor increases by 2.66 % in Y axis as compared to X-axis
Overstrength factor	5.46	5.21	The overstrength factor increases by 4.79 % in X-axis as compared to Y-axis
Time period (sec)	0.43	0.43	The time period is same in X and Y direction
R-factor	6.14	6.01	The R-factor increases by 2.16 % in X-axis as compared to Y-axis

Table 6.34 Performance points of model-16 in X and Y direction				
Performance level	Displacement (mm**)**		Corresponding Base Shear (kN)	
	X direction	Y direction	X direction	Y direction
Life Safety	14.5	14.46	2597.98	2682.89
Collapse Prevention	24.25	24.06	3460.11	3560.48

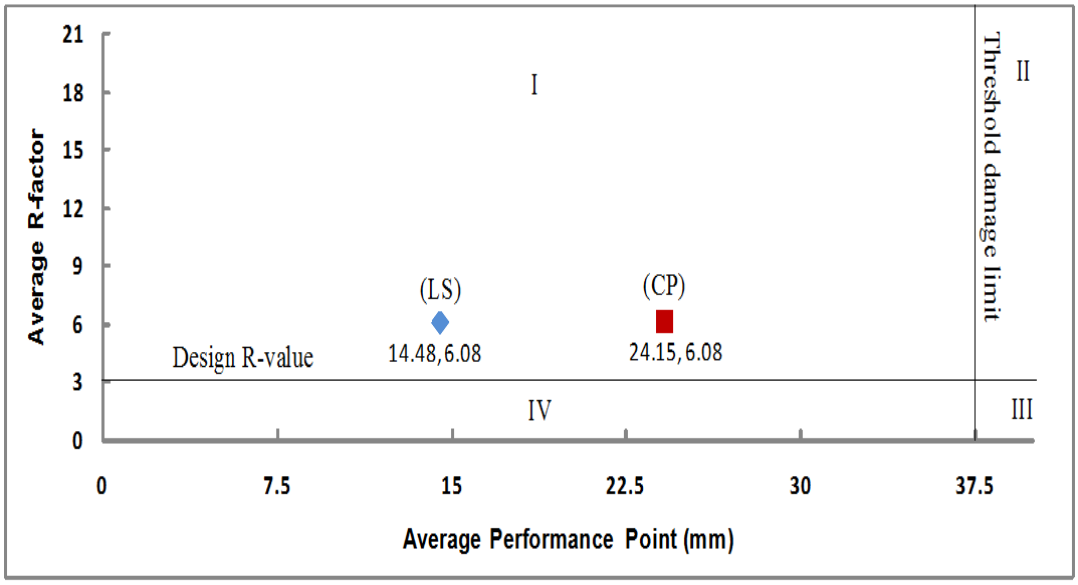

Figure 6.75 Average R-factor versus average performance point graph of model-16

Figure 6.75 shows the average R-factor versus average performance point graph of model-16. The point of intersection of R-factor and performance point for life safety & collapse prevention is located in Ist quadrant so there is no need to retrofit the building according to the "Quadrants assessment method".

6.3.17 Seismic investigation of model-17

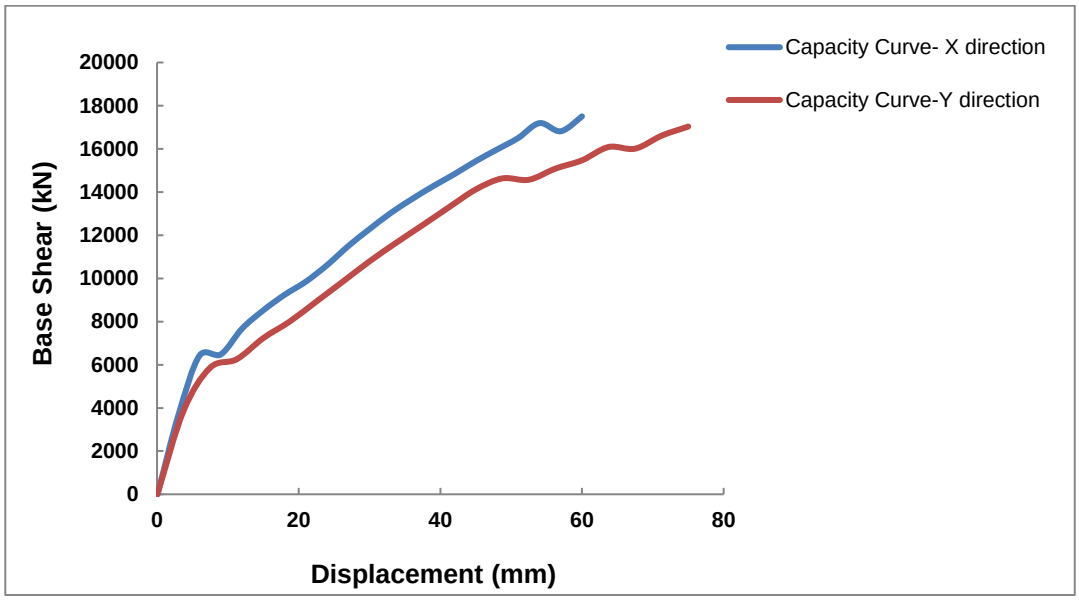

Figure 6.76 Capacity curves of model-17

As shown in Figure 6.76, the ultimate capacity of the building is higher in the X direction as compared to the Y direction due to the structural configuration of the building, and the remaining parameters are discussed in Table 6.35. The performance points of model-17 in X and Y direction are shown in Table 6.36 for life safety and collapse prevention purpose.

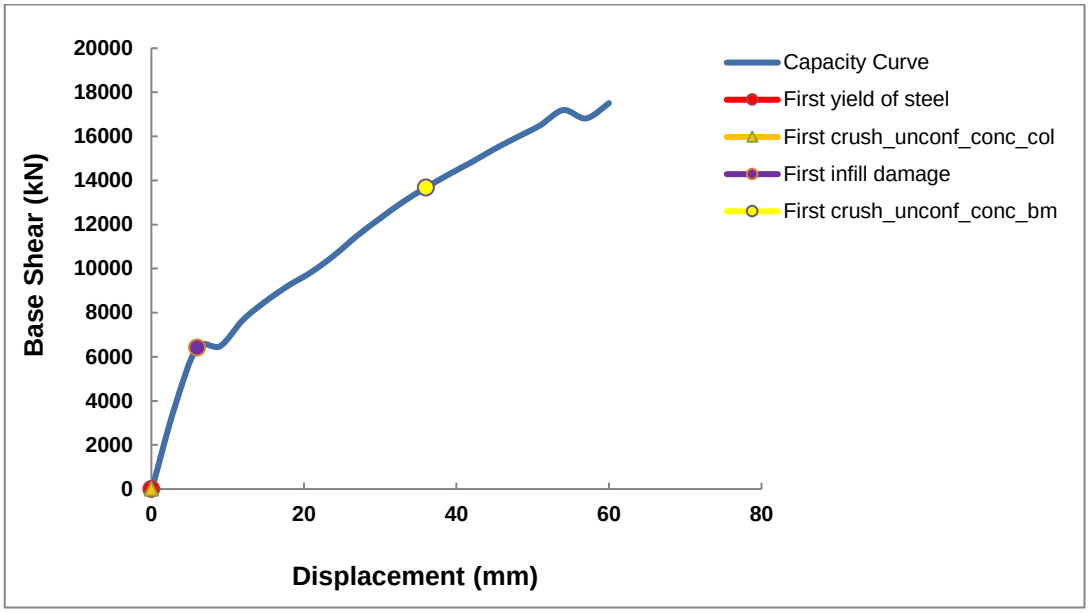

Figure 6.77 Damage pattern of Model-17 in the X direction

Figure 6.77 shows the damage pattern of model-17 in the X direction. The first infill damage occurred at a base shear 6424.24 kN and displacement of 6 mm. The first yielding of steel & first crushing of the unconfined concrete column occurred at a base shear 0 kN and displacement of 0 mm due to the provision of less steel in column. The first crushing of the unconfined concrete beam occurred at a base shear 13674.53 kN and displacement of 36 mm.

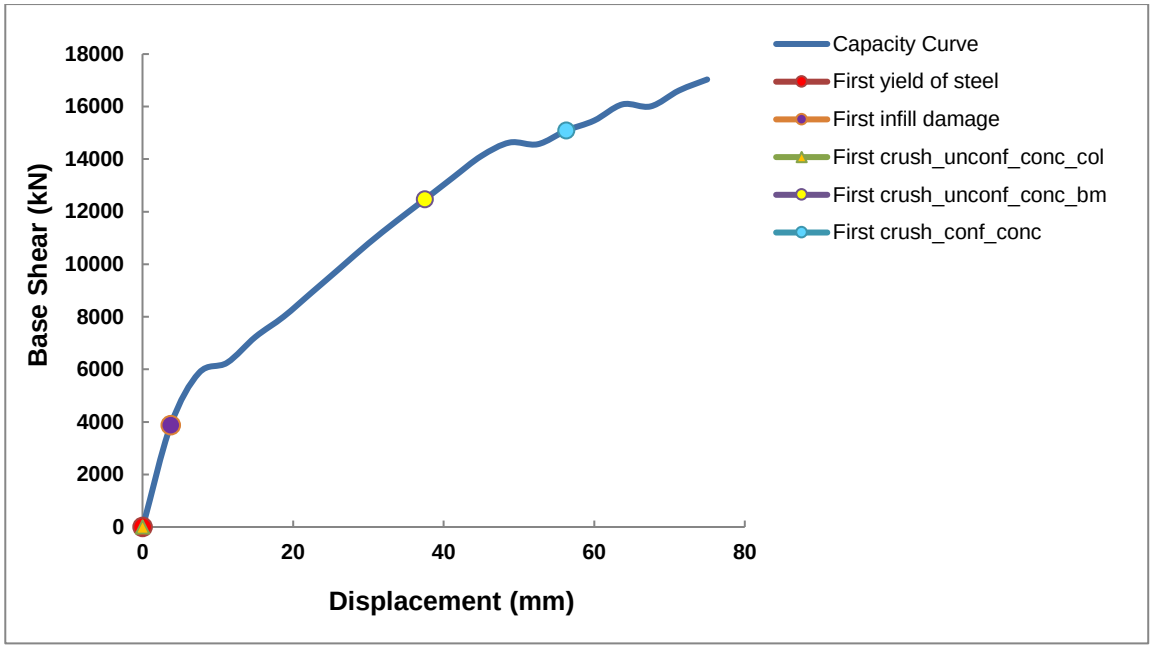

Figure 6.78 Damage pattern of Model-17 in the Y direction

Figure 6.78 shows the damage pattern of model-17 in the Y direction. The first infill damage occurred at a base shear 3874.89 kN and displacement of 3.75 mm. The first yielding of steel & first crushing of the unconfined concrete column occurred at a base shear 0 kN and displacement of 0 mm due to the provision of less steel in column. The first crushing of the unconfined concrete beam occurred at a base shear 12468.62 kN and displacement of 37.50 mm. The first crushing of the confined concrete occurred at a base shear 15084.82 kN and displacement of 56.25 mm.

Table 6.35 Comparison of different parameters of Model-17			
Parameters			Remarks
	In X-axis	In Y-axis	
Ultimate capacity(kN)	17506.56	17032.08	The ultimate capacity increases by 1.02 times in X-axis as compared to Y-axis
Yield displacement (mm)	39.22	47.91	The yield displacement decreases by 18.13 % in X-axis as compared to Y-axis
Maximum Displacement (mm)	60.00	75.00	The maximum displacement increases by 25 % in Y-axis as compared to X-axis
Ductility	1.53	1.57	The ductility increases by 2.61 % in Y-axis as compared to X-axis
Ductility Reduction Factor	1.43	1.46	The ductility reduction factor increases by 2.09 % in Y axis as compared to X-axis
Overstrength factor	4.38	4.26	The overstrength factor increases by 2.81 % in X-axis as compared to Y-axis
Time period (sec)	0.29	0.29	The time period is same in X and Y direction
R-factor	3.13	3.1	The R-factor increases by 0.96 % in X-axis as compared to Y-axis

Table 6.36 Performance points of model-17 in X and Y direction				
Performance level	Displacement (mm**)**		Corresponding Base Shear (kN)	
	X direction	Y direction	X direction	Y direction
Life Safety	6.96	7.53	6441.23	5862.60
Collapse Prevention	13.14	13.96	7994.09	6961.77

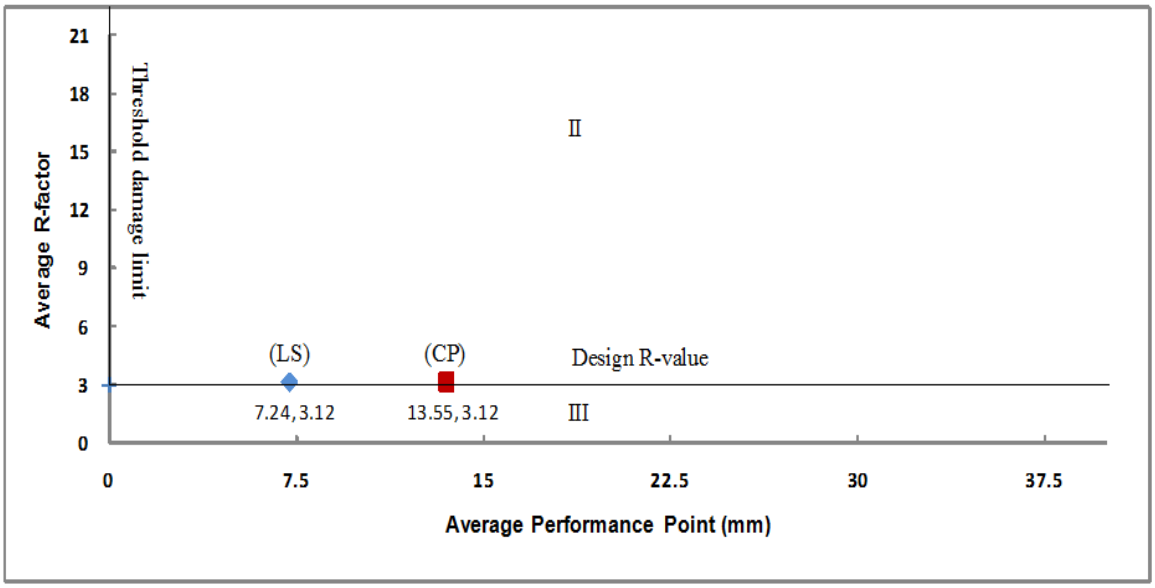

Figure 6.79 Average R-factor versus average performance point graph of model-17

Figure 6.79 shows the average R-factor versus average performance point graph of model-17. The point of intersection of R-factor and performance point for life safety & collapse prevention is located in IInd quadrant so there is need to retrofit the building according to the "Quadrants assessment method".

6.4 Strengthening RC buildings

6.4.1 Retrofit of model-1

A retrofit strategy in accordance with IS 15988:2013 is used to strengthen each deficient structure based on its current deficiencies. Several retrofit strategies may be selected as a retrofit scheme for the structure:

1. Local retrofit: RC jacketing, steel jacketing.
2. Global retrofit: Addition of infills, shear walls, steel braces.

Among the above discussed strategies, RC jacketing is used for the deficient column members with a crushing of the core concrete and having fractured steel failure. In this retrofit technique, M25 concrete is used for jacketing, and the additional steel is used at the corners

and at centre of longer side (6 no. of 16mm diameter steel). 8 mm diameter of stirrups used at 100 mm spacing c/c. The size of the retrofitted columns is 430×580 mm and 430×650 mm, as shown in Figures 6.80 (a) and 6.80 (b) respectively. The same retrofitting plan of the building is shown in Figure 6.81.

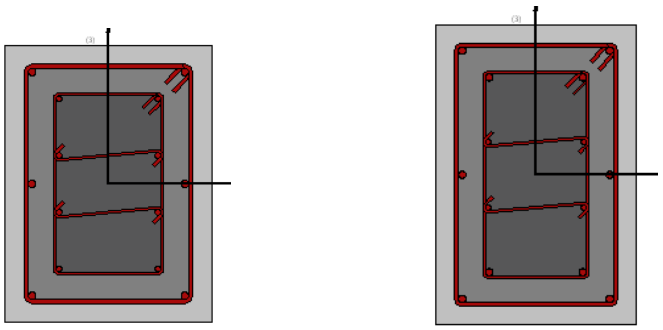

(a) (b)

Figure 6.80 The cross-sections of the columns after the retrofit: (a) 430×580 mm, (b) 430×650 mm.

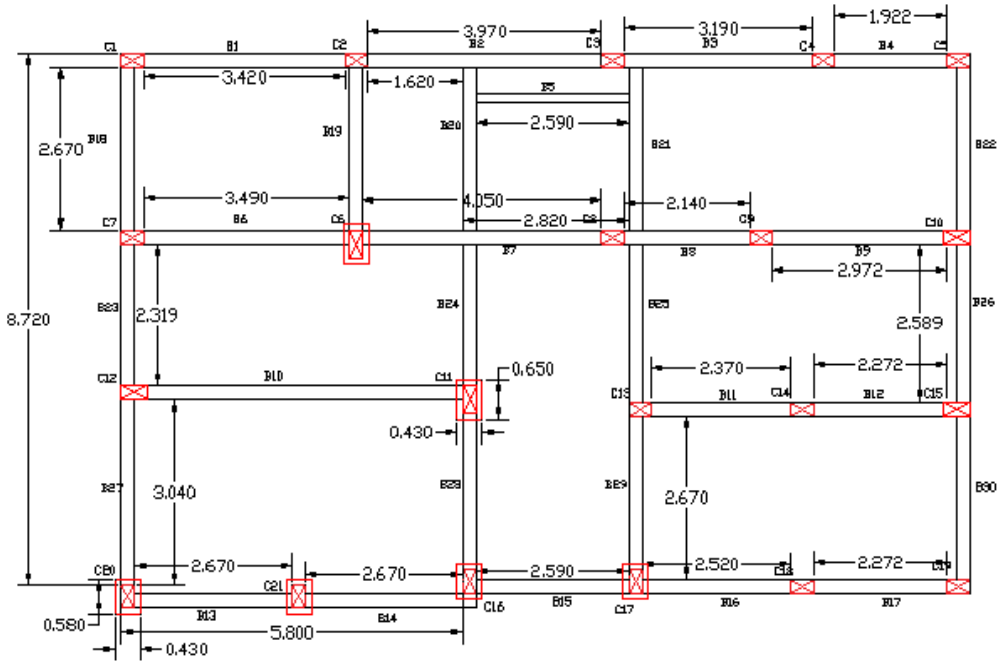

Figure 6.81 Retrofitted plan of Model-1 (units in m).

6.4.1.1 Capacity curves of model-1 before and after the retrofit

As shown in Figure 6.82, the ultimate capacity of the building is increased after the retrofit in the X as well as the Y direction, and the remaining parameters are discussed in Table 6.37. The performance points of model-1 before & after the retrofit in X and Y direction are shown in Table 6.38.

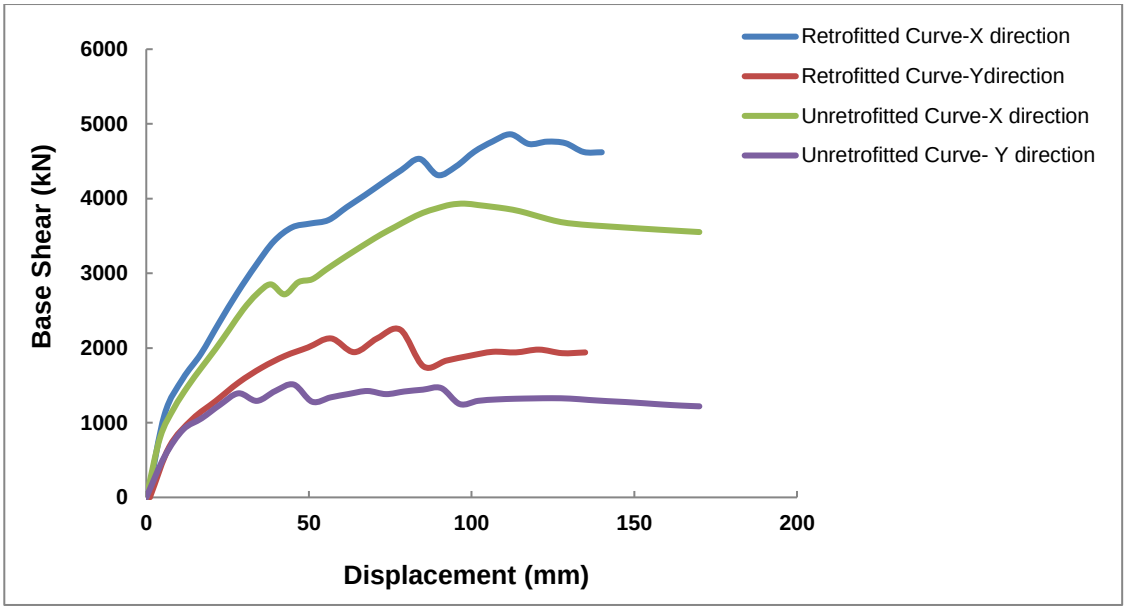

Figure 6.82 Capacity curves of model-1 with and without retrofit.

Table 6.37 Comparison of different parameters of Model-1 before and after the retrofit					
Parameters	Before retrofit		After retrofit		Remarks
	In X-axis	In Y-axis	In X-axis	In Y-axis	
Ultimate capacity (kN)	3933.15	1510.65	4861.01	2244.71	After the retrofit, the ultimate capacity is increased by1.23 times in X-axis and 1.48 times in Y-axis.
Yield displacement (mm)	26.40	13.10	36.06	23.12	After the retrofit, the yield displacement is increased by 1.36 times in X-axis and 1.76 times in Y-axis.
Maximum Displacement (mm)	97.75	45.33	112	78.10	After the retrofit, the maximum displacement is increased by1.14 times in X-axis and 1.72 times in Y-axis.
Ductility	3.70	3.46	3.11	3.38	After the retrofit, the ductility is decreased by 15.94% in X-axis and 2.31% in the Y-axis.
Ductility Reduction Factor	2.53	2.43	2.28	2.40	After the retrofit, the ductility reduction factor is decreased by 9.88% in X-axis and 1.23 % in Y-axis.
Overstrength factor	7.77	2.99	9.47	4.37	After the retrofit, the overstrength factor is increased by 1.21 times in the X-axis and 1.46 times in Y-axis.
Time period (sec)	0.39	0.39	0.34	0.34	After the retrofit, the time period is decreased by 12.82 % in X-axis and Y-axis.
R-factor	9.82	3.63	10.79	5.25	After the retrofit, the R-factor is increased by 1.09 times in X-axis and 1.45 times in Y-axis.

Table 6.38 Performance points of model-1 before & after the retrofit in X and Y direction				
Performance level	Before Retrofit		After Retrofit	
	Displacement (mm)		Displacement (mm)	
	X direction	Y direction	X direction	Y direction
Life Safety	10.62	12.07	7.62	7.9
Collapse Prevention	18.22	25.96	13.53	17.85

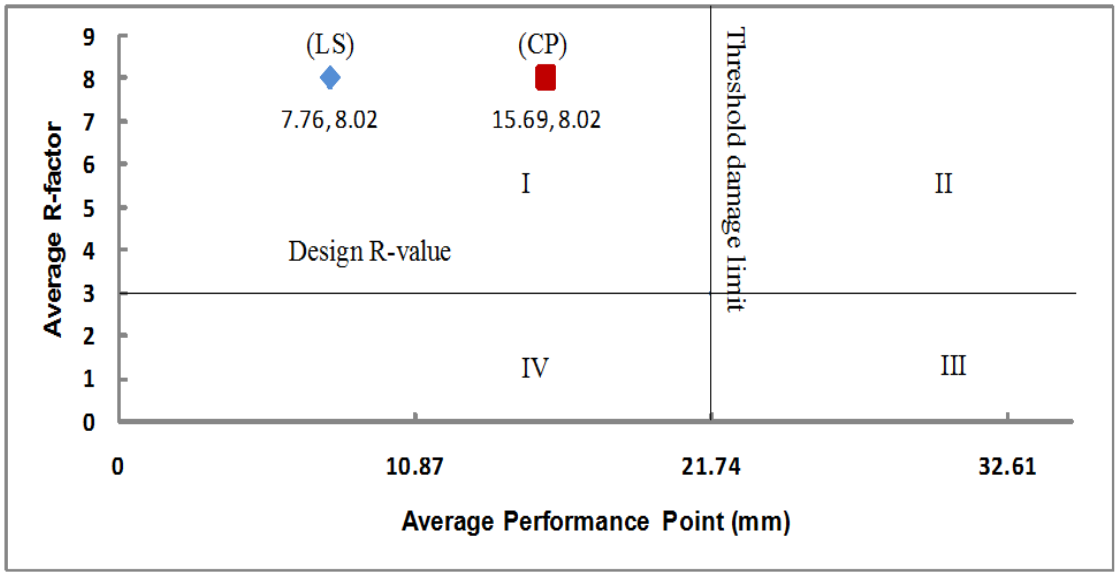

Figure 6.83 Average R-factor versus average performance point graph of model-1 after the retrofit

Figure 6.83 shows the average R-factor versus average performance point graph of model-1 after the retrofit. The point of intersection of R-factor and performance point for life safety & collapse prevention is located in Ist quadrant after the retrofit of building so the structure is in safe zone according to the "Quadrants assessment method".

6.4.2 Retrofit of model-15

Among the different retrofit techniques discussed in section 6.4.1, one sided RC-jacketing is used for the deficient column members having less steel provided the other three sides are not easily accessible; therefore one sided retrofitting has been attempted. In this retrofit technique, M20 concrete is used for jacketing, and the additional steel is used at one side of the column (2 no. of 16 mm diameter steel at corners and 1 no. of 12 mm diameter steel at the center of shorter side). 8 mm diameter of stirrups used at 100 mm spacing c/c. The size of the retrofitted columns is 250×600 mm as shown in Figures 6.84. The same retrofitting plan of the building is shown in Figure 6.85.

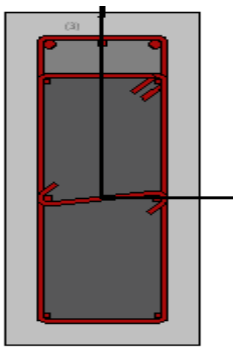

Figure 6.84 The cross-section of the column after the retrofit: (a) 250×600 mm

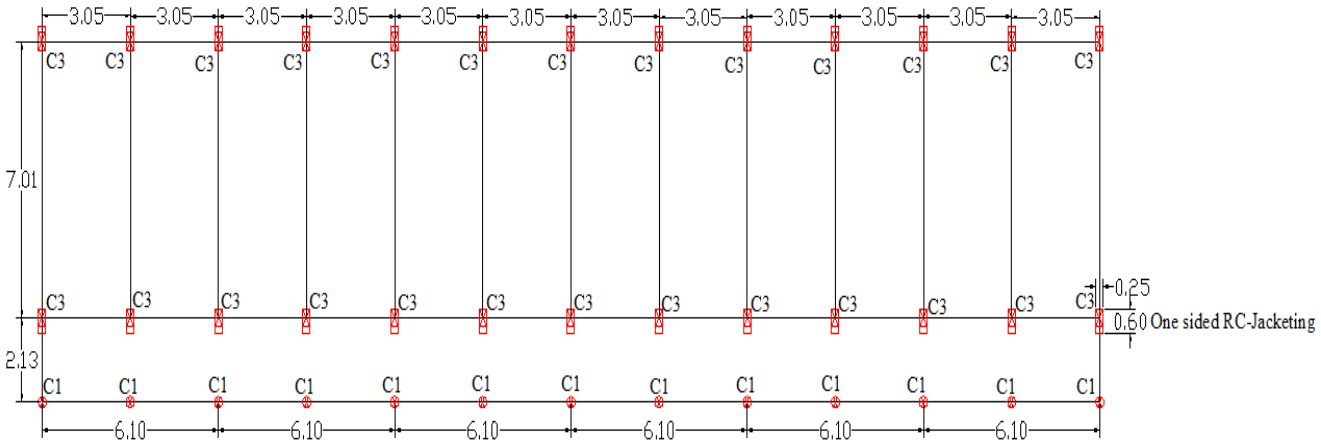

(a) Retrofitted plan of ground floor

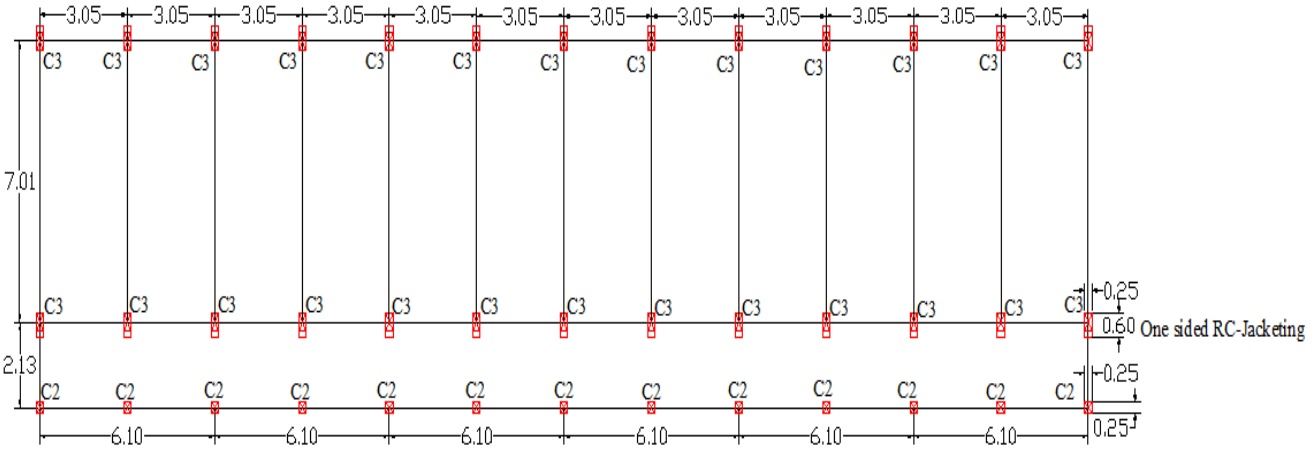

(b) Retrofitted plan of 1st floor

Figure 6.85 Retrofitted plan of Model-15 (units in m)

6.4.2.1 Capacity curves of model-15 before and after the retrofit

As shown in Figure 6.86, the ultimate capacity of the building is increased after the retrofit in the X as well as the Y direction, and the remaining parameters are discussed in Table 6.39. The performance points of model-15 before & after the retrofit in X and Y direction are shown in Table 6.40.

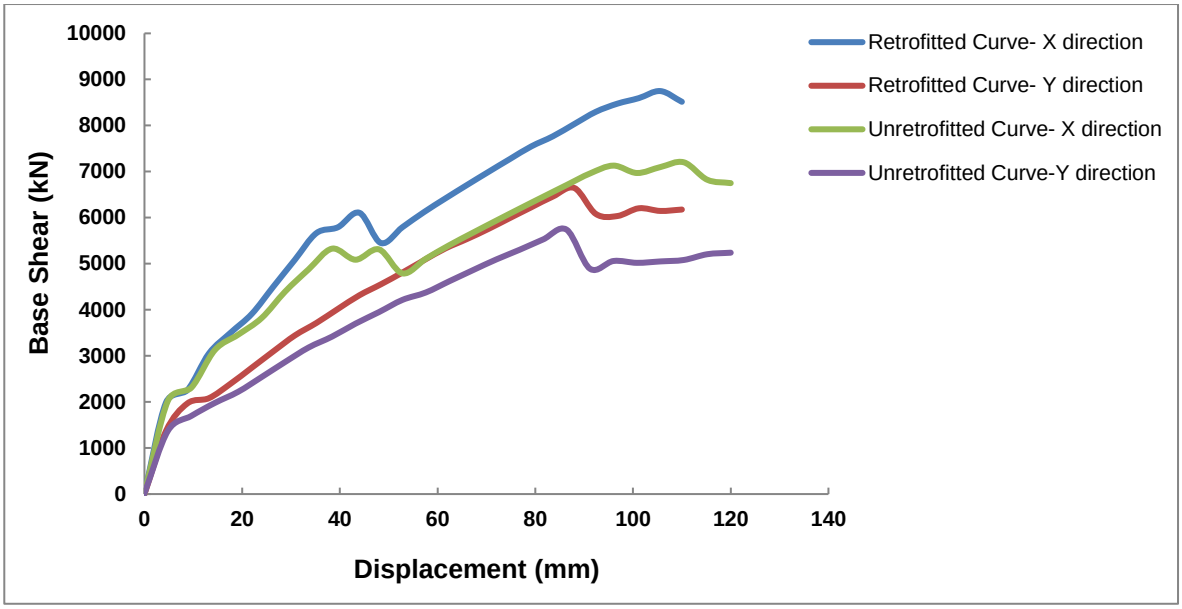

Figure 6.86 Capacity curves of model-15 with and without retrofit.

Table 6.39 Comparison of different parameters of Model-15 before and after the retrofit					
Parameters	Before retrofit		After retrofit		Remarks
	In X-axis	In Y-axis	In X-axis	In Y-axis	
Ultimate capacity (kN)	7201.49	5739.61	8747.67	6643.32	After the retrofit, the ultimate capacity is increased by 1.21 times in X-axis and 1.15 times in Y-axis.
Yield displacement (mm)	22.46	62.46	28.85	65.21	After the retrofit, the yield displacement is increased by 1.28 times in X-axis and 1.04 times in Y-axis.
Maximum Displacement (mm)	110.40	86.40	105.6	88	After the retrofit, the maximum displacement is decreased by 4.34 % times in X-axis and increased by 1.85% times in Y-axis.
Ductility	4.92	1.38	3.66	1.35	After the retrofit, the ductility is decreased by 25.60 % in X-axis and 2.17 % in the Y-axis.
Ductility Reduction Factor	2.97	1.32	2.51	1.30	After the retrofit, the ductility reduction factor is decreased by 15.48 % in X-axis and 1.51 % in Y-axis.
Overstrength factor	5.93	4.73	7.07	5.37	After the retrofit, the overstrength factor is increased by 1.19 times in the X-axis and 1.13 times in Y-axis.
Time period (sec)	0.3	0.3	0.27	0.27	After the retrofit, the time period is decreased by 10 % in X-axis and Y-axis.
R-factor	8.8	3.12	8.87	3.49	After the retrofit, the R-factor is increased by 1.01 times in X-axis and 1.12 times in Y- axis.

Table 6.40 Performance points of model-15 before & after the retrofit in X and Y direction				
Performance level	Before Retrofit		After Retrofit	
	Displacement (mm**)**		Displacement (mm**)**	
	X direction	Y direction	X direction	Y direction
Life Safety	4.47	7.12	1.44	4.8
Collapse Prevention	10.2	13.18	5.38	9.66

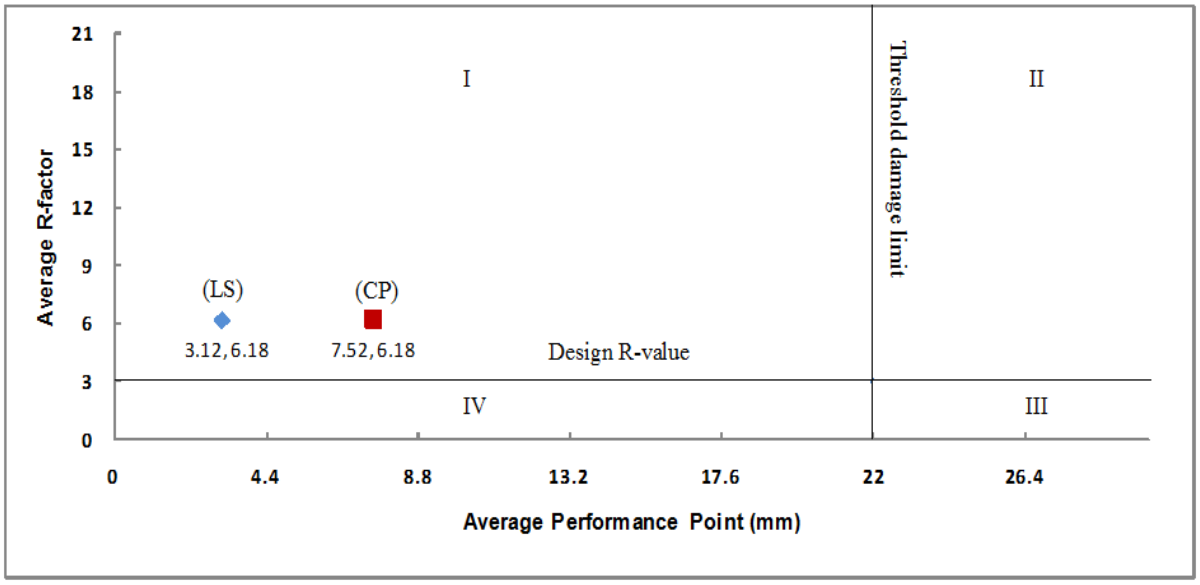

Figure 6.87 Average R-factor versus average performance point graph of model-15 after the retrofit

Figure 6.87 shows the average R-factor versus average performance point graph of model-15 after the retrofit. The point of intersection of R-factor and performance point for life safety & collapse prevention is located in Ist quadrant after the retrofit of building so the structure is in safe zone according to the "Quadrants assessment method".

6.4.3 Retrofit of model-17

Among the different retrofit techniques discussed in section 6.4.1, one sided and full sided RC-jacketing is used for the deficient column members having less steel provided. In this retrofit technique, M25 concrete is used for jacketing, and the additional steel is used at one sided RC-jacketing of the column (3 no. of 16 mm diameter steel). 8 mm diameter of stirrups used at 100 mm spacing c/c. Also, the additional steel is used at full sided RC-jacketing of the column (4 no of 20 mm diameter steel at corner, and 4 no of 16 mm diameter steel at middle side). The size of the retrofitted columns is shown in Figure 6.88 and the same retrofitting plan of the building is shown in Figure 6.89.

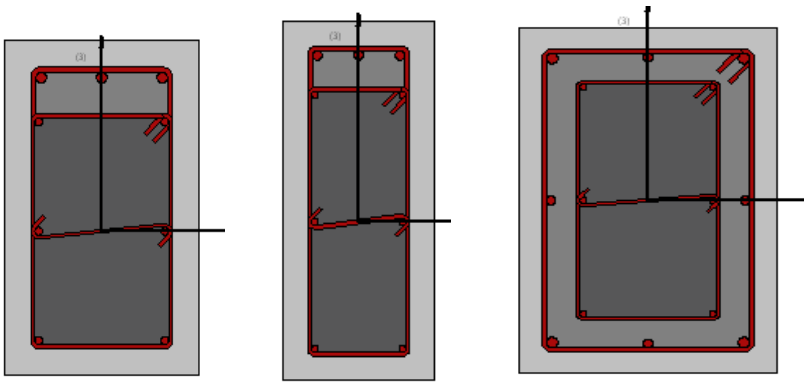

(a) (b) (c)

Figure 6.88 The cross-section of the column after the retrofit: (a) 300×500 mm, (b) 250×600 mm, (c) 450×650 mm

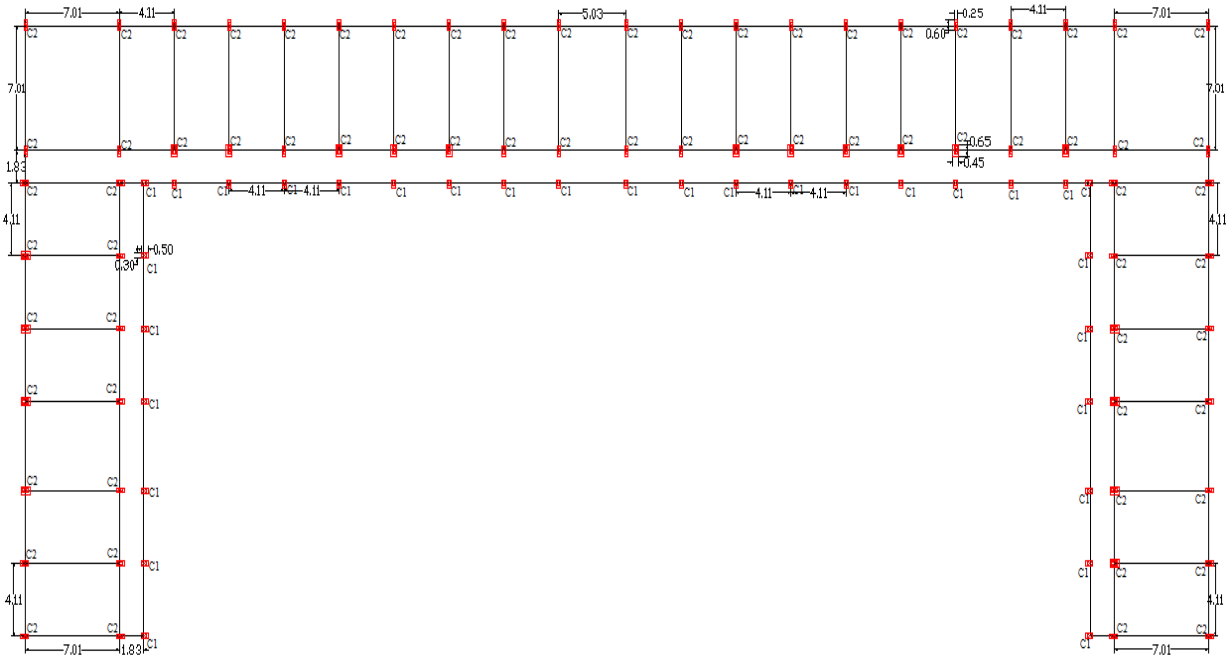

(a) Plan view of Model-17

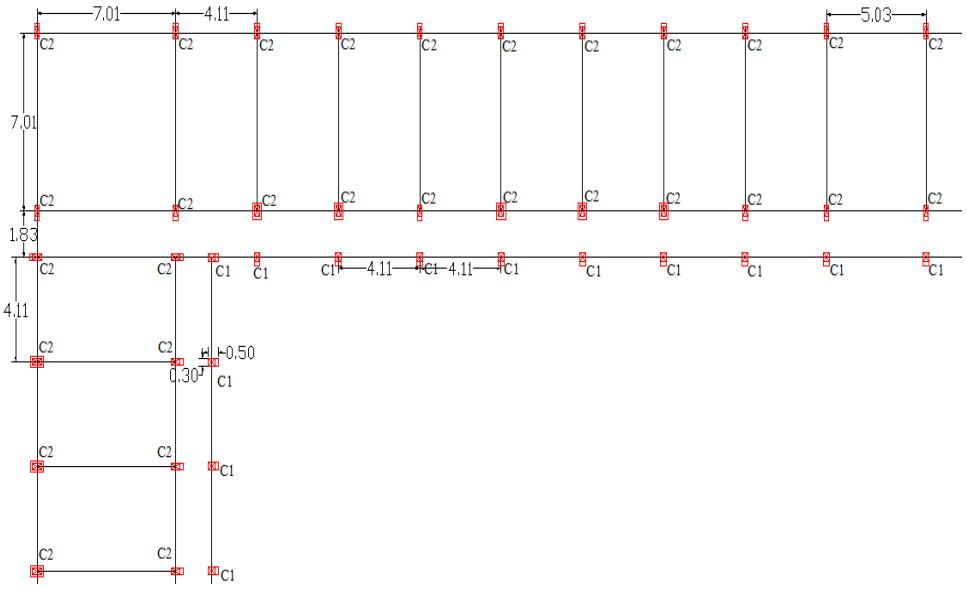

(b) Top left symmetrical view of Model-17

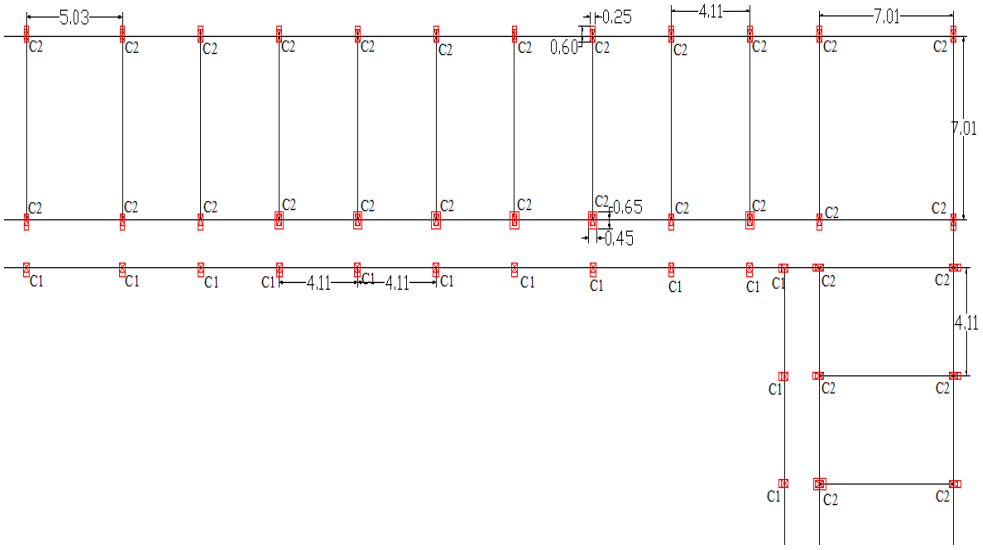

(c) Top right symmetrical view of Model-17

Figure 6.89 Retrofitted plan of Model-17 (units in m)

6.4.3.1 Capacity curves of model-17 before and after the retrofit

As shown in Figure 6.90, the ultimate capacity of the building is increased after the retrofit in the X as well as the Y direction, and the remaining parameters are discussed in Table 6.41. The performance points of model-17 before & after the retrofit in X and Y direction are shown in Table 6.42.

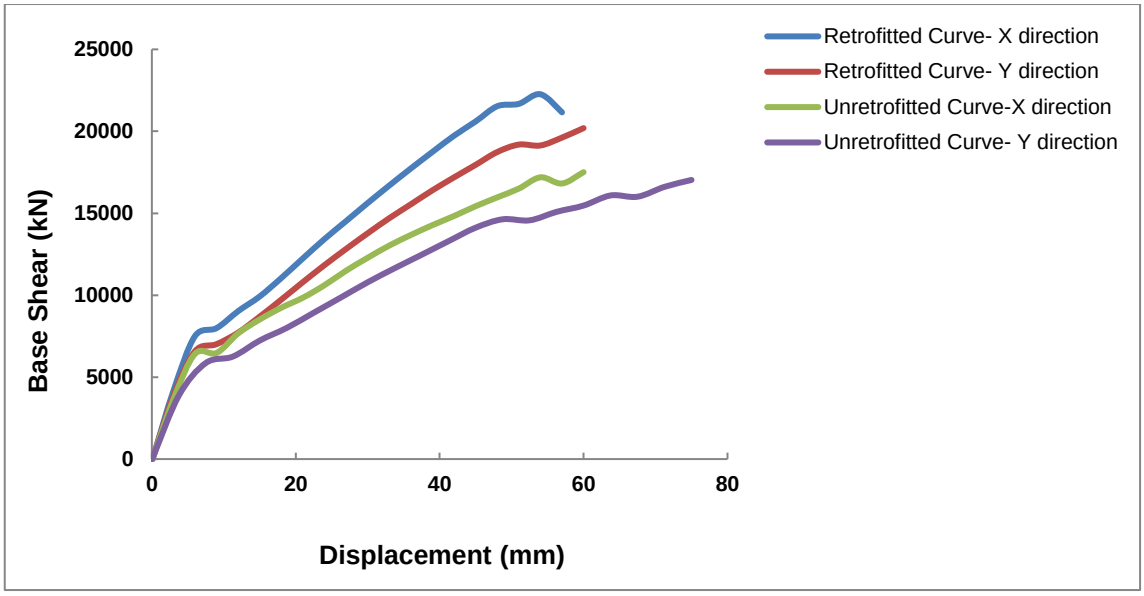

Figure 6.90 Capacity curves of model-17 with and without retrofit

Table 6.41 Comparison of different parameters of Model-17 before and after the retrofit					
Parameters	Before retrofit		After retrofit		Remarks
	In X-axis	In Y-axis	In X-axis	In Y-axis	
Ultimate capacity (kN)	17506.56	17032.08	22261.71	20195.26	After the retrofit, the ultimate capacity is increased by 1.27 times in X-axis and 1.18 times in Y-axis.
Yield displacement (mm)	39.22	47.91	38.81	41.38	After the retrofit, the yield displacement is decreased by 0.98 times in X-axis and 0.86 times in Y-axis.
Maximum Displacement (mm)	60.00	75.00	54.00	60.00	After the retrofit, the maximum displacement is decreased by 10 % in X-axis and decreased by 20 % in Y-axis.
Ductility	1.53	1.57	1.39	1.45	After the retrofit, the ductility is decreased by 9.15 % in X-axis and 7.64 % in the Y-axis.
Ductility Reduction Factor	1.43	1.46	1.33	1.38	After the retrofit, the ductility reduction factor is decreased by 6.99 % in X-axis and 5.47 % in Y-axis.
Overstrength factor	4.38	4.26	5.37	4.87	After the retrofit, the overstrength factor is increased by 1.22 times in the X-axis and 1.14 times in Y-axis.
Time period (sec)	0.29	0.29	0.25	0.25	After the retrofit, the time period is decreased by 13.79 % in X-axis and Y-axis.
R-factor	3.13	3.1	3.57	3.36	After the retrofit, the R-factor is increased by 1.14 times in X-axis and 1.08 times in Y-axis.

Table 6.42 Performance points of model-17 before & after the retrofit in X and Y direction				
Performance level	Before Retrofit		After Retrofit	
	Displacement (mm)		Displacement (mm)	
	X direction	Y direction	X direction	Y direction
Life Safety	6.96	7.53	2.37	2.73
Collapse Prevention	13.14	13.96	6.67	7.53

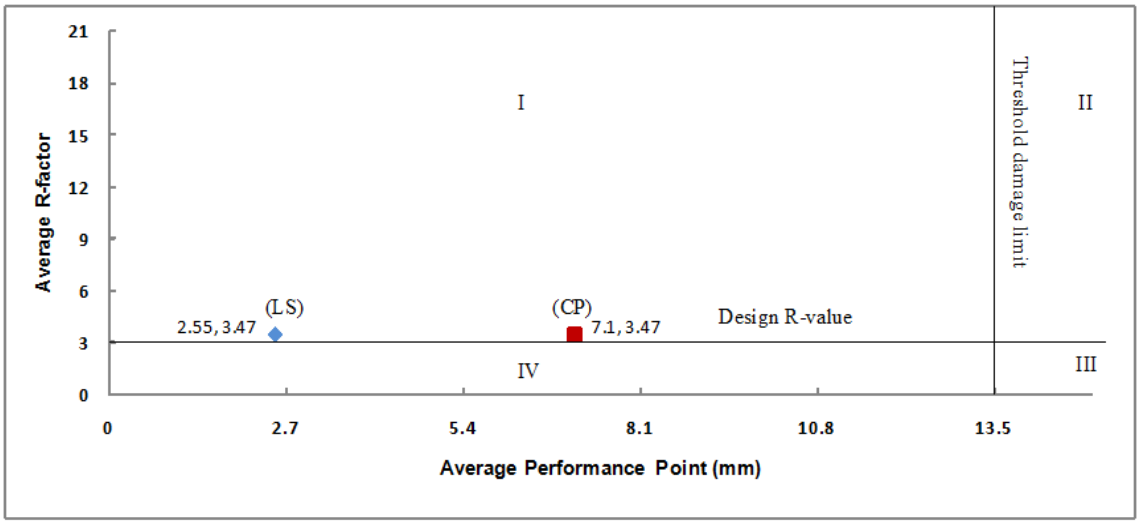

Figure 6.91 Average R-factor versus average performance point graph of model-17 after the retrofit

Figure 6.91 shows the average R-factor versus average performance point graph of model-17 after the retrofit. The point of intersection of R-factor and performance point for life safety & collapse prevention is located in Ist quadrant after the retrofit of building so the structure is in safe mode according to the "Quadrants assessment method".

6.5 Peak base shear

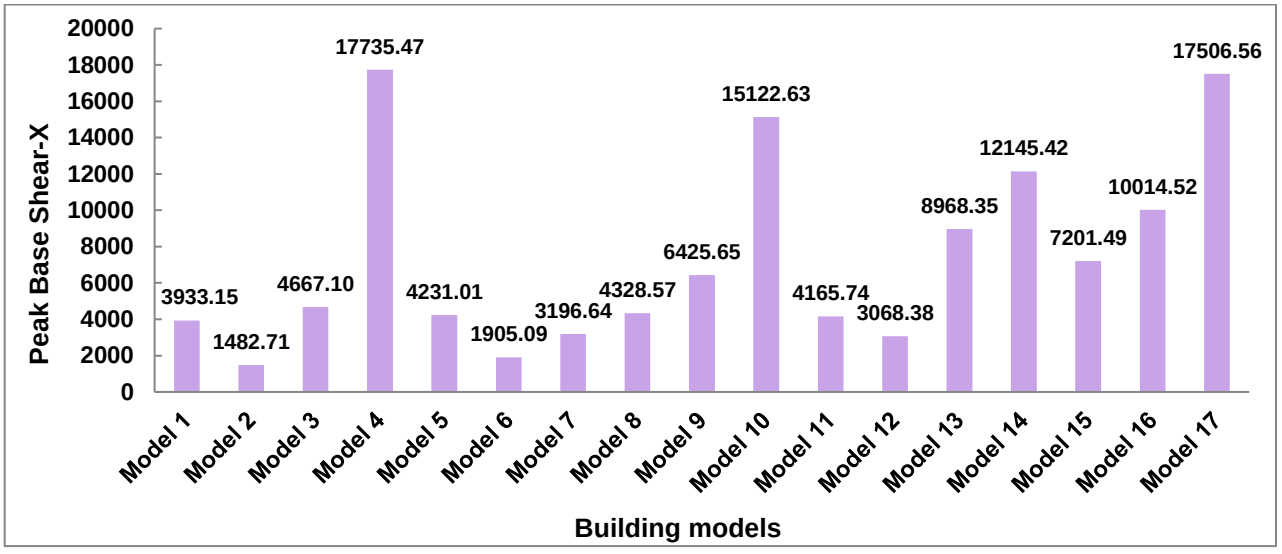

Figure 6.92 (a) Peak base shear graph in X direction

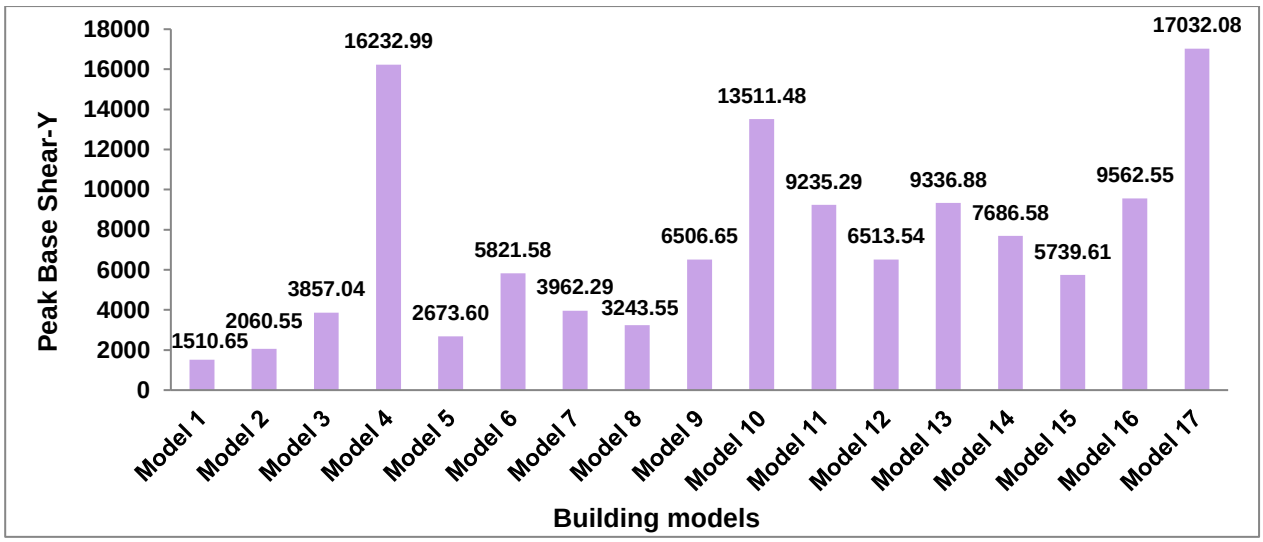

Figure 6.92 (b) Peak base shear graph in Y direction

Figure 6.92 shows the peak base shear graph of all building models in X and Y direction. Model 4, 10 and 17 shows the maximum average peak base shear as compared to all other models due to its good structural and geometrical configuration. Model 1 and 2 shows the minimum average peak base shear due to presence of irregularities in the structure. As per the study, peak base shear depends on the structural and geometrical configuration of the structure.

6.6 Displacement ductility

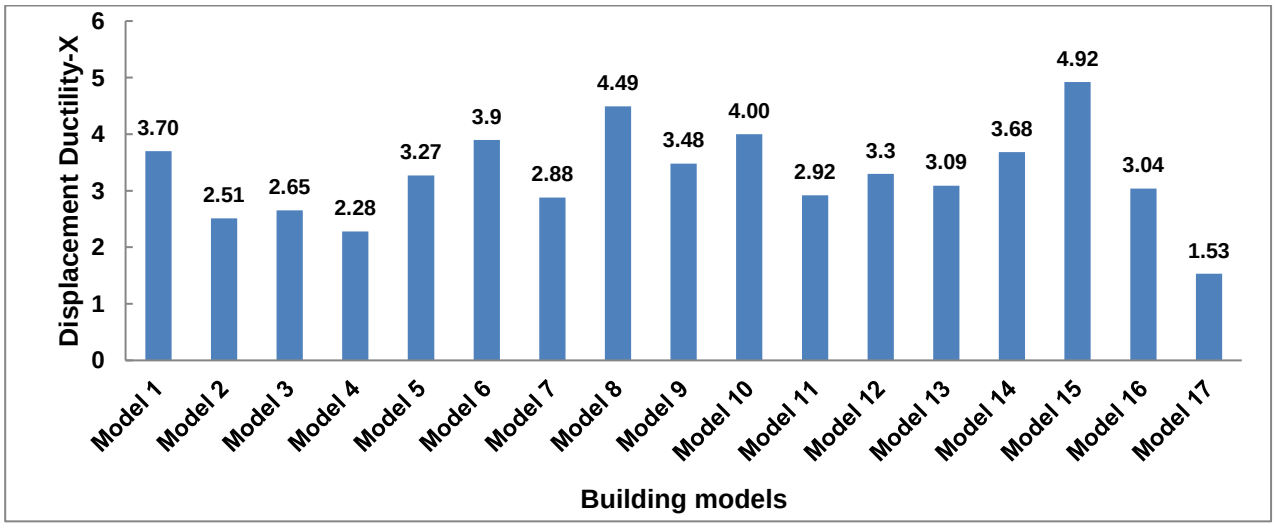

Figure 6.93 (a) Displacement ductility graph in X direction

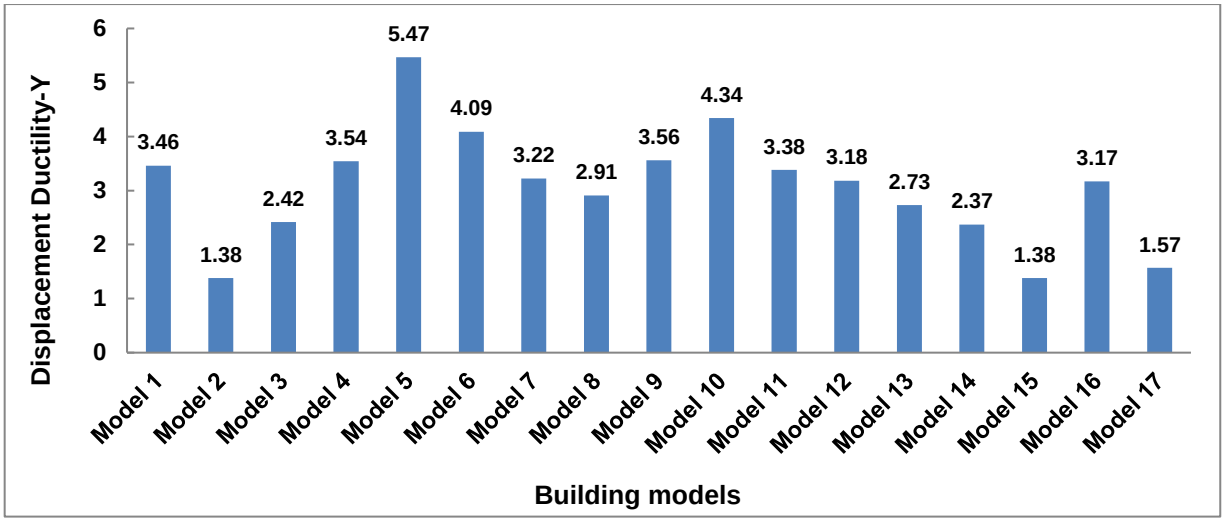

Figure 6.93 (b) Displacement ductility graph in Y direction

Figure 6.93 shows the displacement ductility graph of all building models in X and Y direction. Model 5 shows the maximum average displacement ductility as compared to all other models due to absence of few masonry infill panels. Model 17 shows the minimum average displacement ductility due to high strength in the structure. As per the study, displacement ductility parameter depends on the rigidity of the structure. As the strength of the structure increases, displacement ductility decreases.

6.7 Ductility reduction factor

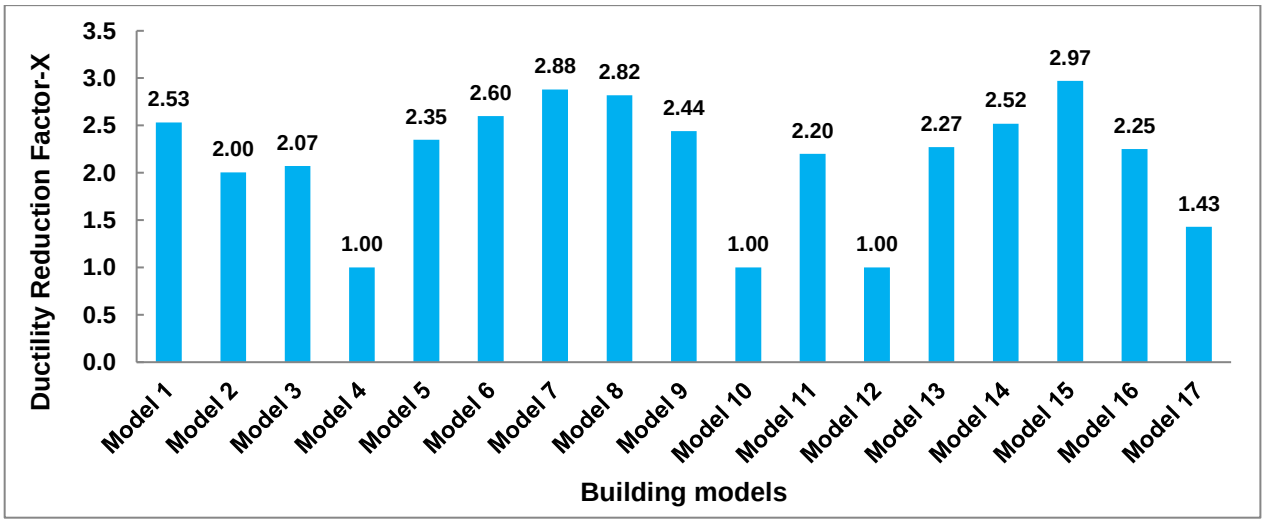

Figure 6.94 (a) Ductility reduction factor graph in X direction

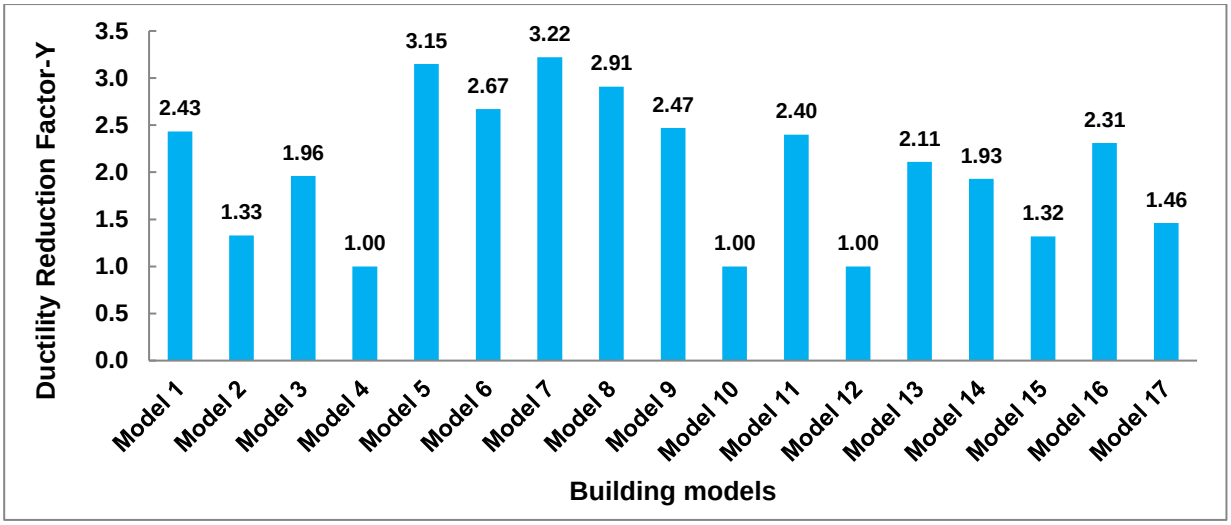

Figure 6.94 (b) Ductility reduction factor graph in Y direction

Figure 6.94 shows the ductility reduction factor graph of all building models in X and Y direction. Model 7 shows the maximum average ductility reduction factor as compared to all other models due to its maximum height of structure. Model 4, 10, and 12 shows the minimum average ductility reduction factor due to less height of structures. As per the study, the ductility reduction factor depends on fundamental time period and ductility parameters. It is observed that as the height of the building increases, the ductility reduction factor increases.

6.8 Overstrength factor

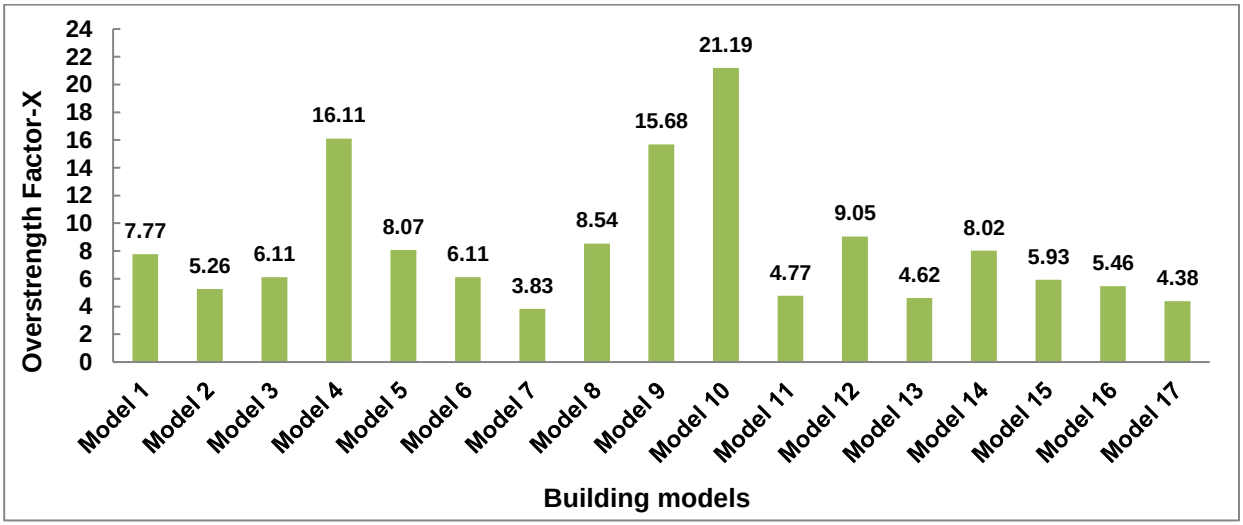

Figure 6.95 (a) Overstrength factor graph in X direction

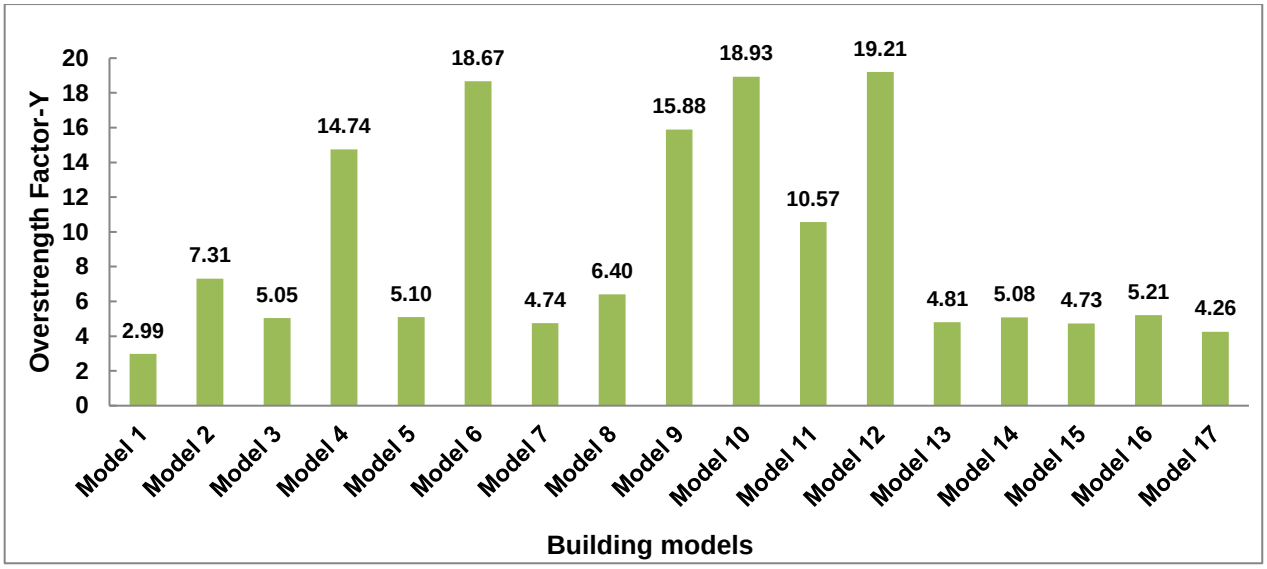

Figure 6.95 (b) Overstrength factor graph in Y direction

Figure 6.95 shows the overstrength factor graph of all building models in X and Y direction. Model 10 shows the maximum average overstrength factor as compared to all other models due to its well planned structural and geometrical configuration. Model 7 shows the minimum average overstrength factor due to high flexibility of structures.

6.9 Response reduction factor

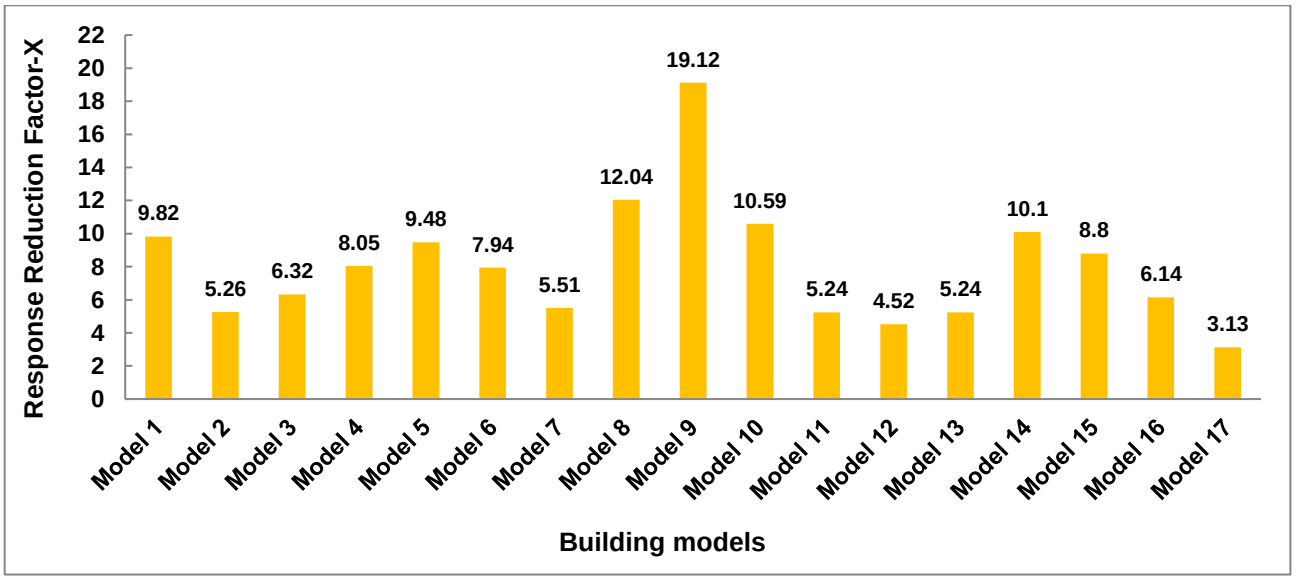

Figure 6.96 (a) Response reduction factor graph in X direction

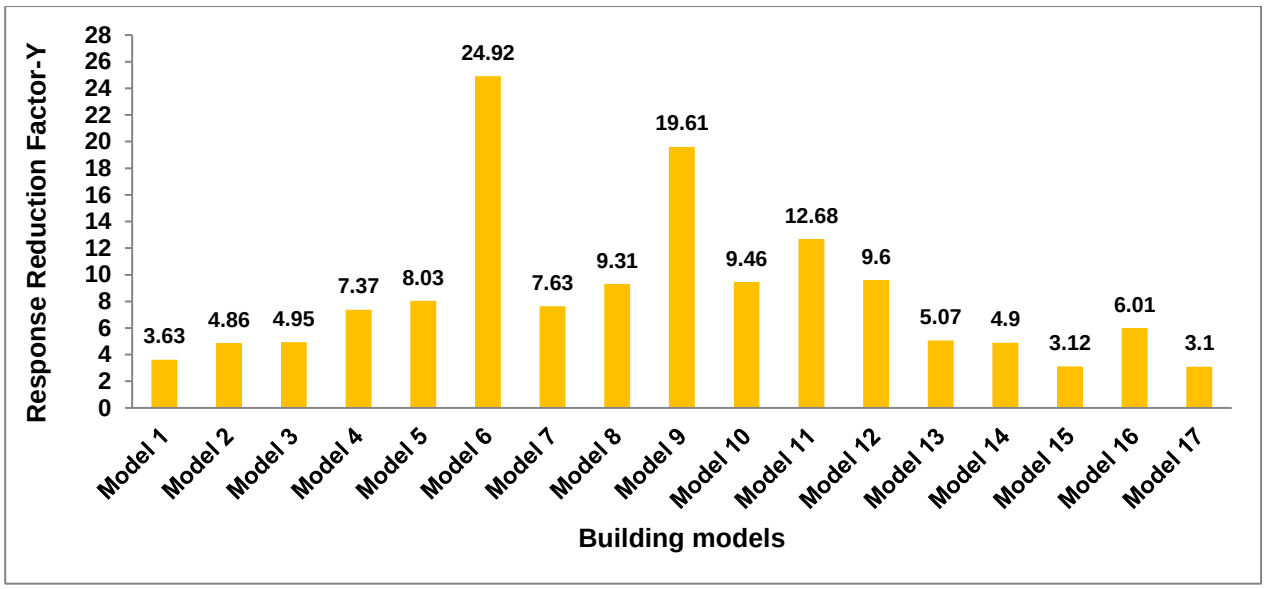

Figure 6.96 (b) Response reduction factor graph in Y direction

Figure 6.96 shows the response reduction factor graph of all building models in X and Y direction. Model 9 shows the maximum average response reduction factor as compared to all other models due to its good structural & geometrical configuration. Model 17 shows the minimum average response reduction factor due to its less reserve strength (overstrength factor) as compared to others. The response reduction factor depends on the ductility reduction factor and overstrength factor of the structure so ultimately it depends on the stiffness, strength and ductility parameters. It is observed that the R-factor is a sensitive parameter which depends upon the many factors, *viz.*, material, structural configuration, geometrical configuration, etc.

6.10 General guidelines for seismic safety of structures

The following general guidelines will be helpful to minimize the future seismic risk in severe earthquake prone area like Koyna-Warna region or elsewhere in the India.

1. Engineers should give an earthquake-resistant design as per the IS 1893 (Part-1):2016 code in severe earthquake prone area.

2. The current construction practice should follow the ductile detailing provisions as per the IS 13920:2016 code.
3. Cosmetic modification of buildings is required for every two-three years especially in buildings constructed in heavy rainfall area.
4. The owner should carry out the regular maintenance of the building.
5. Government authorities should set up a periodic structural audit to ensure safety of structure.
6. Government authorities should establish the demonstration unit to make people aware of the earthquake and make them understand the severity of the risk.
7. Introduce a course curriculum on retrofitting of structures in graduate and postgraduate students as a part of the study.
8. The remedial measures against the deficient structures are: (a) Global retrofitting i.e., addition of shear walls, addition of infill walls, addition of bracings, wall thickening, mass reduction, supplemental damping and base isolation, etc. (b) Local retrofitting i.e., RC-jacketing, FRP-jacketing, steel plating, etc.

6.11 Specific guidelines for seismic safety of structures

The following specific guidelines will be helpful to minimize the future seismic risk in severe earthquake prone area.

1. The masonry infills should be considered while designing and seismic evaluation of the structures because masonry infills play an important role to enhance the stiffness and strength of the structure.
2. Engineers and Architects should provide the symmetrical plan for the construction of any structure. Also, the plan, vertical and torsional irregularities should be avoided while constructing any structure in earthquake prone area.

3. Engineers should design any structure by considering the four important parameters, *viz.*, stiffness, strength, ductility and geometrical configuration.
4. After designing the structure, engineers should evaluate the response reduction factor, overstrength factor, ductility to check its structural integrity because, the response reduction factor is the design tool which shows the level of inelasticity in the structure and that is essentially required in earthquake prone area.
5. Engineers can use the newly proposed "Quadrants assessment method" to check the need of intervention or retrofit the structure in a quick manner to avoid the seismic risk of structures.
6. Engineers can use the newly proposed "Material strain limit approach" to identify the local structural damages in concrete and steel material. This approach can be more useful while retrofitting any RC structure.

6.12 Concluding remarks

This chapter gives the results of earthquake disaster risk index (EDRI) method, adaptive pushover analysis, quadrants assessment method, and material strain limit approach in detail. The chapter also discussed the adopted retrofit strategies to deficient reinforced concrete structures and compared the seismic performance of RC buildings before and after the retrofit.

7. CONCLUSIONS

7.1. Concluding Remarks

This study proposes a refined procedure for the seismic evaluation of reinforced concrete buildings based on the combination of the “Quadrants assessment method” and “Material strain limit approach”. Also for the preliminary assessment purpose, seismic risk index of all existing RC buildings is evaluated by using Earthquake Disaster Risk Index (EDRI) method. Herein, seventeen existing RC buildings from the Koyna-Warna region are seismically evaluated and suggested the retrofit strategies to deficient buildings. The following conclusions can be drawn:

- Seismic risk of RC buildings in the Koyna-Warna region is evaluated to create the awareness in concerned government organization, engineers, architects and local people to take an initiative for the risk mitigation program.
- Based on the RVS study of 120 surveyed RC buildings, it is found that the Koyna-Warna region has 46.7% of reinforced concrete sample buildings falling in the possible collapse category as many buildings are constructed as a non-engineered in a hilly region, aging of structures, heavy rainfall conditions, etc. About 0.8 % and 21.7 % of sample buildings are falling in no damage and slight damage condition. The percentage of RC buildings in moderate and severe damage stage is 10.8 % and 20 % respectively. Also, irregular plan shapes, inadequate lintel bands, cracks in structural members, vegetation on the wall are the common observations in RC buildings that make them seismically more vulnerable.

- Based on the visual observation, some structural defects have been observed in the surveyed RC buildings, viz., the corrosion of reinforcement starts due to inadequate concrete cover provided to the structural members, poor construction practice, deterioration of concrete due to heavy rainfall condition, shear cracks on columns due to inadequate stirrup spacing, diagonal cracks occurred at the opening of windows due to inadequate sill band, opening of windows closer to the corner of the masonry infills.
- Model-1, Model-15 and Model-17 are vulnerable to earthquakes due to the soft storey effect, less provision of steel in columns. So there is a need to retrofit these structures based on the "Quadrants assessment method". The structural deficiencies are identified through the "Quadrants assessment method" and "Material strain limit approach". The remaining all other buildings are found to adequately resist earthquakes due to their structural integrity. The ultimate capacity, overstrength factor, response reduction factor of the retrofitted buildings are increased significantly in the X and Y direction as compared to the unretrofitted building, due to the RC jacketing of the deficient column members. The performance points of Model-1, Model-15 and Model-17 are transferred from other Quadrants (II^{nd} / III^{rd} / IV^{th}) to the I^{st} Quadrant due to the application of RC jacketing. The performance points of the other remaining RC buildings are already located in the I^{st} Quadrant due to their inherent structural integrity. So there is no need to retrofit these RC buildings based on the "Quadrants assessment method".

- As per the present study, the computed values of the response reduction factor (R) are more than the value suggested in the IS 1893 (Part-1):2016 code for RC-infilled frames obtained from adaptive pushover analysis. It is observed that the over-strength factor is significantly influenced by the presence of masonry infill in the RC frame. As a result, the response reduction factor is higher in the RC-infilled frame. Also based on the observation, as the R-factor increases, the performance point of the structure decreases.
- In the current construction practice, engineers should follow strictly the earthquake resistant design and ductile detailing provisions for improvement in the performance of the structure. Also try to adopt the energy dissipation devices like damper, semi-interlocked bricks infill, shape memory alloy material, lintel beam with a view to achieving the satisfactory performance of the structure. Strong column-weak beam concept should be adopted while designing any RC structure. Structural member size should be maximum in such a way that reinforcement should not bend at the beam column joint to avoid the congestion of reinforcement.
- The “Quadrants assessment method” is a global and quick approach for the seismic assessment of the structures based on the actual response reduction factor and performance point. The material strain limit is the effective local approach for the seismic assessment of the RC structures based on the threshold strain limit of concrete and steel to identify the actual damage state of structural members.

- Based on the present study, it is concluded that the proposed combination of the "Quadrants assessment method" and "Material strain limit approach" can give a rapid, reliable and refined procedure for the seismic evaluation and retrofit of any RC structure.
- Based on the findings of this work we should consider the masonry infill in the RC frame structure to enhance the structural integrity of the structure. As highlighted by several studies together with ours, the R-factor is sensitive to material strength, geometrical and structural configuration of the structure so it is difficult to predict the precise R-value for the particular structure. The practicing engineers should calculate the R-value for every structure instead of using the codal provision in earthquake prone area.

7.2 Scope for the Future Research

In this section, some of the possible areas of research which can be further explored in future are presented below:

- The present work may be extended to seismically assess the reinforced concrete structures through the nonlinear dynamic time history analysis.
- To evaluate the seismic performance of different housing typologies, *viz.*, brick masonry structures, stone masonry structures in earthquake prone areas and compare their relative structural efficiency.
- To study the various other retrofit strategies for the deficient structures based on the cost to benefit ratio.

- To assess the seismic performance of the deficient reinforced concrete structures having energy dissipation devices, *viz.,* tuned mass dampers, viscous fluid dampers, metallic damper, friction damper.